Author:
Gill Olivas, Beatriz

Title:
Rock comminution of subglacial lake sediments as a potential source of energy and nutrients to the Subglacial Lake Whillans microbial ecosystem.

Rock comminution of subglacial lake sediments as a potential source of energy and nutrients to the Subglacial Lake Whillans microbial ecosystem

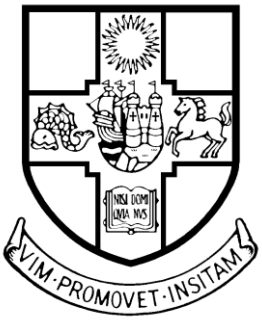

Beatriz I. Gill Olivas

A dissertation submitted to the University of Bristol in accordance with the requirements for award of degree of Doctor of Philosophy in the Faculty of Science.

School of Geographical Sciences

December 2018

Word Count:27,857

Abstract

Throughout the past couple decades, the study of subglacial environments has shown microbial ecosystems exist under ice sheets and glaciers. The recent access to Subglacial Lake Whillans (SLW) provided, for the first time, the opportunity to observe these environments directly. So far, SLW has been shown to have a diverse and active microbial ecosystem despite the limited access to typical energy sources, such as the atmosphere or in-washed organic matter and oxidising agents. Therefore, SLW, like most other sub ice-sheet environments, is limited to energy sources that exist within it. In this thesis, samples from four depths of a shallow SLW sediment core, were used to evaluate the potential energy contributions from mechanochemical reactions. To do this, samples were crushed and wetted under anoxic conditions and gases released during crushing and the subsequent 40-day incubation of the crushed sediments were measured. Results showed considerable amounts of hydrogen and carbon dioxide, as well as methane (albeit at a lower concentration), which could serve as abiotic sources of energy to methanogenic and methanotrophic microbial communities found in SLW. Further experiments and analysis, to investigate the origins of these gases, revealed crushing produced significant amounts of surface free radicals and H_2O_2, offering the potential for a wide range of REDOX conditions and reactions to develop in subglacial environments, and consequently, the potential for nutrient cycling within these environments. Finally, analysis of trace gases within the vial headspace and of the water chemistry after incubation provided some further insight into previously overlooked effects of sediment comminution. The presence of several hydrocarbons within the headspace, together with the concentrations of acetate, DOC and DOM within the water hint at the potential recycling of ancient organic matter. Analysis of the water chemistry also showed evidence of fluid inclusion release and the effects of comminution on subglacial weathering.

Acknowledgements

Firstly, I would like to thank my supervisor, Martyn Tranter, who has guided me from beginning to end of this project. Particularly for his continued support and advice, and for the numerous coffee meetings, which gave me the energy and encouragement to finish this Ph.D. I would also like to thank my second supervisor, Sandra Arndt, who was very helpful, particularly at the early stages of this project when I was attempting to use a Reactive-Transport model. I hope to be able to use all those skills in future projects.

Thank you to Mark Skidmore, and the WISSARD team, for providing the samples without which this project would not be possible. Many thanks also go out to Jon Telling, who was instrumental in the initial development stages of this project, and who's enthusiasm kept me interested in this project throughout its duration. Also, thank you to Simon O'Doherty for his interest in this project and for his invaluable help with developing a method to measure trace gases in my samples.

I would like to thank Fotis and James, for all their assistance in the LOWTEX lab, and for putting up with my constant requests for instrument repairs, and for doing everything possible to allow me to complete the lab work necessary for this project. A special thanks goes out to my "lab pals", Moya and Guillaume, who have kept me company through the long days in the lab and who made lab work so much more fun. As well as for all the help they provided outside the lab, with never-ending calculation discussions and for all the times they have been there to bounce ideas off.

Many thanks as well to the people of Browns, there's too many to name, but a general thanks for all the lunch breaks which have kept me going past the mid-day slump. Thank you, Tim, for the countless songs that made the morning walks into work more entertaining, to Ale, for being there whenever I've needed someone to chat, and to the many others for the numerous coffee breaks and conversations.

I would like to thank my mum and my 'yaya', for their encouragement, love and support throughout the years, my brothers and their families for offering a distraction from work and for generally being there, and to Marimar and Eduardo for always showing an interest.

To Anja, Leire and Monica, thanks for staying so close, even when far.

A very special thanks to Thom, for being that friendly face in the lab at the start of this Ph.D., and for his incredible support throughout the past couple of years.

To my dad, whose memory still encourages me to do my best, and to Felipe, wish you could both share this with me.

Authors Declaration

I declare that the work in this dissertation was carried out in accordance with the requirements of the University's *Regulations and Code of Practice for Research Degree Programmes* and that it has not been submitted for any other academic award. Except where indicated by specific reference in the text, the work is the candidate's own work. Work done in collaboration with, or with the assistance of, others, is indicated as such. Any views expressed in the dissertation are those of the author.

SIGNED: ..... DATE:.....

Table of Contents

List of Figures

List of Tables

Chapter 1 Introduction

1.1 Background

Subglacial environments were believed to be devoid of life as recently as 30 years ago. However, microbial life has now been found in a range of subglacial environments, from small alpine glaciers to polar ice sheets (e.g. Sharp et al. (1999), Wadham et al. (2004), Tranter et al. (2005), Skidmore et al. (2005) and Mikucki et al. (2009)). The occurrence of recently divided cells suggest that subglacial environments have an active microbial ecosystem (Sharp et al. (1999), Skidmore et al. (2000)), and are believed to have a large impact on the types of geochemical weathering reactions that occur within them (Tranter et al, 2002). However, our understanding of the sources of energy that maintain this biome is still limited. Subglacial ecosystems, particularly below large ice sheets, are isolated from the most common sources of energy (such as sunlight, atmospheric gases or in-washed nutrients), and therefore they are required to derive their energy from other sources, which include oxidizable and reducible minerals and organic matter found in-situ(Sharp and Tranter, 2017). Smaller polythermal glaciers can often get atmospheric gases, such as oxygen, recharged from the atmosphere as supraglacial water drains into the subglacial environment through a series of moulins and crevasses (Tranter et al., 2005). However, in larger ice-sheets, sources oxidising agents and legacy organic matter is limited (Wadham et al., 2010, Tranter and Wadham, 2013).

Microbes are often found in association with subglacial debris (Sharp et al., 1999), since this provides a source of energy, in the form of potential electron acceptors (e.g. organic carbon and sulphides), and a source of nutrients, such as phosphorous and nitrogen (Tranter et al., 2005). There, they can exploit both macro-aerobic and micro-anaerobic conditions - indeed most subglacial systems will host cycling between oxic and anoxic conditions (Skidmore et al., 2005). In aerated environments, where surface water reaches the bed, microbes will exploit aerobic weathering processes, such as oxidation of sulphide by oxygen (Bottrell and Tranter, 2002) or they will catalyse chemical weathering of glacial flour components, including silicates (Rogers and Bennett, 2004). Under anaerobic conditions, they will take advantage of anaerobic redox reactions, such as reduction of manganese, iron and sulphate, or the oxidation of sulphide by iron (III) (Wadham et al., 2007) and, if organic carbon is available, methanogenesis (Wadham et al., 2012). In some

cases, microbes may even drive glacier beds and margins to anoxia, as is the case in Finesterwalderbreen, Svalbard (Wadham et al., 2004), where there is a readily available supply of kerogen and sulphides from shale, which can be used by microbes, and where the hydrological profile prevents interaction with the atmosphere. This has also been suggested to be true of Subglacial Lake Vostok, Antarctica (Wadham et al., 2004). However, the organic matter sources available to subglacial microbes are finite, and this can pose an issue when trying to understand the survival of microbial ecosystems beneath large ice masses such as Antarctica, where they have been isolated for hundreds of millennia.

The extreme nature of these environments has lead microbial ecosystem in these environments to adapt and utilise the nutrient sources available to them. Some of the most notable microbes which have been observed include those beneath Taylor Glacier, Antarctica, which cycle sulphur from sulphate rich marine brine, utilising iron (III) as a terminal electron acceptor and giving the Blood Falls, Antarctica, their distinctive red colour as emerging Fe(II)-rich waters adsorb atmospheric oxygen and precipitate ferric oxy-hydroxides (Mikucki et al., 2009). There is also widespread evidence of methanogens below ice. Boyd et al. (2010) provide genetic, biochemical and geochemical evidence of active methanogens living in subglacial sediments at Robertson Glacier (Canada). There has also been evidence of microbial cells below the Greenland ice sheet correlated with the excess CO_2 and CH_4 produced (Tung et al., 2006). Additionally, some active methanotrophic bacteria below Greenland have been found which could consume some of the methane produced by methanogens (e.g. Stibal et al. (2012b), Dieser et al. (2014)). More recently, both methanogens and methanotrophs were found within Subglacial Lake Whillans, the first subglacial lake to be cleanly sampled (Christner et al., 2014, Michaud et al., 2017).

A new shift in our understanding of the factors impacting on the energetic underpinning of subglacial microbial communities came from the finding that H_2 could be produced abiotically by the comminution of rocks at glacier beds (Telling et al., 2015). There is an array of bacterial species that are capable of utilising H_2 as an energy source, both in anaerobic and aerobic subglacial systems. These include strains of Thiobacillus (Lanoil et al., 2009), Rhodoferax and Geobacter (Hamilton et al., 2013), as well as a range of methanogens (e.g. Boyd et al. (2010), Stibal et al. (2012b)). Results from Telling et al.

(2015) showed H_2 concentrations as a result of comminution of fresh unweathered rock were more than enough to support rates of methanogenesis previously reported in the Greenlandic sediments analysed by Stibal et al. (2012b), showing the potential for erosion to be a significant contribution to the energy requirements of these systems. This could also provide an ongoing source of energy to these isolated systems. Telling et al. (2015) used unweathered fresh rock, yet most large glacier masses, including Antarctica, are often underlain by ancient sediments. Those beneath Antarctica are highly weathered (Tulaczyk et al., 1998). Further, recent access for the first time to a subglacial lake (Subglacial Lake Whillans (SLW)) revealed the presence of methanogenic bacteria capable of using H_2 as an energy source, as well methanotrophs which utilise CH_4 (Michaud et al., 2017). Therefore, understanding the possible contributions of erosion, despite sediments being highly physically and chemically weathered, to this microbiome is key to comprehending the ongoing survival of these extreme ecosystems.

1.2 Literature Review

1.2.1 The Subglacial Environment

Glacial landscapes account for ~10% of the Earth's surface (Anesio and Laybourn-Parry, 2012). Ice, in the form of glaciers, is one of the Earth's biggest agents of erosion (Knight, 1997), and impacts on regional physical erosion indirectly via isostatic rebound during glacial/inter-glacial cycles (Hallet et al., 1996). Subglacial erosion in the polar regions has been measured to be as rapid as 4.8 mm a^{-1} in Greenland (Cowton et al., 2012), and is considerably higher in soft bedded glaciers and in Antarctica, with rates of between 0.5 m a^{-1} (Davies et al., 2018) and 1 m a^{-1} (Smith et al., 2012, Smith et al., 2007) in West Antarctica. The main subglacial erosion processes are plucking and abrasion. Plucking is the movement of rocks and boulders as they become detached and trapped within basal ice, to be transported and deposited further downstream. In cold based glaciers, where sliding is negligible due to the greater adhesive strength between the rock and the ice, plucking is the main form of erosion (Benn and Evans, 2010a). Abrasion is the erosion of rock surfaces by the scouring action (striation) and polishing of the bedrock by the basal layer of the ice (Benn and Evans, 2010a). Abrasion produces large volumes of glacial flour, which refers to the finest fraction of subglacial till. Glacial flour can be described as the fresh mineral fragments, usually smaller than 100 μm, that can only be explained by abrasion (Sudgen and John, 1976). Typically, these mineral fragments are also coated in

micron sized particles (Tranter, 2003). During the formation of glacial flour, the high pressures produce strained and amorphous surfaces which readily release cations (Anderson et al., 1997). Further, mechanical grinding and milling of quartz and other silicate and oxide minerals resulted in fracture or local plastic deformation within mineral structures (Petrovich, 1981). This then affects the dissolution kinetics in three ways: it increases the surface area, increases the solubility of a solid (due to the Kelvin effect), slowing the effect of approaching saturation, and, finally it increases the dissolution rate constant (Petrovich, 1981). This, combined with the lack of precipitates, that might hinder rock-water interactions on their surface (Tranter, 2003), renders these particles highly reactive relative their parent material and will be readily weathered in contact with water, provided that there is a supply of protons to displace cations from the silicate mineral surfaces.

1.2.2 Subglacial Biogeochemistry

It is generally accepted that subglacial systems include a variety of aquatic environments, similar to terrestrial 'wetlands', including streams and rivers, saturated sediments and lakes (Priscu et al., 2008). In Antarctica alone there are almost 400 subglacial lakes (Wright and Siegert, 2012), potentially with a range of water chemistry conditions which could harbour a wide diversity of microbial ecosystems. However, despite the interest in subglacial environments, their very nature has limited our understanding of them. Most of our biogeochemical knowledge of subglacial environments to date has been inferred from glacial runoff (Hodson et al., 2002, Sharp et al., 1999, Tranter, 2006, Tranter et al., 2002b) or from accreted ice (Priscu et al., 1999). Although these data sets are essential to understanding the overall characteristics of the subglacial drainage system, they are not without their limitations, making subglacial lake samples all the more valuable.

To date, the composition of subglacial waters has been thought to be controlled by an array of different factors, including abiotic factors, such as mineralogy, the existing concentration of ions in the water, the rock-water contact area, the time water is contact with reactive surfaces and the availability of dissolved atmospheric gases (Benn and Evans, 2010b), and biotic factors, such as the metabolically active microbial species present, will also affect weathering reactions in subglacial environments (Skidmore et al., 2010) and in turn, their chemistry. However, it is the source of the melt and the path the

melt subsequently follows that will primarily determine the composition if the meltwaters (Tranter et al., 1997).

1.2.2.1 Carbonate Weathering

Due to the characteristically fast dissolution kinetics of carbonates, initial weathering reactions between glacial flour and water are characterised by carbonate weathering, particularly when CO_2 is present (Brown et al., 1996). Carbonates appear mainly as limestone (primarily in the form of calcite) and dolomite in the rock record, making up almost a fifth of the Earth's surface (Langmuir, 1997). However, they make up very little of most glacial bedrocks, but are ubiquitous in almost every bedrock, being found as disperse phases in most rock types. Their dissolution kinetics are often six orders of magnitude higher than those of silicates (Lerman, 1988), and so their presence, in concentrations even as low as 0.1%, will dominate the ensuing water chemistry (Langmuir, 1997). Plummer et al. (1978) suggest that carbonate dissolution occurs by the reactions shown in equations 1, 2 and 3 (below) all of which occur simultaneously at the calcite surface (Brantley, 2003).

$$CaCO_{3\,(s)} + H^+_{(aq)} = Ca^{2+}_{(aq)} + HCO_3^-{}_{(aq)} \quad (1)$$

$$CaCO_{3\,(s)} + H_2CO_3^0{}_{(aq)} = Ca^{2+}_{(aq)} + 2HCO_3^-{}_{(aq)} \quad (2)$$

$$CaCO_{3\,(s)} + H_2O_{(l)} = Ca^{2+} + HCO_3^-{}_{(aq)} + OH^-_{(aq)} \quad (3)$$

The rates of dissolution of different carbonates can vary considerably. For example, dolomite is significantly less soluble than calcite and it can take weeks or even months before it reaches equilibrium (Langmuir, 1997). There are a number of factors which can influence the solubility and saturation state of carbonates. These include dissolution and exsolution of CO_2 (Langmuir, 1997), the common ion effect (Langmuir, 1997), temperature (Langmuir, 1997), surface area (Rickard and Sjoberg, 1983) and roughness of the carbonate particles(Compton et al., 1986).

Carbonate dissolution in subglacial environments is effectively in a closed system with respect to CO_2, where the rate of CO_2 consumption typically exceeds the rate of CO_2 renewal by dissolution of atmospheric gases (Raiswell, 1984), because the ice acts as a barrier between atmospheric CO_2 and the solution. The limited availability of atmospheric CO_2 means that carbonic acid from CO_2 dissolution will be limited to that produced by certain methanogens and oxidation of organic matter (Tranter et al., 2002a),

limiting reactions shown in equation 1 and 2. However, dissolution by equation 2 might be compensated by the presence of sulphuric acid produced during sulphide oxidation. So, the initial carbonate dissolution in subglacial environments is primarily controlled by hydrolysis (Hodson et al., 2000), as shown in reaction 3, in combination with further reactions such sulphide oxidation and oxidation of organic matter which are required to drive further carbonate dissolution (Tranter et al., 2002b).

Despite carbonates (e.g. calcite) and sulphides (e.g. pyrite) only being a minor component of subglacial sediment, they largely control weathering reactions (Tranter et al., 1993). This is particularly true of fast draining glaciers or small alpine glaciers, where the contact time between sediment and water is shorter and the fast reaction kinetics of these minerals are the most relevant (Wadham et al., 2010). Common subglacial carbonate

Table 1-1 Common subglacial weathering reactions described in Tranter et al. (2002b).

PRINCIPAL SUBGLACIAL WEATHERING REACTIONS	
Carbonate hydrolysis	(4)
$Ca_{1-x}(Mg_x)CO_3$ (s) + H_2O (l) ⇆ (1-x)Ca^{2+}(aq) + xMg^{2+} (aq) + HCO_3^- (aq) + OH^- (aq)	
Silicate (feldspar) hydrolysis	(5)
$KAlSi_3O_8$ (s) + H_2O (l) ⇆ $HAlSi_3O_8$ (weathered surfaces) + K^+ (aq) + OH^- (aq)	
Carbonation of carbonate	(6)
$Ca_{1-X}(Mg_x)CO_3$ (s) + CO_2 (aq) + H_2O (l) ⇆ (1-x)Ca^{2+}(aq) + xMg^{2+}(aq) + 2HCO_3^-(aq)	
Carbonation of feldspar	(7)
$CaAl_2Si_2O_8$ (s) + 2CO_2 (aq) + 2H_2O (l) ⇆ Ca^{2+} (aq) + 2HCO_3^- (aq) + $H_2Al_2Si_2O_8$ (weathered surfaces)	
Fe (III) as an oxidising agent	(8)
FeS_2 (s) + 14Fe^{3+} (aq) + 8 H_2O (l) ⇆ 15Fe^{2+} (aq) + 2SO_4^{2-} (aq) + 16H^+ (aq)	
Coupled sulphide oxidation and carbonate dissolution	(9)
4FeS_2 (s) + 16$Ca_{1-X}(Mg_x)CO_3$ (s) + 15O_2 (aq) + 14H_2O (l) ⇆ 16(1-x)Ca^{2+} (aq) + 16xMg^{2+} (aq) + 16HCO_3^- (aq) + 8SO_4^{2-} (aq) + 4$Fe(OH)_3$ (s)	
Coupled sulphide oxidation and silicate dissolution	(10)
4FeS_2 (s) + 16$Na_{1-x}K_xAlSi_3O_8$ (s) + 15O_2 (aq) + 86H_2O (l) ⇆ 16(1-x)Na^+ (aq) + 16xK^+ (aq) + 8SO_4^{2-} (aq) + 4$Al_4Si_4O_{10}(OH)_8$ (s) + 32H_4SiO_4 (aq)) + 4$Fe(OH)_3$ (s)	

weathering mechanisms include: hydrolysis (Equation 3 and Table 1-1: Equation 4), carbonation (Table 1-1: Equation 6), or the coupled sulphide oxidation and carbonate dissolution reaction (Table 1-1: Equation 9) (Tranter et al., 2002b). The presence of large microbial communities in subglacial environments has been suggested to promote sulphide oxidation (Sharp et al., 1999). Carbonate weathering reactions will continue until the 'ultimate steady-state concentration', or the 'saturation index' (SI) of this mineral is reached (Brown et al., 2001). However, in some cases the steady-state concentration will not be determined by the SI but by the surface area of calcite exposed to dissolution and the water flux (Brown et al., 2001). In small scale glaciers, where water residence time is relatively short (0.1 – 10 years), steady state is seldom reached (Skidmore et al., 2005).

1.2.2.2 Sulphide oxidation

Although often considered to be slow, abiotic rates of sulphide oxidation can in fact be comparable or, in some cases, faster than microbially mediated sulphide oxidation (Mortimer et al., 2011). Partly due to this reactivity, abiotic and microbially catalysed sulphide oxidation, which is often coupled to either carbonate or silicate dissolution, will dominate subglacial weathering reactions (Skidmore et al., 2005, Skidmore et al., 2000). The oxidation of sulphides in subglacial environments produces acidity, which in conjunction with an influx of atmospheric gases (such as oxygen and carbon dioxide) and microbe CO_2 respiration decreases the pH of subglacial water and lowers the saturation with respect to carbonates (Tranter, 2003). This reaction is only second to acid hydrolysis in providing protons to solution subglacial environments. Lowering the pH of solutions decreases the saturation index with respect to carbonates, thus allowing carbonate dissolution to continue (Tranter et al., 2002b). Sulphide oxidation preferentially dissolves carbonates because of their considerably faster dissolution rate. The carbonate: silicate dissolution ratio is approximately 5:1 in subglacial environments compared to the 1.3:1 global average ratio (Tranter, 2003).

Some studies have suggested sulphide oxidation is limited by the oxygen content from supraglacial sources that filtered to the basal layer through crevasses or from bubbles within the basal ice which are released during basal melt (Skidmore et al., 2000). However, boreholes drilled to the glacier bed showed that the SO_4^{2-} concentration exceeds that allowed by the oxygen concentration in supraglacial environments by a

factor of 2 to 3 (Tranter et al., 2002b). Therefore, it is likely that microbial activity in certain subglacial environments drives the bed into anoxic conditions (Wadham et al., 2004). Fe (III) is then used as an oxidising agent (Table 1-1, Equation 8), rather than O_2, in these environments. Sources of Fe(III) could include the oxidation products of pyrite and other Fe(II) silicates, as well as magnetite and hematite (Tranter, 2003).

Microbes can also play a part in sulphur recycling within these environments (Mikucki et al., 2009). This has been observed in other environments (Schink, 2006), however the mechanisms by which this occurs is not fully understood (Turchyn et al., 2006). Evidence from the Blood falls (Antarctica) suggests the sulphate is biologically reduced to sulphite by either assimilatory or dissimilatory metabolisms (Mikucki et al., 2009). Sulphate reduction does not go all the way to hydrogen sulphide (no H_2S is present), suggesting that the metabolism in the brine requires sulphates to be recycled through intermediates, and these sulphur intermediates must be reoxidised to sulphate (Mikucki et al., 2009). Sulphur is thus catalytically cycled to facilitate the oxidation of organic matter in a system where Fe (III) is the terminal acceptor (Mikucki et al., 2009).

1.2.2.3 Silicate Weathering

Silicate rocks dominate the subglacial environment, these include a range of minerals, from feldspars, which are relatively reactive, to quartz whose dissolution is so slow that it is often considered to be virtually unreactive. Even feldspars have considerably slower dissolution and weathering kinetics compared to carbonates (Langmuir, 1997). Thus, it is not until glacial flour has a longer water contact time, on the order of years, that silicate weathering becomes more dominant (Wadham et al., 2010), particularly if supplies of disseminated carbonates are exhausted. Longer water residence times mean that pH continually increases, and carbonate saturation is reached, allowing silicate dissolution to occur. Although less kinetically favourable, the limited external inputs (such as atmospheric gases or atmospheric deposition of nutrients) to subglacial ecosystems below large ice masses, results in silicate weathering dominating carbonate weathering (Wadham et al., 2010). Feldspar dissolution can be described by several kinetic equations describing each of the four stages in their dissolution (Lerman, 1988), and each becomes increasingly slower. Initially, feldspar undergoes hydrolysis very rapidly with water, but then dissolution slows down radically as the cations on the mineral surface are replaced

by H^+, leaving behind a leached mineral surface layer (Lerman, 1988). However, even at its slowest stage, feldspar dissolution is still relevant to glacial timescales.

Silicate mineral dissolution can be controlled by a number of factors, which can be divided into extrinsic and intrinsic factors (White and Brantley, 2003). Extrinsic factors include changes in climate and biology (White and Brantley, 2003) and some of the factors suggested earlier (Section 1.2.2.1), such as pH, temperature and surface history (Lasaga, 1984). It has also been suggested that the presence of organic matter can catalyse the dissolution rate of some rocks (Lasaga, 1984). Intrinsic factors include the change in roughness over time, which accounts for approximately a third of the decrease in the reaction rate (White and Brantley, 2003), or the feldspar structure, related to the Al and Si disorder, which can yield an eight-fold increase of dissolution rates at a fixed composssition (Zhang and Luettge, 2009).

However, glacial flour, which is formed by crushing (or comminution), has a large surface areas and areas of high surface energy (Tranter, 2003), which are favourable to silicate dissolution. This promotes some of the common silicate weathering reactions, including silicate hydrolysis (Table 1-1: Equation 5) and carbonation of feldspar (Table 1-1: Equation 7; Tranter et al. (2002b)). It is likely that because sources of CO_2 to subglacial environments are limited, the coupled sulphide oxidation and silicate dissolution reaction (Table 1-1: Equation 10) becomes more important (Skidmore et al., 2010).

Silicates contain trace concentrations of nitrogen (e.g. in micas and feldspars) and potassium (e.g. in feldspars and biotite; Holloway and Dahlgren (2002)), and thus their dissolution can provide microbial ecosystems with nutrients to sustain life, and indirectly microbial respiration furthers silicate carbonation. It is now believed that microbial population dynamics can heavily influence subglacial weathering rates (Sharp et al., 1999).

1.2.3 Subglacial Ecosystems

Despite the apparently limited energy sources found sub-glacially, subglacial ecosystems have been characterised in a range of sites, including Alpine (Sharp et al., 1999), Arctic (Bhatia et al., 2006, Sharp et al., 1999) and Antarctic (Mikucki et al., 2009, Stibal et al., 2012a) glaciers, as well as below the Greenlandic (Yde et al., 2010) and Antarctic (Christner et al., 2014, Lanoil et al., 2009, Mikucki et al., 2016) Ice Sheets.

There is evidence that microbial cells below ice are not just in a dormant state, but that they are active and have adapted to live under ice (e.g. Wadham et al. (2004), Tranter et al. (2005), Skidmore et al. (2005), Mikucki et al. (2009), Skidmore et al. (2010)). Due to the lack of sunlight below the ice these microbes have evolved to produce their energy from sources other than photosynthesis, which include organic carbon from overridden soils or introduced by the surface (Boyd et al., 2010, Stibal et al., 2012b), geothermal heat energy or redox and weathering reactions (Lanoil et al., 2009, Mikucki et al., 2009, Skidmore et al., 2005). The ever increasing evidence of microbial presence underneath glaciers, together with an increased understanding of the microbial communities present, has led to a shift in understanding of how subglacial weathering takes place (Tranter et al., 2005). It was previously believed that chemical weathering only took place under oxic conditions. However, it has now been established that subglacial weathering of rocks can occur in a variety of conditions expanding from oxic to completely anoxic environments (Tranter et al., 2005).

The most widespread microbial organisms below glaciers are chemolithotrophic microbes, which derive their energy from rock weathering processes (Tranter et al., 2005) and the oxidation of organic carbon sources (Stibal et al., 2012b). Microbial populations found within subglacial environments include strains of Thiobacillus (Lanoil et al., 2009), Rhodoferax and Geobacter (Hamilton et al., 2013), as well as a range of methanogens (Boyd et al., 2010, Stibal et al., 2012a, Stibal et al., 2012b). Microbes are often associated with subglacial debris, since the debris provides potential source of energy, from organic carbon and sulphides, and nutrients, such as phosphorous and nitrogen (Tranter et al., 2005). In aerated environments, where surface water reaches the bed, microbes will exploit aerobic processes such as aerobic acetate mineralisation (Foght et al., 2004). They have also been shown to catalyse chemical weathering of glacial flour components, including silicates (Rogers and Bennett, 2004). Microbes have also adapted to exploit anaerobic reactions which might occur in a distributed drainage system, such as reduction of manganese, iron and sulphate, oxidation of sulphide by Fe (III) (Mikucki et al., 2009) and, if organic carbon is available, methanogenesis (Stibal et al., 2012b). Furthermore, microbes can themselves cause glacier beds and margins to become anoxic, as in Finsterwaldrbreen (Wadham et al., 2004). This occurs when there is a readily available supply of kerogen and sulphides from shale, which are utilised by

microbes, and the hydrological profile prevents interaction with the atmosphere (Wadham et al., 2004).

Although it was originally believed that the there was little species diversity within these microbial ecosystems (Skidmore et al., 2005), further investigation of these environments has shown them to sustain extensive and abundant microbial ecosystems (Boyd et al., 2010, Dieser et al., 2014, Hamilton et al., 2013, Mikucki et al., 2009). Despite the extreme nature of these environments, i.e. any microorganism living there must be able to live under constantly dark, constantly cold and oligotrophic conditions, as well as being able to adapt to freeze-thaw and seasonal cycling between oxic and anoxic environments (Skidmore et al., 2005), microbial assemblages have adapted to utilise the limited energy and nutrient sources available to them. There is widespread evidence of methanogens below ice, Boyd et al. (2010) provide genetic, biochemical and geochemical evidence of active methanogens living in subglacial sediments at Robertson Glacier, Canada. It was also found that concentrations of microbial cells below the Greenland ice sheet correlated with the excess CO_2 and CH_4 produced (Tung et al., 2006). It has been shown that methane hydrate formation is strongly dependant on the basal temperature of the ice sheet and that significant hydrate is likely to be produced under frozen bed conditions with relatively high organic carbon concentrations (above 2%). Therefore, the bed of the Antarctic ice sheet could be a significant methane pool (Wadham et al., 2012). It has also been suggested that the source of the organic carbon is important for maintaining methanogenesis (Stibal et al., 2012b). There is evidence of active methanotrophic bacteria below Greenland (Dieser et al., 2014) and Antarctica (Michaud et al., 2017), which could counteract some of the methane produced by methanogens.

1.2.4 Abiotic Sources of Energy in Other Extreme Environments

Subglacial ecosystems are highly erosive extreme environments, yet to date most studies focus solely on chemical weathering as a source of nutrients to these environments and the microbial effects on weathering and nutrient cycling, with very little attention on the effect that mechanical forces can have on the subglacial environment. Studies into environments such as fault zones and hydrothermal vents have found mechanochemical reactions can provide a substantial energy source to bacterial ecosystems (Kelley et al., 2005). However, studies looking at their possible contribution to subglacial environments are limited to one, by Telling et al. (2015).

1.2.5 Fluid Inclusions

Fluid inclusions in silicate minerals can arise during the formation of ores, the crystallization of magma, diagenesis and during metamorphic reactions (Sisson et al., 1993). Fluid inclusions contain traces of gases and fluid from the environment where they were formed. Whilst igneous rocks, such as quartz or granite, contain fluid inclusions which are rich in different carbon bearing gases (Konnerupmadsen and Rosehansen, 1982), sedimentary and metamorphic rocks contain fluid inclusions characterised by the environments of their formation, with traces of the sea water composition and atmospheric gases from their time of formation (Goldstein, 2001). Thus, their composition will be as varied as the mechanisms by which they form.

Fluid inclusions can be released back into the environment though faulting, erosion, or comminution, of rocks. However, their contributions to the environment will be highly dependent on the origins of these rocks. They commonly have high salinity, and this is particularly true of fluid inclusions formed during diagenesis or metamorphic reactions (Goldstein, 2001). Fluid inclusions can also release a number of gases, including high volumes of CO_2 and methane(Martinelli and Plescia, 2005), or H_2S and N_2 (Naumov et al., 2009). N_2 released from fluid inclusions is in fact considered the main source of N during weathering of silicate rocks (Montross et al., 2013).

1.2.6 Rock-Water Reactions

Beside the release of fluid inclusion during erosion and faulting, there are a number of mechanochemical reactions that can occur as a result of ground up rocks reacting with water. These include reactions involving mineral surface free radicals (Kita et al., 1982) and serpentinization (Jones et al., 2010, Kelley et al., 2005), which are also often related to Fisher-Tropsch Type (FTT) reactions, and radiolysis (Lin et al., 2005).

1.2.6.1 Surface free radicals

Surface free radicals can be formed when silicate or aluminosilicate minerals and rocks containing covalent bonds (e.g, granite or quartz) are crushed (Kita et al., 1982). When the Si-O-Si or Al-O-Si bonds in silicates or aluminosilicates are broken, these produce surface free-radicals (Kameda et al., 2004) (Equation 11; Hasegawa et al. (1995)). It has been suggested that the Si· can then react with water to produce H_2 (Equations 12 and 13; Kita et al. (1982)).

$$\equiv Si\text{-}O\text{-}Si\equiv \rightarrow \equiv Si\bullet + \bullet O\text{-}Si\equiv \quad (11)$$

$$Si\bullet + H_2O \rightarrow SiOH + H\bullet \quad (12)$$

$$H\bullet + H\bullet \rightarrow H_2 \quad (13)$$

These reactions were first suggested to explain the concentrations of H_2 produced at fault zones during earthquakes (Wakita et al., 1980). Since then, these mechanisms have been widely studied in relation to active fault zones (Takehiro et al., 2011) and their production during the crushing of quartz (Damm and Peukert, 2009, Kita et al., 1982, Saruwatari et al., 2004). However studies relating to their possible relevance in a cold, highly erosive environments such as the subglacial ecosystem have been limited to that of Telling et al. (2015).

Other free radicals can also be produced when rocks other than silicates are crushed. Crushing of pyrite can produce ·OH through the Fenton reaction (Borda et al., 2003), where Fe (III) is reduced to Fe (II) on sulfur-deficient defect sites on pyrite, which dissociates H_2O to ·OH and H^+ (Equation 14, Borda et al. (2003)). It has also been suggested that two ·OH radicals can combine to form H_2O_2 (Equation 15, Borda et al. (2001)).

$$\equiv Fe\ (III) + H_2O_{(ads)} \rightarrow \equiv Fe\ (II) + \bullet OH_{(ads)} + H^+ \quad (14)$$

$$\bullet OH + \bullet OH \rightarrow H_2O_2 \quad (15)$$

1.2.6.2 Serpentinization

Another abiotic rock-water reaction capable of producing H_2 is serpentinization. During serpentinization Fe (II) is oxidised to Fe (III) through the reduction of water to H_2 (Mayhew et al., 2013), this process can be described simply by equation 16 (McCollom, 2009), where $(FeO)_{rock}$ represents the ferrous component of an igneous silicate mineral and $(Fe_2O_3)_{rock}$ represents the ferric component of an Fe-bearing secondary mineral. Typically these reactions occur with Fe (II) in olivine or pyroxene minerals, which then produce secondary minerals such as serpentine or magnetite (Equation 17, Neubeck et al. (2014)). In nature, this reaction is typically associated to environments with high pressures and/or temperatures, such as seafloor settings and hydrothermal vents (Janecky and Seyfried, 1986, Kelley et al., 2005, Marques et al., 2008). However, it has been studied at a range of temperatures and pressures, with temperatures ranging from

over 300°C down to 22°C (Kelley et al., 2005, Neubeck et al., 2011, Stevens and McKinley, 2000b, McCollom, 2009) in laboratory settings. Serpentinization reactions are more favourable at temperatures above ~15°C (McCollom, 2009), however even at temperatures as low as 22°C, laboratory experiments have been shown to produce significant amounts of H_2 when crushed basalt reacts with water (Stevens and McKinley, 2000b). The by-products of serpentinization (e.g. magnetite and serpentinite) can also act as catalysts for further reactions between H_2 and inorganic carbon to form CH_4 and other hydrocarbons (Jones et al., 2010).

$$2(FeO)_{rock} + H_2O \rightarrow (Fe_2O_3)_{rock} + H_2 \quad (16)$$

$$\underset{\text{olivine}}{(Mg_{0.88}Fe_{0.12})_2SiO_4} + \underset{\text{water}}{1.34H_2O} \rightarrow \underset{\text{serpentinite}}{0.5Mg_3S_2O_5(OH)_4} + \underset{\text{brucite}}{0.26Mg(OH)_2} + \underset{\text{magnetite}}{0.08Fe_3O_4} + \underset{\text{dihydrogen}}{0.08H_2} \quad (17)$$

1.2.6.3 Fischer-Tropsch Type (FTT) reactions

Fischer-Tropsch reactions are well known to the oil and petroleum industry, they are catalysed, abiotic reactions by which CH_4 and other, longer hydrocarbons can be formed from CO and H_2 (Schulz, 1999). Fischer-Tropsch Type (FTT) reactions, sometimes called the Sabatier reaction, refer specifically the formation of CH_4 through the catalysed hydrogenation of CO_2, in an aqueous or gaseous state (Equation 18) (Neubeck et al., 2011). FTT reactions are often associated to serpentinization, not only because the H_2 produced can be used in these reactions, but also because they are often catalysed by some of the secondary minerals serpentinization produces, such as magnetite (Neubeck et al., 2011). However, it is also worth noting this reaction is likely to have a number of intermediates, such as the reduction of CO_2 to CO, and the formation of by-products such as formate (Okland et al., 2014). Like serpentinization, FTT reactions have also been studied at a range of temperatures and pressures, mostly relevant to hydrothermal systems (Bradley and Summons, 2010, Etiope and Ionescu, 2015, Proskurowski et al., 2008), yet these reactions have still been shown to be relevant at temperatures as low as 30°C (Neubeck et al., 2011).

$$CO_2 + 4H_2 \rightarrow CH_4 + 2H_2O \quad (18)$$

1.2.7 Isotopic Fractionation of Gases

A number of studies have been carried out to identify and differentiate between the different isotopic signatures associated to the origin, both abiotic and microbial, of carbon-bearing gases. Some publications have focused on the isotopic signatures of microbial processes, such as Whiticar (1999) which provided a comprehensive investigation of fractionation of CH_4 and CO_2 during bacterial formation and oxidation of methane through a series of field and laboratory methods. Whiticar (1999) created an isotope discrimination diagram, which can be used to identify the dominant origin of CH_4 by its isotopic signatures (Figure 1-1). Others have tried to constrain the possible abiogenic sources of hydrocarbons formed in the mantle by investigating isotopic signatures within hydro-carbons in fluid inclusions (Potter et al., 2013). Isotopic signatures of hydrocarbons have also been used to investigate the abiotic sources of hydrocarbons in hydrothermal vents, such as FTT reactions (Proskurowski et al., 2008).

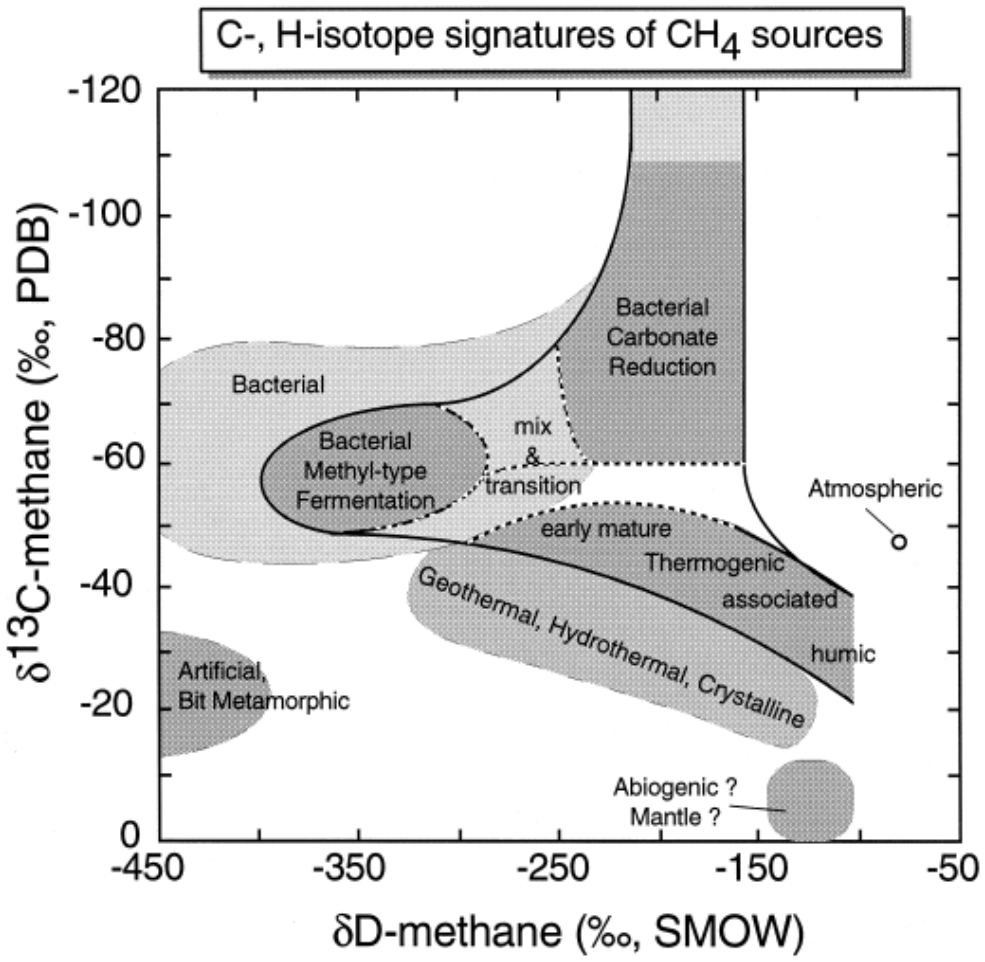

Figure 1-1 Classification diagram for the origin of CH_4 through the use of d ^{13}C-CH_4 and d D-CH_4 (taken from Whiticar (1999)).

1.3 Summary

Subglacial environments have been shown to have a diverse active microbial ecosystem. Yet, our current understanding of the sources of energy to these systems is limited to surficial sources, which filter through into the subglacial ecosystem, relic organic matter and the energy and nutrients derived from weathering reactions. These sources are very limited and/or finite. Microbial communities in other extreme environments have been shown to be supported by a number of abiotic processes associated to rock-water reactions. Here we aim to examine their possible contribution in a subglacial setting, and their potential to continue to sustain the microbial ecosystem.

1.4 Aims and Objectives

The main aim of this study is to explore alternative sources of energy to subglacial microbial ecosystems, other than those of traditional chemical weathering and sedimentary organic matter, which could sustain microbial life. The aim of this project is to explore whether comminution of old weathered sediment can provide these ecosystems with a source of energy. In order to do this, we will pursue the following objectives:

1. To examine whether the comminution of highly weathered, subglacial lake sediment at 0^{o}C is capable of producing bio-utilisable gases, such as H_2 and CH_4.
2. To understand the origins of these bio-utilisable gases and the mechanisms by which they form.
3. Finally, to explore if sediment comminution has other effects on the subglacial ecosystem that might help or hinder microbial life in this environment.

1.5 Roadmap

This thesis consists of three central research chapters, each dealing with some aspect of crushing of Subglacial Lake Whillans sediment. These are preceded by two chapters. First, an introductory chapter, in which a broad overview of the project is given (Section 1.1), followed by an overview of the current state of our scientific knowledge in the field of subglacial weathering and the wider subglacial environment, as well as some the chemical reactions associated to rock crushing (Section1.2), followed by a set of aims and

objectives for this project (Section 1.4). The second chapter describes the site from which the sediments used for this project were taken and the sampling techniques used to collect them, as well as outlining some of the main findings associated with the site. Each research chapter in this thesis is associated to one of the research objectives highlighted in Section 1.4. The first research chapter (Chapter 3) attempts to quantify the possible contribution of bio-utilisable gases to SLW as a result of crushing. The second research chapter (Chapter 4) studies the possible origins of these gases and the mechanisms by which they might form. The third, and final, research chapter (Chapter 5), looked at any other potential effects of sediment comminution on the subglacial ecosystem. Overarching findings and conclusions, as well as limitations to this work and further research ideas are detailed in the final chapter (Chapter 6).

Chapter 2 Site Description and Sampling

2.1 Subglacial Lake Whillans

Subglacial Lake Whillans (SLW) lies approximately 800 m beneath the Whillans Ice Plain (Christner et al., 2014), which is part of the Siple-Gould Coast ice stream system (Fricker and Scambos, 2009)(Figure 2-1). SLW is an active lake which drains every few years through a series of hydrologically linked subglacial lakes in this area, which eventually drain into the ocean (Fricker and Scambos, 2009). Active-source seismic data and ice-penetrating radar estimate the maximum lake depth to be approximately 8 and 15 m at low- and high- stand respectively (Christianson et al., 2012, Horgan et al., 2012). During drainage events, ~0.15 km^3 of water is lost during a six month period, with a water flux of ~10 $m^3\ s^{-1}$ (Christianson et al., 2012, Fricker et al., 2007).

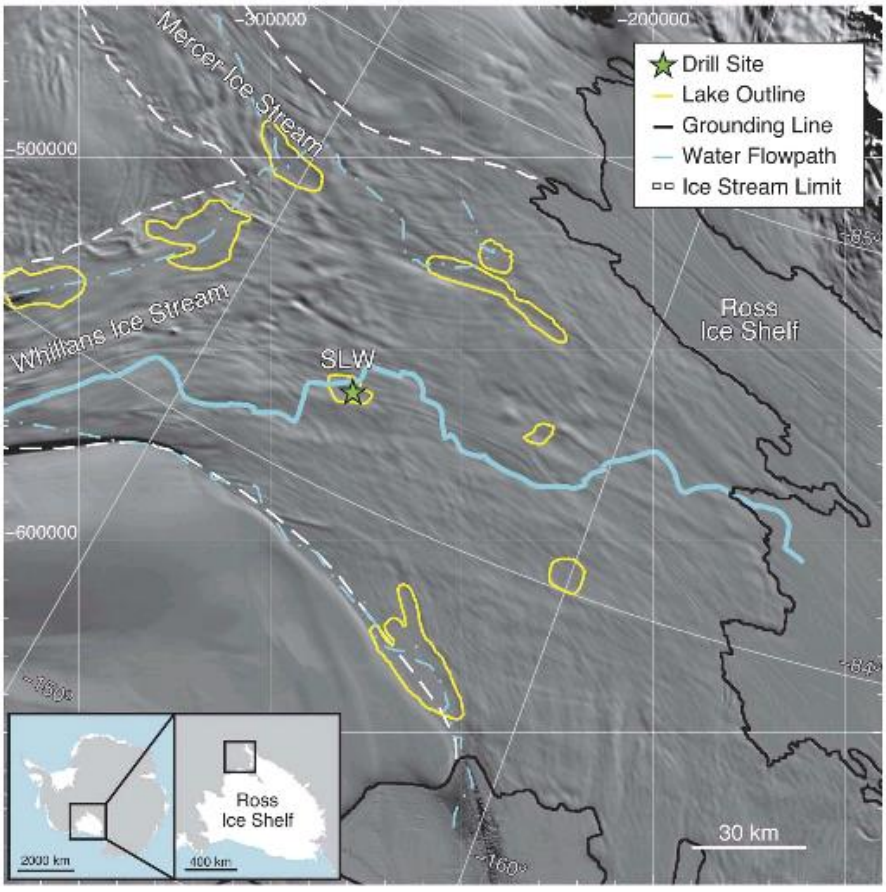

Figure 2-1 Location of SLW and the SLW drill site. (Figure from Priscu et al. (2013)).

Sampling took place in late January 2013 at the deepest point in the lake (84.240 °S, 153.694 °W, Christner et al. (2014)). A hot water drilling system was used to create a borehole (with a 60 cm minimum diameter). To ensure the clean access of the lake, microbial cells in the drilling water, or on any exposed surfaces of the hose, cables and any equipment deployed, were reduced and killed by the use of four complementary methods: filtration, ultraviolet radiation, pasteurization and disinfection using 3% (w/v) H_2O_2 (Priscu et al., 2013). Drilling water was derived from melting surface snow and ice on the overlying ice sheet. This was circulated through a water treatment system, which filtered out micron and sub-micron (>0.2 μm) sized particles. Next, the filtered water was irradiated with two germicidal UV wavelengths, and, finally, it was pasteurised at 90°C to reduce the presence of any remaining viable microbes (Christner et al., 2014). Water samples were taken before and after each stage of the processing to monitor contamination levels (Priscu et al., 2013). The drill hose and any instrument cables were deployed through a borehole collar containing 12 amalgam pellet UV lamps (Christner et al., 2014). Borehole sampling instruments and tools were all spray-saturated with 3% H_2O_2 (w/v) and placed in sealed polyethylene bags until their deployment (Christner et al., 2014). All personnel wore single use protective apparel during borehole operations (Christner et al., 2014). The efficiency of this technology was thoroughly tested before its use, and the results of these test are detailed in Priscu et al. (2013). Sediment core samples were taken using a UWITEC gravity multi-corer, with a diameter of 6 cm and a 50 cm length (Tulaczyk et al., 2014), which provided a 38cm long sediment core (Michaud et al., 2016).

The SLW sediment cores were composed primarily of silicates, principally quartz and feldspars (Table 2-1), although there was some evidence of pyrite within the sediments (Figure 2-2) . The grain size distribution of SLW sediments was dominated by silt and clay fractions, with some slightly coarser materials (Table 2-2). Analysis of stable isotopes in sediment pore waters indicate that the water is primarily derived from basal-ice melt, with only a minor sea-water component, which reaches a maximum of 6% at the bottom of the 38 cm long core (Figure 2-3) (Michaud et al., 2016). Analysis of the SLW waters showed oxygen levels to be below saturation with respect to oxygen (~16% of surface air-saturated water) (Christner et al., 2014). Pore water ion profiles are consistent with those of a silicate weathering dominated system (Michaud et al., 2016).

Table 2-1 Mineralogical composition of SLW sediment grains within the 63 – 125 µm size fraction (taken from Michaud et al. (2016)).

Mineral type	Percent (%)
Alkali Feldspar	4
Biotite	2
Chlorite	1
Garnet	2
Hornblende	0.5
K-Feldspar	12
Plagioclase	19
Quartz	59
Unknown	0.5

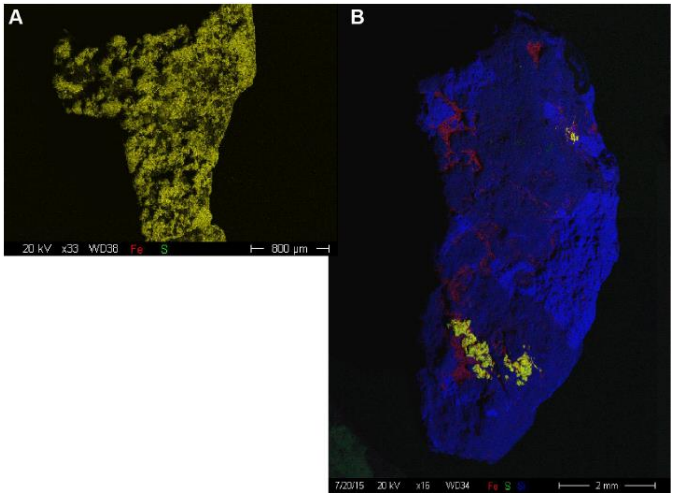

Figure 2-2 Elemental maps from two SLW pyrite containing clasts. A. Pyrite grain, as determined by its predominantly Fe and S composition. B. Quartz grain with Pyrite inclusions (taken from Michaud et al. (2016)).

Table 2-2 Grain size distribution of SLW sediments (taken from Michaud et al. (2016)).

Grain size diameter (µm)	Wentworth size class	wt %
>250	Medium sand and coarser	20.9
125-250	Fine sand	12.9
63-125	Very fine sand	16.3
<63	Silt and clay	49.9

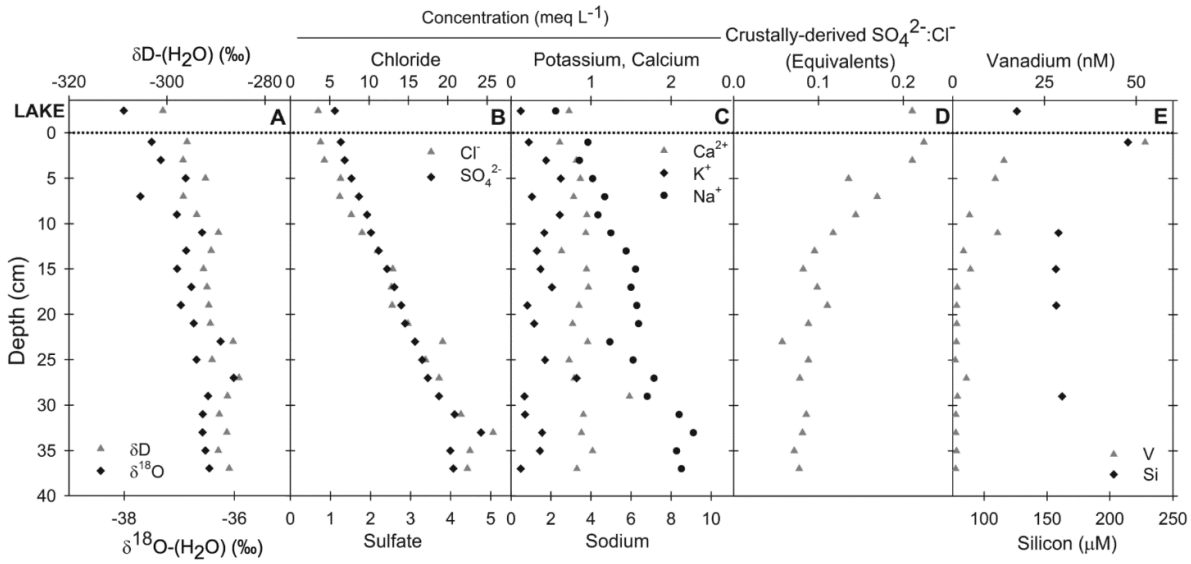

Figure 2-3 Pore-water profiles of SLW sediment cores and lake waters(taken from Michaud et al. (2016)). A: Water stable isotopes. B: Chloride and sulfate of water (not corrected for sea-water component). C: Crustally derived calcium, potassium and sodium. D: Ratio of crustally derived sulfate to chloride. E: Silicon and vanadium concentrations. Dotted line represents the water-sediment interface.

There was also some evidence of sulphide oxidation, carbonate dissolution and carbonation reactions (Table 2-3, Christner et al. (2014)).The concentration of major ions increased down the sediment pore water profile, indicating there might be a concentrated, presumably saline, solute source at a depth (Figure 2-3)(Michaud et al., 2016).

SLW has both a notable NH_4^+ component, accounting for 73% of the dissolved inorganic nitrogen pool (Table 2-3), and relatively high DOC concentrations (Table 2-3) (Christner et al., 2014). It has been suggested that this DOC is a result of upwards diffusion from the ancient marine sediments. There is also some evidence of acetate and formate (Table 2-3), suggesting SLW has a labile source DOC in its waters (Christner et al., 2014).

Table 2-3 Lake Whillans borehole, water and pore water chemistry (taken from Christner et al. (2014)).

Parameter	Borehole*	Water column†	Sediments‡
Physical			
Temperature (°C)§	−0.17 (0.25)	−0.49 (0.03)	n.d.
Conductivity (µS cm^{-1} @ 25 °C)‖	5.3	720 (10)	860
pH‖	5.4	8.1 (0.1)	7.3
Redox (mV (SHE))‖	n.d.	382	n.d.
Microbiological			
Cell density (cells ml^{-1})	6.9×10^2 (51.0)	1.3×10^5 (0.4×10^5)	n.d.
Cellular ATP (pmol l^{-1})	0.04 (0.002)	3.70 (1.00)	n.d.
[^{3}H]thymidine¶	n.d.	13.7 (1.3)	46.6 (5.6)
[^{3}H]leucine¶	n.d.	2.9 (0.4)	0.9 (0.04)
^{14}C-bicarbonate (ng C l^{-1} d^{-1})	n.d.	32.9 (4.2)	n.d.
Carbon and nutrients			
Dissolved oxygen (µmol l^{-1})	n.d.	71.9 (12.5)	n.d.
DIC (mmol l^{-1})	n.d.	2.11 (0.03)	n.d.
DOC (µmol l^{-1})	n.d.	221 (55)	n.d.
Acetate (µmol l^{-1})	n.d	1.3 (0.2)	n.d.
Formate (µmol l^{-1})	n.d	1.2 (0.3)	n.d.
PC#	n.d.	78.5 (7.4)	384.2 (37.0)
PN#	n.d.	1.2 (0.4)	21.5 (1.7)
PC:PN (molar)	n.d.	65.4 (0.3)	17.9 (0.4)
NH_4^+ (µmol l^{-1})	n.d.	2.4 (0.6)	n.d.
NO_2^- (µmol l^{-1})	n.d.	0.1 (0.1)	n.d.
NO_3^- (µmol l^{-1})	n.d.	0.8 (0.5)	9.1
PO_4^{3-} (µmol l^{-1})	n.d.	3.1 (0.7)	7.3
DIN:SRP (molar)	n.d.	1.1 (0.4)	n.d.
Major ions (µeq l^{-1})			
Na^+	n.d.	5,276 (18)	6,977
K^+	n.d.	186 (4.2)	293 (1.0)★
Mg^{2+}	n.d.	507 (12)	596 (101)★
Ca^{2+}	n.d	859 (29)	860 (104)★
F^-	n.d.	31.5 (0.4)	34.0
Cl^-	n.d.	3,537 (3.4)	4,943
Br^-	n.d.	6 (0.01)	7 (0.4)★
SO_4^{2-}	n.d.	1,111 (0.4)	1,230
HCO_3^-	n.d	2,111 (35)	2,238**

Parameter	Borehole*	Water column†	Sediments‡
Stable isotopes††			
$\delta^{18}O$ of H_2O	n.d.	−38.0‰	−37.5‰
$\Delta^{17}O$ of NO_3^-	n.d.	−0.1 to 0.2‰	n.d.

1. *Borehole water sampled by hydrocast at 672 mbs before lake entry.
2. †Water column data represent averages (± s.d.) from hydrocasts collected on 28 January 2013 (cast 1), 30 January (cast 2) and 31 January (cast 3) 2013, except for [^{3}H]leucine incorporation, which is an average of cast 1 and 3 only.
3. ‡The sediment data correspond to measurements from the upper 2 cm of surficial sediments.
4. §Average (± s.d.) of *in situ* measurements made through the lake water column at ~10 cm intervals with a SBE 19*plus*V2 SeaCAT Profiler CTD on 28 January and 30 January 2013.
5. ‖Based on measurements from discrete water samples brought to the surface.
6. ¶Macromolecular incorporation rates of tritium were converted to cellular carbon and presented along with bicarbonate incorporation as average ng C l^{-1} d^{-1} (± s.d.) for water or average ng C d^{-1} gram dry weight $^{-1}$ (± s.d.) of sediment.
7. #Average (± s.d.) µmol l^{-1} for water and average (± s.d.) µmol g dry weight sed^{-1} for surficial sediment.
8. ★Surficial sediment porewater major ions are the average (± range) of two replicates.
9. **Calculated based on charge balance.
10. ††Values are per thousand and reported relative to V-SMOW. The range of 2 measurements is given for $\Delta^{17}O$ of NO_3^-.
11. n.d., no data available.

Extensive analysis of the microbial populations found in SLW have shown a chemosynthetically driven, active, microbial ecosystem (Christner et al., 2014). There is some evidence of heterotrophic microbes, however their low growth efficiency suggest that most of their carbon demand goes into cellular maintenance, rather than growth (Vick-Majors et al., 2016). Results so far have shown that there is an abundance of chemolithotrophic bacteria and archea, suggesting that the oxidation of iron (II), sulphur and nitrogen compounds may be important primary production pathways in these environments (Achberger et al., 2016). Further, 16s RNA analysis showed this microbial community includes bacteria that have the genetic capability for either sulphur oxidation as well as sulphur reduction (Purcell et al., 2014). The presence of methanogenic and methanotrophic bacteria down the sediment core also suggest there is potential for CH_4 cycling within SLW sediments (Michaud et al., 2017).

Despite the potential for a number of nutrient cycling reactions to take place, modelled oxygen and nitrogen demands of this ecosystems have shown they are both limiting to the growth and it is suggested that the cycles between oxic and anoxic conditions play a key role in nutrient cycling with the SLW porewaters (Vick-Majors et al., 2016).

2.2 Whillans Grounding Line

The hydrological system below the Whillans Ice Stream (WIS), which feeds SLW and a number of other active subglacial lakes found in this area, continues to drain all the way to the grounding line and into the Southern Ocean (Carter et al., 2013). The Whillans Grounding Line (WGL) is found approximately ~100km downstream from SLW (Figure 2-4)(Begeman et al., 2017). The WGL is under a slightly thinner layer of ice than SLW, with surveys showing ice thickness varying from ~760m at the grounded area down to 740 m at the seaward end of the grounding zone (Muto et al., 2013). There is evidence that the WIS transports subglacial sediment in the basal ice. This is melted out and deposited at the WGL (Muto et al., 2013), creating a grounding-zone wedge, or a "till delta" (Anandakrishnan et al., 2007). Further, the subglacial sediments found in this area appear to be saturated with ice-water inland of the grounding line (Christianson et al., 2016).

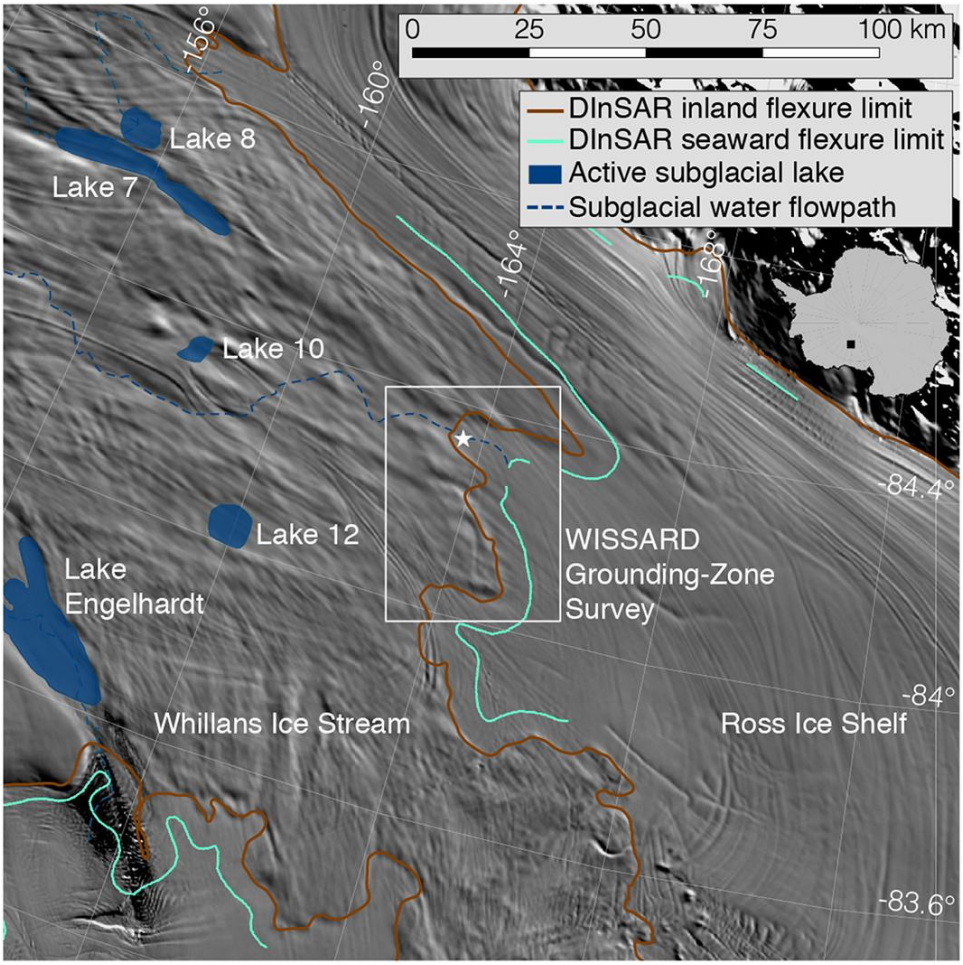

Figure 2-4 Whillans Grounding Zone drill site indicated by white star. Figure from Christianson et al. (2016)

The WGL subglacial environment was accessed by the WISSARD team using the same clean-access technology described above (Section 2.1), with sediment samples collected using UWITEC gravity multi-corer (Figure 2-5A) (as before, Section 2.1), of which an amalgamated fraction (Figure 2-5B) of the sediment cores extracted was used for the experiments described in this thesis. Sediment samples were collected by the WISSARD team at the WGL in mid-January 2015 (Begeman et al., 2017). The WGL subglacial environment had a much deeper water column of 10 m, the water found here was fully marine and had an active community of marine organisms (Scherer et al., 2015).

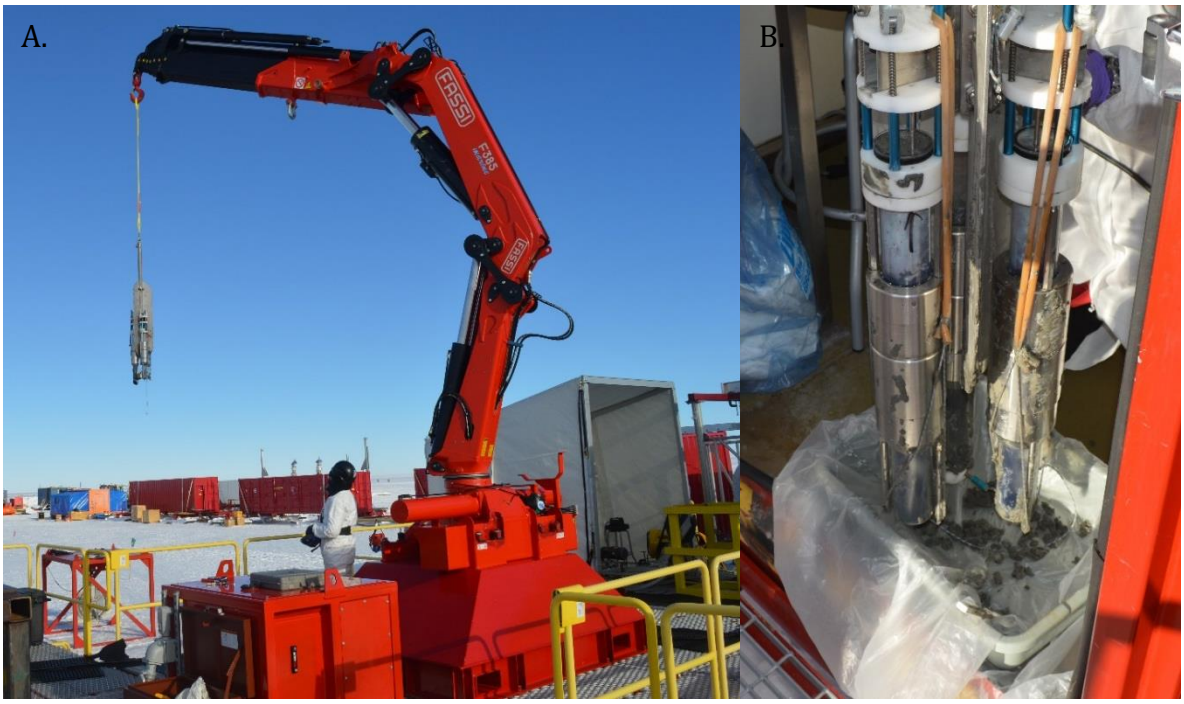

Figure 2-5 A. UWITEC gravity multi-corer in operation at WGL. B. Sediment cores taken at WGL and example of amalgamated sediment used in experiments. (Pictures courtesy of Martyn Tranter)

Chapter 3 Sediment Comminution: A Source of Microbially Relevant Gases

3.1 Introduction

This chapter addresses the first research objective of this thesis (Section 1.4), namely to examine whether or not hydrogen gas is produced during and following the crushing of highly weathered Subglacial Lake Whillans sediment. Laboratory experiments were conducted to determine if crushing of these ancient subglacial sediments would produce bio-utilisable gases, specifically H_2 in the first instance. Sediments from four different depths of a core directly extracted from SLW were crushed. Any bio-utilisable gases, such as H_2, CO_2 and CH_4, released during the initial crushing of the sediments (FIRST-CRUSH) were analysed and quantified. These are likely to have arisen from pore spaces and fluid inclusions in the sediment. Next, either two or three different treatments were carried out on sediment from each depth. These treatments are referred to as DIS-WET (disaggregated and wetted), CRUSH-WET (crushed and wetted), CRUSH-DRY (crushed and left dry).

3.2 Methods

3.2.1 Sample Preparation and Treatment

Sediment samples for four different depths from a Subglacial Lake Whillans core were provided by the Whillans Ice Stream Subglacial Research Drilling (WISSARD) project, by courtesy of Mark Skidmore and John Priscu (Montana State University) and stored at -20^{o}C until used in the experiments. Each depth had a wet mass of between 24 g and 56 g (Appendix A). The weight available for each depth determined the number of treatments that could be carried out on each sample. Samples from the middle two depths had to be combined to allow all treatments to be carried out on them. A list of the sample depths and the treatment of the sediment, described below, can be seen in Table 3-1.

Table 3-1 List of sample depths and treatments to Subglacial Lake Whillans sediments. * = an amalgamation of two depths.

SAMPLE	DEPTH (CM)	CRUSH-WET	DIS-WET	CRUSH-DRY	BLANKS
SLW TOP	0 – 4	✓	--	--	✓
SLW MIDDLE*	14 - 16 and 28 – 30	✓	✓	✓	✓
SLW BOTTOM	36 – 38	✓	✓	--	✓

All samples were oven dried at 75°C (pasteurisation temperature) until a constant weight was reached. Each dried sample was gently disaggregated in a laminar flow hood using a mortar and pestle, previously cleaned with milliQ water and disinfected with 70% ethanol. The sediment was sieved, and the <200 μm fraction was used either as the "disaggregated" control (DIS-WET), or for crushing (FIRST CRUSH, CRUSH-WET and CRUSH-DRY). The "SLW Middle" sample consisted of sediment from two depths (Table 3-1), which were amalgamated, by sieving them together and further mixing the sieved sediment using a clean (rinsed six times with milli-Q water and autoclaved) spatula.

DIS-WET: some 11g of the <200 μm fraction was transferred into a Coy Vinyl Anaerobic Chamber with a zero grade nitrogen atmosphere, and 3 g triplicates were weighed into 25 ml borosilicate serum vials, which had been previously acid washed, rinsed six times with milliQ water and furnaced at 450°C for 4 hours. These were sealed with Belco blue butyl rubber stoppers, which had been previously boiled in 0.1 M NaOH for an hour, rinsed six times with milliQ water, autoclaved and air dried within the laminar flow hood, and crimp sealed. All the vials for each treatment were taken out of the anaerobic chamber and flushed with zero grade N_2 for 2 minutes to remove any trace of atmospheric gases. This was done by piercing the stopper with a needle connected to a zero grade N_2 gas line, and after two seconds piercing it again with another needle, so keeping the positive pressure out of the vial with a continuous N_2 stream for 2 minutes. After this, both needles were removed when the flush of N_2 out of the vial stopped.

All sampling of gas and transfer of water was undertaken by piercing the vial stopper with a needle attached to a gas tight syringe. A headspace sample was taken at the

beginning of each experiment, when all samples were dry, by simultaneously adding 5 ml of zero grade Nitrogen and removing 5 ml of the headspace. Some 4 ml of anoxic water, autoclaved and sparged with zero grade nitrogen for an hour, was added to the vials, and then 4 ml of the vial headspace was removed to keep the atmospheric pressure. Samples were gently shaken for 1 minute to mix the water and the sediment. 5 ml of gas was then removed, simultaneously replacing with zero grade nitrogen. Samples were incubated at 0°C, with further gas samples taken in the same way at after 24 hrs, 48 hrs, 120 hrs, 3 weeks and 6 weeks.

FIRST-CRUSH: another 11 g subsample of the <200 μm fraction was weighed in the laminar flow hood and transferred into a gas tight agate ball mill, together with five agate balls, previously cleaned with 70% ethanol and left to dry in the laminar flow hood. The headspace of the ball mill was flushed for 5 mins with zero grade nitrogen gas before the sediment was milled for 30 minutes at 500 rpm in a Fritsch Planetary Mono Mill Pulverisette 6. The headspace of the ball mill was sampled before and after milling using the valves attached.

CRUSH-DRY: the milled sediment was transferred to the anaerobic chamber, and, as with the disaggregated control, 3 g of sediment was weighed into 25 ml borosilicate serum vials, in triplicate. Three further 25 ml borosilicate vials were also sealed in the anaerobic chamber, to be eventually used as water blanks (**BLANKS**). The vials were sealed with Belco blue butyl rubber stoppers and crimp sealed. A head space gas sample was collected as above (DIS-WET), and at the same times, following the same procedures. However, no water was added to the sediment.

CRUSH-WET: these incubations were the same as CRUSH-DRY, except that 4 ml of anoxic water was added to the sediment, as described in DIS-WET above.

3.2.2 Headspace Analysis

CO_2, CH_4, ethylene (C_2H_4), ethane (C_2H_6), propane (C_3H_8), i-butane (C_4H_{10}) and n-butane (C_4H_{10}) were determined using an Agilent 7890A Gas Chromatograph, fitted with a 0.5 ml sample loop. Helium (He) was used as the carrier gas, passed through a Porapak Q 80-100 mesh, 2.5 m x 1/8 inch x 2 mm SS column and a methaniser, and analysed on a Flame Ionization Detector (FID). He, H_2, O_2 and N_2 were also determined using the Agilent 7890A Gas Chromatograph. However, these gases were analysed using a 1 ml sample loop, with

Argon (Ar) as the carrier gas, a Hayesep D 80–100 mesh, 2 m × 1/8 inch SS column, in series with a molecular sieve 5a, 60–80 mesh, 8ft × 1/8 inch column and a Thermal Conductivity Detector (TCD). The oven temperature was set at 25°C for the initial 4 mins of all analytical runs, and then the temperature ramped up at rate of 50°C min^{-1} until the oven reached a temperature of 200°C. This temperature was maintained for 2.5 mins, when the run was concluded.

The concentrations of headspace gases were calculated based on a 100 ppm Helium 11 gas standard standard-curve (for H_2: 4.1 ppm to 493 ppm, R^2 = 0.9988, n = 6, linear to 493 ppm; for CH_4: 1.6ppm to 195ppm, R^2 = 0.9988, n = 7, linear to 195 ppm). Standards were run daily and gave a coefficient of variation of 1.94% (n = 75) for H_2, with a detection limit of 4 ppm, equivalent to 1.56 nmol g^{-1}, and a coefficient of variation of 7.22% (n = 75) for CH_4, with a detection limit of 0.166 ppm, equivalent to 0.065 nmol g^{-1}. Gas concentrations were then converted to molar concentrations using the ideal gas law, corrected for dilution of gases during sampling and for gases dissolved within the water. The results were also blank corrected and normalised to dry sediment mass. A full description of the steps taken during corrections can be seen in Appendix B.

3.3 Results

3.3.1 FIRST CRUSH

Gases released during crushing were analysed directly after the completion of the milling process (Table 3-2). All gases detected after this initial crush had a relatively high concentration, well above atmospheric concentrations of these gases. Most gasses detected showed broadly similar values of production down the SLW core. The exception is CO_2, which did show large variations. Maximum concentrations were found in both the middle depth runs, which produced almost three times more CO_2 than the bottom layer. The top layer of sediment produced the least CO_2 (only 4.9 nmol g^{-1}), just over a tenth of that produced at the bottom of the core.

Table 3-2. FIRST CRUSH - gases released during the initial crushing of the sediment. Units are normalised to nmol g^{-1}.

SAMPLE	H2	CO_2	CH_4	C_2H_4	C_2H_6
TOP SLW	110	4.9	9.0	2.5	0.26
MIDDLE SLW 1	96	130	13	2.8	0.24
MIDDLE SLW 2	85	120	7.8	1.6	0.18
BOTTOM SLW	110	44	10	3.2	0.33

3.3.2 Hydrogen Production

3.3.2.1 BLANKS

No H_2 was detected (concentration was less than 4ppm) throughout the 40-day incubation for any of the blank control vials (Table 3-3).

3.3.2.2 DIS-WET

Disaggregated samples produced some H_2, ranging from 8.9 to 18 nmol g^{-1} at the end of the time series. About 50% of the H_2 was produced during the first five days of incubation. The H_2 production appeared to stabilise after 23 days (552 hours) of incubation (Figure 3-1).

3.3.2.3 CRUSH-DRY

Crushed dry samples also did not produce any H_2 throughout the 40-day incubation (Figure 3-1), even though H_2 was released during the initial milling (Table 3-2) and was produced from the wetted disaggregated sediment (Figure 3-1). This suggests that the N_2 flushing prior to start of the experiment was successful at removing any H_2 attached to the sediment particles, and that subsequent H_2 production from crushed sediment is dependent on the availability of water.

3.3.2.4 CRUSH-WET

H_2 production occurred rapidly within the first five days. Over 70% of the final concentration was produced during this period, after which the H_2 production slowed down (Figure 3-1). There was a clear distinction in H_2 production from wetted crushed sediment between the top layer and the middle and bottom layers of the core. The top layer produced roughly 59 nmol of H_2 per gram of crushed sediment after a 40-day incubation, whilst the other two core depths produced just over one sixth of this,

producing an average of 11.8 nmol of H_2 per gram of crushed sediment (Figure 3-1). The H_2 concentrations measured in the deeper cores are of the same order of magnitude as values (~20 nmol g^{-1}) found by Telling et al. (2015). It is interesting to note that the crushed and wetted sediment of the middle and bottom depths yielded only slightly higher H_2 concentrations than their disaggregated counterparts, (e.g. at 120 hrs middle CRUSH-WET had produced 8.15 nmol g^{-1} versus the DIS-WET samples which had produced 6.26 nmol g^{-1}; similarly for the bottom depth the CRUSH-WET and DIS-WET samples produced 9.13 and 6.03 nmol g^{-1} respectively (Table 3-3)).

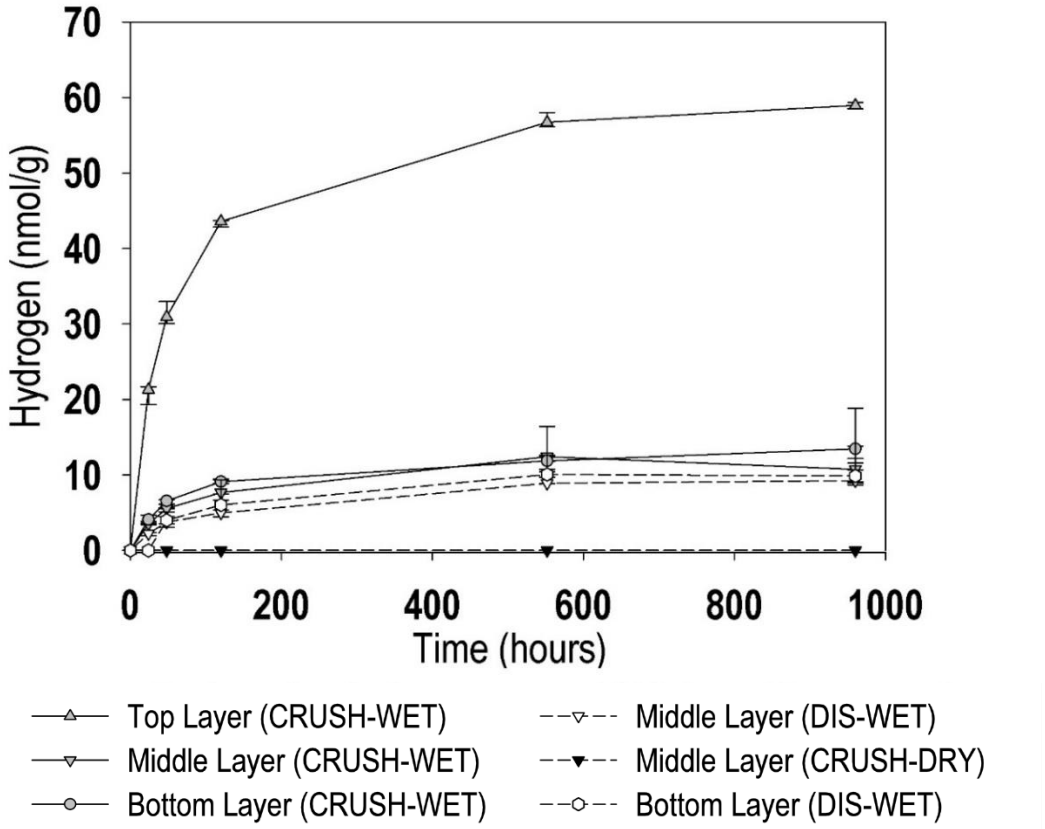

Figure 3-1. Temporal production of H_2 from wetted disaggregated (DIS-WET) and crushed (CRUSH-WET) SLW sediment, versus crushed but unwetted (CRUSH-DRY) sediment. Each point represents the median value, and error bars denote the maximum and minimum concentrations.

Table 3-3. Average temporal production of H_2 from wetted disaggregated (DIS-WET) and crushed (CRUSH-WET) SLW sediment, and crushed but unwetted (CRUSH-DRY) sediment. All samples (except BLANKs) have been blank corrected. Concentrations for BLANK vials were converted to nmol g^{-1} assuming the mean mass of sediment for that depth was in the vial.

TIME POINT (HRS)	TOP CRUSH-WET	MIDDLE CRUSH-WET	MIDDLE DIS-WET	MIDDLE CRUSH-DRY	BOTTOM CRUSH-WET	BOTTOM DIS-WET	BLANK
	Mean H_2 produced (nmol g^{-1})						
0 (DRY)	0.00	0.00	0.00	0.00	0.00	0.00	0.00
0.17	0.00	0.00	0.00	0.00	0.00	0.00	0.00
24	20.8	3.53	2.19	0.00	4.21	0.00	0.00
48	31.3	5.58	3.99	0.00	6.47	4.00	0.00
120	43.4	8.15	6.26	0.00	9.13	6.03	0.00
540	57.0	11.9	11.4	0.00	12.1	10.1	0.00
960	59.0	10.5	12.4	0.00	13.0	9.88	0.00

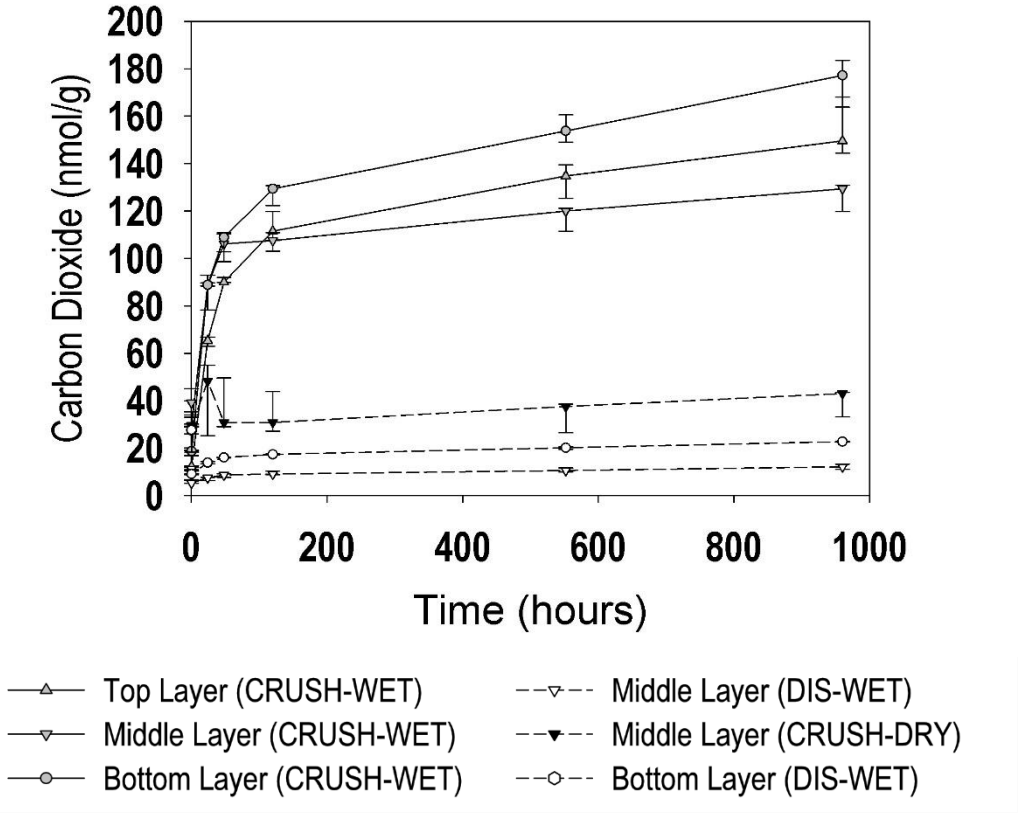

Figure 3-2 Temporal production of CO_2 from wetted disaggregated (DIS-WET) and crushed (CRUSH-WET) SLW sediment, versus crushed but unwetted (CRUSH-DRY) sediment. Each point represents the median value, and error bars are the maximum and minimum concentrations.

Table 3-4. Average temporal production of CO_2 from wetted disaggregated (DIS-WET) and crushed (CRUSH-WET) SLW sediment, and crushed but unwetted (CRUSH-DRY) sediment. All samples (except BLANKs) have been blank corrected. Concentrations for BLANK vials were converted to nmol g^{-1} assuming the mean mass of sediment for that depth was in the vial.

TIME POINT (HRS)	TOP CRUSH-WET	MIDDLE CRUSH-WET	MIDDLE DIS-WET	MIDDLE CRUSH-DRY	BOTTOM CRUSH-WET	BOTTOM DIS-WET	BLANK
	Mean CO_2 produced (nmol g^{-1})						
0 (DRY)	9.90	39.9	9.95	30.8	25.4	27.6	1.60
0.17	11.7	31.3	5.58	26.8	18.2	4.52	5.02
24	65.1	89.0	7.13	42.8	86.6	13.8	7.39
48	90.7	105	8.53	36.5	108	16.0	2.86
120	113	107	9.39	34.0	127	17.3	3.15
540	133	117	10.7	34.2	154	20.1	2.96
960	154	127	12.1	39.9	175	22.7	3.27

3.3.3 Carbon Dioxide Production

3.3.3.1 Blank Controls

There was some CO_2 detected in the blank controls (Table 3-4), but these data are not included in Figure 3-2 because the values (< 2 nmol g^{-1}) were only a fraction of the CO_2 concentrations in the sample vials (Table 3-4).

3.3.3.2 DIS-WET

These sediments produced the least CO_2, with an average of 17.4 nmol g^{-1} at the end of the incubation period (Figure 3-2). The disaggregated samples showed a similar trend to the crushed samples below, albeit producing eight (in the bottom layer) and ten (for the middle layer) times less than their crushed counterparts (Table 3-4).

3.3.3.3 CRUSH-DRY

These sediments produced intermediate CO_2 concentrations (Figure 3-2), giving a final CO_2 concentration of 39.9 nmol g^{-1} (Table 3-4). There was a slow, but constant, increase in CO_2.

3.3.3.4 CRUSH-WET

These wetted, crushed sediment samples yielded most CO_2 during the first 5 days of the incubation and produced a total of between 126 and 270 nmol CO_2/g of crushed sediment at the end of the 40 day incubation period (Table 3-4). The crushed sediments from the top, middle and bottom layers had produced 73%, 85% and 73% of the total CO_2 yielded after five days (Figure 3-2). The CO_2 production slowed down slightly for both the top and bottom crushed layers but continued to increase after the initial five days. The CO_2 production for the middle layer appeared to slow down after 48 hours and was much lower than the other two depths.

3.3.4 Methane Production

3.3.4.1 BLANKS

CH_4 was detected in the blanks. However, the values (Table 3-5) were always ~1/3 lower than the concentration found in sample runs.

3.3.4.2 DIS-WET

These produced less CH_4 than both the crushed treatments, producing only an average of 0.047 nmol g^{-1} after 40 days of incubation (Figure 3-3).

3.3.4.3 CRUSH-DRY

The crushed, unwetted sediment produced methane (0.28 nmol g^{-1} after 40 days, Table 3-5), albeit less than the wet counterpart (Figure 3-3).

3.3.4.4 CRUSH-WET

The wetted crushed sediments released the most CH_4, which showed a similar trend to CO_2 (Figure 3-3). Approximately 50% of the CH_4 for the top and bottom depths was produced within the first 5 days of the incubation. By contrast, only 40% of the CH_4 yielded was produced in the first 5 days for the crushed amalgamated middle depths (Figure 3-3). The incubation was terminated after 40 days, but there is no evidence to suggest that CH_4 generation would have slowed down after this point. The crushed sediment from the top and bottom layers of the SLW core produced almost twice as much CH_4 per gram (1.5 and 1.4 nmol g^{-1} after 40 days respectively) than the middle core (0.83 nmol g^{-1} after 40 days) (Table 3-5).

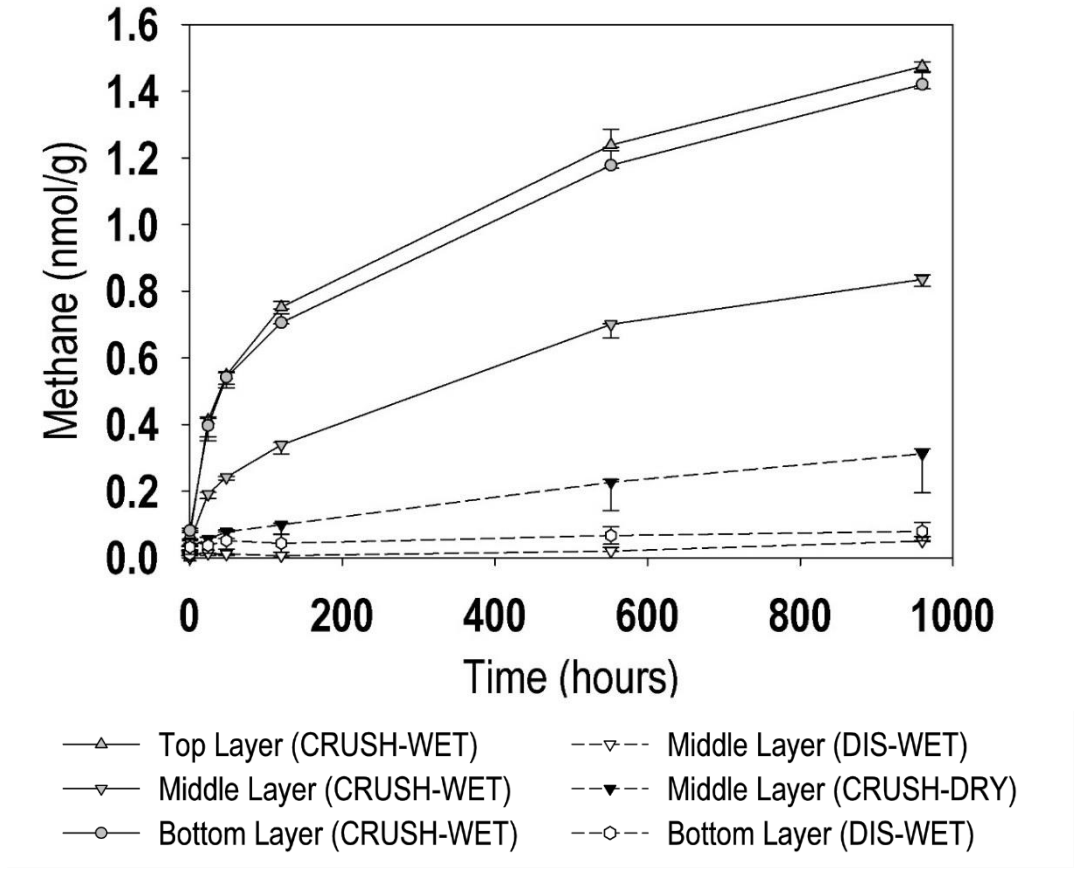

Figure 3-3 Temporal production of CH_4 from wetted disaggregated (DIS-WET) and crushed (CRUSH-WET) SLW sediment, versus crushed but unwetted (CRUSH-DRY) sediment. Point represents median value; error bars are maximum and minimum concentrations.

Table 3-5 Average temporal production of CH_4 from wetted disaggregated (DIS-WET) and crushed (CRUSH-WET) SLW sediment, and crushed but unwetted (CRUSH-DRY) sediment. All samples (except BLANKs) have been blank corrected. Concentrations for BLANK vials were converted to nmol g^{-1} assuming the mean mass of sediment for that depth was in the vial.

TIME POINT (HRS)	TOP CRUSH-WET	MIDDLE CRUSH-WET	MIDDLE DIS-WET	MIDDLE CRUSH-DRY	BOTTOM CRUSH-WET	BOTTOM DIS-WET	BLANK
	Mean CH_4 produced (nmol g^{-1})						
0 (DRY)	0.00	0.03	0.01	0.03	0.02	0.01	0.02
0.17	0.08	0.05	0.01	0.03	0.08	0.03	0.14
24	0.39	0.19	0.01	0.05	0.39	0.04	0.18
48	0.54	0.24	0.01	0.07	0.57	0.05	0.17
120	0.76	0.33	0.01	0.09	0.71	0.04	0.20
540	1.25	0.69	0.02	0.20	1.19	0.07	0.24
960	1.47	0.83	0.05	0.28	1.43	0.08	0.28

3.4 Discussion

3.4.1 First Crush

Gases analysed after the initial dry crush of the sediment revealed that not only was hydrogen released, as Telling et al. (2015) previously suggested, but also CO_2 and a range of hydrocarbons (Table 3-2). H_2 can be released from fluid inclusions (Konnerupmadsen and Rosehansen, 1982), where it is often accompanied by carbon dioxide and hydrocarbons, such as methane and ethane. The presence of these gases after the initial crushing of subglacial sediment serves as evidence supporting fluid inclusions as the main source of these gases to the ball mill headspace. Crushing could have also released gases trapped in inter-grain spaces. The relative proportions of the gases released from fluid inclusions will vary with different lithologies (Konnerupmadsen and Rosehansen, 1982) and the gases themselves will have different isotopic signatures depending on their origin (Potter et al., 2013). However, identifying the precise source of the gases according to gas ratios and isotopic signatures is difficult, due to the complex interactions between different formation processes.

There are other conceivable sources of these gases to the headspace. A possible source of H_2 during crushing of the SLW sediment could be due to surface radicals reacting with any moisture in the atmosphere. The sediment samples were dried prior to crushing, and N_2 gas used as the headspace was passed through a water trap. Therefore, any moisture from this source within the ball mill headspace should be minimal. There could be some water released from ruptured fluid inclusions, which could enhance the H_2 production, as suggested by Takehiro et al. (2011), or even some water produced through prototrophy when clay minerals are crushed (Kameda et al., 2004). However, the possible contribution of H_2O from fluid inclusions is difficult to quantify without knowing the amount of fluid inclusions present and the possible contribution of H_2O as a result of prototropy has not been widely studied, and so is also difficult to quantify. Studies are limited to prototropy in kaolinite during grinding. These studies have suggested an increase in free moisture of 3.9% after 30 mins grinding (G. Miller and Oulton, 1970), however without knowing the mineralogical composition of our samples in detail it is difficult to estimate how much moisture might be available to our samples after crushing.

The presence of CO_2 in the initial crush of the sediment is consistent with the release from ruptured fluid inclusions, but the high variability in results suggests that there are other possible sources. Carbonates in the sediment are a likely control on CO_2 release, and the difference in CO_2 production at different depths could be the result of different carbonate contents. This is partly supported by the increase in bicarbonate concentrations in pore waters below the top 3 cm of the sediment core found by Michaud et al. (2016). The top layer of sediment released significantly less CO_2 than the other two depths, possibly due to the sediment being in contact with the lake waters, dissolving the surface carbonate into the large body of lake water (Figure 3-4). Further, SLW is an active lake (Fricker et al., 2007), so water in equilibrium with solid carbonates will be flushed away, resulting in lower surface carbonate contents. Carbonate preservation, and the potential for calcite precipitation increases down the core, particularly if the sulphate reduction zone is reached and the waters become increasingly supersaturated with respect to calcite (Meister, 2013).

Mechanochemical reactions can also produce CO_2 when mechanical energy is applied to carbonates, as shown by both lab and field observations (Dickinson et al., 1992, Italiano et al., 2008, Martinelli and Plescia, 2004). Therefore, reactivation of calcite through

mechanochemical reactions is a likely source of CO_2 during milling. Furthermore, carbonates are highly soluble, and equilibrate between the liquid and gaseous forms of dissolved CO_2 (Figure 3-4). Thus, if water is created during grinding through prototropy, or any of the processes mentioned previously, this water could react with carbonates and release CO_2. However, as mentioned also previously, due to the limited studies conducted looking at prototropy during crushing, quantifying the contributions from these sources is challenging.

The release of both methane and ethane during the initial sediment crushing is consistent with their release from fluid inclusions (Potter et al., 2013). Ethylene release from fluid inclusions has not been reported to date, however, there are often a number of other hydrocarbons released from fluid inclusions, such as CH_4, C_2H_6, C_3H_8. Therefore, we contend, C_2H_4 release from fluid inclusions would not be unlikely. It is also possible that CH_4 and other hydrocarbons could be released due to either thermal decomposition of organic matter in the sediment or even the Sabatier reaction(Section 1.2.6, Equation 18), where CO_2 and H_2 react to produce CH_4 (Bradley and Summons, 2010). However, this has only been measured at higher temperatures and pressures.

3.4.2 Hydrogen

H_2 was produced during the incubation of both crushed and disaggregated sediments with water, whereas crushed sediments which were left dry did not produce any detectable H_2. This strongly suggests that H_2 produced during the incubations was a result of processes associated with water, other than the slow release of fluid inclusion. Abiotic H_2 production by rock-water interactions has been widely studied in high pressure, high temperature environments (Kita et al., 1982, Takehiro et al., 2011), but their possible contribution to the subglacial environment are limited to one study only, conducted by Telling et al. (2015). Telling et al. (2015) suggested that H_2 could be produced by reactions between H_2O and silicate radicals formed on the surface of freshly crushed, but unweathered, rock (Section 1.2.6, Equation 12). Our H_2 generation time series is consistent with those of the Telling et al. (2015) studies and suggests that surface free radicals also produce H_2 when H_2O reacts with the freshly crushed, highly weathered subglacial sediment found in SLW.

Concentrations of H_2 produced by crushing SLW sediments (Table 3-3) were of the same order of magnitude as found by Telling et al. (2015) and Kita et al. (1982), despite the

highly weathered nature of the sediments and the finer initial particle size. Telling et al. (2015) found an increase in H_2 production associated with longer crushing times; this occurred as a result of the increased surface area and increased molar silica surface area exposed after longer crushing periods. Similar results were expected for these experiments due to the extended crushing of CRUSH-WET samples (30 mins) versus DIS-WET samples (which only experienced a short period of gentle disaggregation using a pestle and mortar) (Figure 3-1). A possible reason for the lack of difference between DIS-WET and CRUSH-WET samples might be due to the nature of the sediments. Subglacial waters originating from large ice bodies such as ice-sheets and glaciers are often characterised by relatively high concentrations of the products of silicate weathering , due to the longer residence times of water (Wadham et al., 2010). This is also true of SLW waters (Michaud et al., 2016). The highly (both physically and chemically) weathered nature of the sediments, together with the already fine nature of subglacial sediments (Table 2-2), is likely to result in only small changes to the molar silicate surface area. The exception is the very top layer of sediment, which might contain less weathered sediment from the melt out and deposition of sediment in the basal layer of ice. These coarser sediments have the potential to increase their molar silicate surface areas upon crushing, unlike the middle and bottom layers, which do not have this comparatively fresh source of sediment.

Despite the middle and bottom cores being finer and more weathered, they still produced significant H_2 concentrations upon crushing. Takehiro et al. (2011) suggested fine grained sediment particles could form chemical bonds, with each other, which produce hydrogen during crushing. It is possible that this source of H_2 is more relevant to deeper sediments, whereas the top layer of sediment has a more important contribution from the reaction of silica free radicals with water.

3.4.3 Carbon Dioxide

Carbon Dioxide was produced by every sample during incubation, although the concentrations varied between treatments and sample depths. CO_2 produced during incubation is likely the result of a number of reactions, where the main control is likely to be the carbonate content of the sediment. Carbonate rock weathering through hydrolysis is a relatively fast and well documented reaction. Carbonate weathering involves equilibrium reactions between carbonate minerals, carbonic acid and CO_2 (Figure 3-4).

Therefore, when a carbonate solid is put into water in a CO_2 free system, a series of reactions will take place until all dissolved, gaseous and solid carbonate are in equilibrium (Figure 3-4). CRUSH-WET samples had higher CO_2 production compared to DIS-WET and CRUSH-DRY samples as a result of the increased surface area, which would be expected from milling the sediment. This has the potential to expose reactive, but previously inaccessible, carbonates to water, causing hydrolysis (Equation 4) and, consequently, CO_2 production (Figure 3-4).

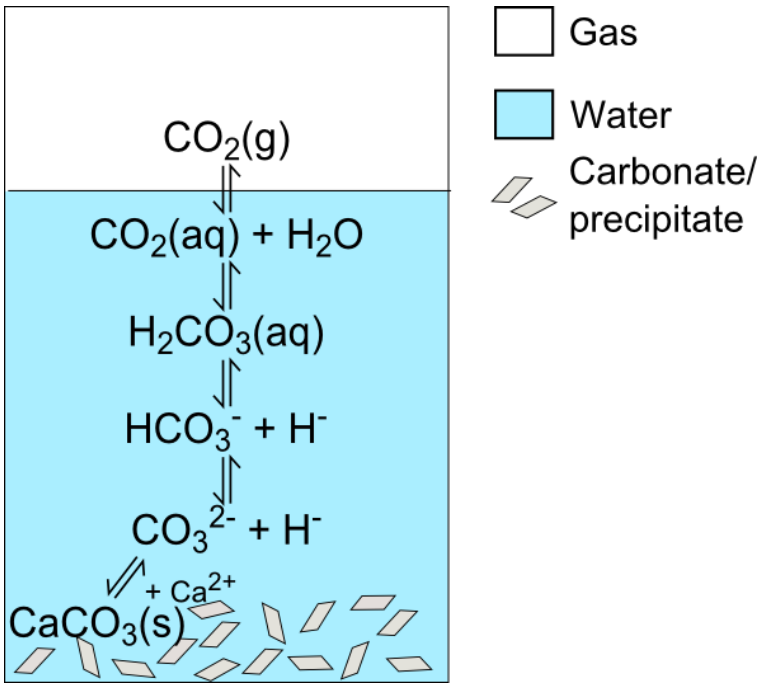

Figure 3-4 Carbonate equilibrium between solid, aqueous and gaseous species

Mechanochemical reactions, as highlighted earlier, could also be an abiotic source of CO_2 to the system, although they are often overlooked. Release of CO_2 as a result of mechanochemical activation of calcite has been studied and widely reported (Beyer and Clausen-Schaumann, 2005), it is often observed and studied in relation to seismic events at active fault zones (Langenhorst and Poirier, 2000, Martinelli and Plescia, 2004) and is likely to take the form of equation 19. This source of CO_2 could explain the CO_2 production that is found in CRUSH-DRY samples, particularly the initial rapid CO_2 production, as this mechanically activated carbonate continues to release CO_2 after the initial crush.

$$CaCO_3 \xrightarrow[\text{energy}]{\text{mechanical}} CaO^- + CO_2\,(g) \qquad (19)$$

Finally, there is a possible contribution to the CO_2 from oxidation of organic matter. Subglacial sediments contain ancient organic matter, and although this material is highly

refractory, crushing may increase its lability (Schillawski and Petsch, 2008). Further, it is likely hydrogen peroxide is formed through the reaction of water with silica radicals and the subsequent pairing of hydroxyl radicals to form H_2O_2 (Chapter 4, Equation 15). H_2O_2 is a powerful oxidising agent, which is capable of oxidising organic matter present in the sediment, and thus could result in the formation of CO_2 (Equation 20, where "CH_2O" represents organic matter).

$$CH_2O + H_2O_2 \rightarrow CO_2 + 3H_2O \qquad (20)$$

3.4.4 Methane

Methane was also released during sediment incubations, as highlighted in Section 3.3.4. The sources and processes of methane formation during crushing are less well understood. The concentrations of methane were much lower than other gases and the rate of production was much more constant. Methane was produced by CRUSH-DRY samples, suggesting there might be some slow release from ruptured fluid inclusions. The increase in CH_4 in wetted samples, however, suggests that slow release from fluid inclusions is not the only source of CH_4. Fischer-Tropsch Type (FTT) reactions (Section 1.2.6, Equation 18) have previously been suggested, which use H_2 and CO_2 to produce CH_4 in high pressure environments (Neubeck et al., 2011). However, both these processes have only been measured at temperatures above 30°C. Further, these reactions require a catalyst, and often this is Fe^{2+} (Jones et al., 2010). Rates of reaction for FTT reactions tend to be slow and steady, producing between 0.1 and 10^{-5} μmol kg^{-1} h^{-1} depending on the carbonate saturation, our rates of production fall in the middle of this range, producing roughly 1.5 x 10^{-3} μmol kg^{-1} h^{-1}.

3.4.5 Subglacial Relevance: Abiotic H_2 and CO_2 sources to sustain methanogenesis

Previous experiments (Telling et al., 2015) concluded that the rates of H_2 production in the first 120 hours after crushed sediment is wetted (H_2 concentrations at end of the experiment were between 4 and 60 nmol g^{-1}) were more than sufficient to maintain the flux (150 nmol H_2 m^{-2} d^{-1}) necessary to sustain rates of methanogenesis in Leverett Glacier, southwest Greenland. The concentrations obtained by crushing of SLW (Figure 3-1) were comparable to the range of values found by Telling et al. (2015), with the top layer CRUSH-WET samples (58.9 nmol g^{-1}) producing similar concentrations to those of the Engabreen schist (~60 nmol g^{-1}) and the middle and bottom CRUSH-WET and DIS-WET sediments (average of 11.4 nmol g^{-1}) producing similar concentrations to the

Leverett gneiss or Ellsworth quartzite (~7.5 nmol g^{-1} and ~10.5 nmol g^{-1}, respectively)(Telling et al., 2015). Thus, crushed SLW sediment could potentially sustain methanogenic bacteria in SLW, or in other areas of the drainage basin where crushing of similar sediment likely occurs. Rates of methanogenesis have not been measured in SLW, but it has been suggested that the CH_4 found in the upper layers of the sediment column underlying SLW is the result of an upwards CH_4 flux. Methanogens have been found in deeper sediment, in support of this assertion (Figure 3-5). However, H_2 and CO_2 sources to sustain this methane flux have not been assessed.

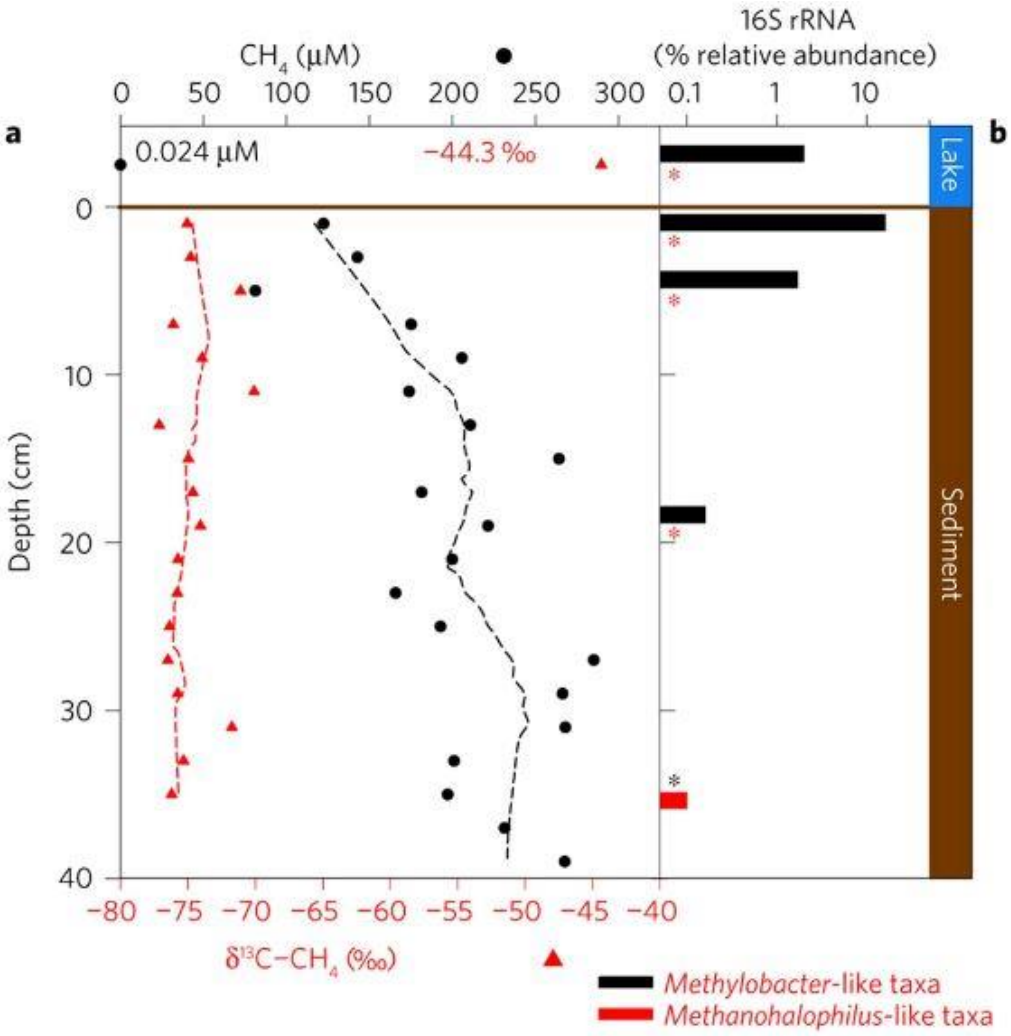

Figure 3-5 Concentration of CH_4, stable isotope composition and abundance of active methanogenic and methane oxidising taxa in the SLW water column and sediment pore waters (Source: Michaud et al. (2017). a) Concentration of CH_4 and values of $\delta^{13}C–CH_4$. Dashed lines represent running averages (calculated using a Loess smoothing function). CH_4 values and stable isotope values for SLW water column are shown next to points. b) Percentage relative abundance of methanogenic and CH_4 oxidising and archeal taxa relative to the 16S r RNA analysis of molecules. Red and black asterisks denote methanogenic and methanotrophic genera were below detection limit, respectively.)

Michaud et al. (2017) estimate a CH_4 flux of 6.8±1.8 (mean ± SE) mmol CH_4 m^{-2} yr^{-1} to the top (0-2cm) layer of the sediment to sustain methanotrophs at this depth. The ratio of H_2:CH_4 is 4:1, given a CO_2 reduction source for the methane (Equation 21). Therefore, 6.8 x 4 or 27.2 mmol H_2 m^{-2} yr^{-1} is required to maintain the annual CH_4 flux by CO_2 reduction.

$$CO_2 + 4H_2 \rightarrow CH_4 + 2H_2O \qquad (21)$$

Little is known about the erosion or comminution of sediments in Subglacial Lake Whillans, but we can calculate how much comminution is required to maintain such an H_2 flux as follows. A single 30 minute crush or gentle disaggregation of sediment produced 21 nmol g^{-1} (top layer) and 2.2 nmol g^{-1} (middle layer), respectively, within 24 hours of wetting and a subsequent 40 day incubation releases a further 38 nmol g^{-1} and 10 nmol g^{-1} of H_2, respectively.

Bulk density of wet sediment for the top 5 cm of SLW sediments was measured as 1.69915 g cm^{-3} (Hodson et al., 2016a). This value was used to calculate the mass of sediment in a 1 m^2 area to a depth of 1cm (16991.5 g). To calculate how much H_2 would be released during the initial crushing of sediment we multiplied the grams of sediment in a m^2 by the number of nmol g^{-1} released during initial crushing (for the top layer 106 nmol g^{-1}; Table 3-2).To calculate how much H_2 could be produced per m^2 after a 40 day incubation of crushed sediment with water, the final nmol g^{-1} of H_2 in the top layer of sediment (CRUSH-WET H_2 production in the top layer of sediment after a 40 day incubation: 59 nmol g^{-1}; Table 3-2) was multiplied by the grams of sediment in a m^2. Therefore, a single 30 minute crushing event in the top 1 cm of sediment has the potential to produce 1.8 mmol m^{-2} during crushing and a further 1.0 mmol m^{-2} after a subsequent 40 day incubation. This, in total, accounts for 2.8 mmol or just over 10% of the ~27.2 mmol m^{-2} required to sustain the methane flux in SLW (Michaud et al., 2017). We would therefore require either ten 30 minute crushing events, a more prolonged sustained period of crushing, or erosion to extend to the top 10 cm of sediment to sustain measured methane fluxes in SLW (Michaud et al., 2017).

The sources of CO_2 to the system will be more extensive, and therefore are unlikely to limit CH_4 production. DIC measured in situ was of 2.11 mmol L^{-1} (Christner et al., 2014) in the lake waters and the bicarbonate concentration in the top sediment depth was of 3.2 mmol L^{-1} and increased down the core (Michaud et al., 2016). Both the lake waters or

the porewaters could therefore provide sufficient CO_2 for the production of CH_4. Finally, crushing of sediments during erosion and the subsequent reaction of these sediments with water will also produce some CO_2. The CO_2 released to this system by crushing can be crudely estimated following the same calculations as for H_2.

Wet bulk density of SLW was used as before (1.69915 g cm^{-3}, Hodson et al. (2016a)) to calculate the mass of a 1 m^2 area (16991.5 g). Then to calculate the CO_2 produced during crushing, this mass was multiplied by the of nmol of CO_2 g^{-1} released during initial crushing (for the top layer 4.9 nmol g^{-1}; Table 3-2). To calculate CO_2 production per m^2 after a 40 day incubation of crushed sediment with water, the final nmol of CO_2 g^{-1} in the top layer of sediment (CRUSH-WET CO_2 after a 40 day incubation: 154 nmol g^{-1}; Table 3-2) was multiplied by the grams of sediment in a m^2. A single 30 minute crushing event in the top 1 cm of sediment has the potential to produce 84 µmol m^{-2} during crushing and a further 2.6 mmol m^{-2} after a subsequent 40 day incubation. The CH_4:CO_2 ratio is 1:1 (Equation 21) for CH_4 production, thus this single crushing event and subsequent incubation, alone, has the potential to just over one third of the CO_2 required to sustain the methane flux in SLW (Michaud et al., 2017). Three further crushing events and incubations or crushing over the top 3 cm of the core could provide the system with enough CO_2.

Analysis of micro-fabrics and micro-structures within the SLW core indicates that there is ductile deformation with shear under low basal pressure and little erosion (Hodson et al., 2016b). Although further experiments would be necessary to constrain the potential H_2 and CO_2 produced under these conditions, our results indicate that even after gentle disaggregation SLW sediments can produce significant amounts of these gases. Middle depth DIS-WET samples produced 37 µmol H_2 m^{-1} and 121 µmol CO_2 m^{-1} within 24 hours and a further 173 µmol H_2 m^{-1} and 85 µmol CO_2 m^{-1} after a 40 day incubation. A single gentle disaggregation event and subsequent incubation of the top 1 cm SLW sediment can provide the system with just under 1% and 3% of the required H_2 and CO_2, respectively. Thus, for disaggregation to account for the CH_4 flux measured, it would have to occur over a depth and the process would have to occur repeatedly or for a prolonged time. Additionally, these values might be further underestimated by disregarding any pre-existing gases trapped in inter-grain spaces which would be released during the disaggregation process.

Erosion in subglacial environments, particularly in warm based glaciers, is primarily in the form of abrasion (Benn and Evans, 2010a). This includes a range of forms of abrasion from large scale erosion in the form of freeze-on debris in basal ice, to smaller scale erosion when sediment particles abrade against each other. Although erosion within subglacial lake Whillans might not be enough to incise channels into the bed, it is enough to move silt sized particles (Hodson et al., 2016b). Some level of erosion, even if very gentle, is likely to be occurring during filling and, particularly, draining events as particles abrade each other during transportation. It is difficult to know exactly how much abrasion occurs in situ, but it becomes more likely that erosion will become more relevant during large draining events.

During these draining events, more abrasion is likely to occur in the lake margins, as the ice starts to sink and makes contact with the basal sediment. In 2004, when the lake is believed to have drained almost entirely and the ice stream was grounded over the entirety of the lake bed (Hodson et al., 2016b), a considerable amount of erosion could have occurred as large portions of the basal ice came into contact with the surface sediments of the lake. This could provide the subglacial environment with large amounts of bio-available gases. These draining events, albeit not to this extent, occur on a semi regular basis. Between 2004 and SLW sampling in 2013, two fill-and-drain events occurred, each lasting approximately 2 years (Hodson et al., 2016b). During the periods when the ice is grounded on the lake margins and lake bed, erosion is unlikely to be limited to the top 1 cm of the sediment, therefore the numbers presented earlier greatly underestimate how much gas could be produced per m^2 during these periods. Erosion could be potentially providing this ecosystem with a cyclical energy source that sustains the microbiome. However, further experiments are required to quantify the effect of ductile deformation with shear in subglacial sediments, particularly over longer periods of erosion during drain-and-fill events and during periods where the ice stream is mostly grounded, such as 2004 (Hodson et al., 2016b).

Maybe even more importantly, SLW is part of a continuous drainage system (Fricker and Scambos, 2009). SLW not only receives water from the upper Whillans Ice Stream (WIS), but also is believed to be supplied with water from both the Kamb Ice Stream (KIS)(Carter et al., 2013) and the Mercer Ice Stream (MIS) (Fricker and Scambos, 2009), funnelling any products of erosion from further upstream. This water piracy from other ice streams has

increased the filling rate of SLW and has the potential to bring with it dissolved gases such as H_2, CO_2 and CH_4, which could account for the difference in CH_4 flux estimated by Michaud et al. (2017) and the potential abiotic CH_4 production measured here.

3.5 Conclusions

SLW sediments, although highly weathered, have the potential to produce a range of microbially relevant gases both during crushing and subsequent rock-water reactions. Quantifying to what extent this is occurring in SLW is difficult due to the rather limited nature of the data at this time. However, relatively little erosion is necessary to produce these gases, and taking into account the interconnectedness of the hydrological system of which SLW is part of, it is not unlikely that abiotic processes might be contributing bio-utilisable compounds to the microbial ecosystem.

Chapter 4 Investigating Mechanisms of Gas Production

4.1 Introduction

This chapter addresses the second research objective (Section 1.4), and attempts to examine the mechanisms by which bio-utilisable gases were produced during crushing of subglacial sediments. This chapter describes some of the additional techniques and tests carried out in an attempt to unravel the possible sources of gases produced after crushing (Chapter 3), including some experiments which did not return any results. Previous studies have suggested free radical reactions as an abiotic H_2 source, and this chapter attempts to show this is also the case for SLW samples. Further, we attempt to confirm our hypothesis that hydroxyl radicals are also formed during crushing. Other possible sources for H_2 are suggested, and possible sources of CH_4 are investigated through the use of isotopic analysis of gases and through additional experimental incubations.

4.2 Methods

4.2.1 Silica radicals

The production of silica radicals by the crushed and disaggregated sediments was measured by the use of 2,2-diphenyl-1-picrylhydrazyl (DPPH), a radical scavenger, based on the methods in Damm and Peukert (2009). The DPPH solution was prepared by dispersing 50 mg of DPPH in 1 litre of ethanol. The absorption of the solution was measured at 515 nm using a Shimadzu UV min 1240 UV-VIS spectrophotometer. Ethanol was used to dilute the solution to an absorbance close to 1 at this wavelength. 0.01 g of sample was weighed into serum vials under a grade zero N_2 atmosphere, and the vials were then crimped shut. 5 ml of DPPH was injected into the vials and allowed to react for one minute. The solution was transferred into centrifuge tubes, and centrifuged for 10 minutes at 4500 rpm. The solution was decanted into 1cm path length plastic cuvettes and measured using the Shimadzu UV min 1240 UV-VIS spectrophotometer.

4.2.2 Hydroxyl Radicals

A number of methods were used in attempts to measure hydroxyl radicals (·OH) formed in solution. These experiments were all tested using crushed pyrite, a mineral well known for its ability to produce ·OH.

4.2.2.1 Phenol Spectrophotometric method (Borda et al., 2003)

This method measures the concentration of phenol produced when benzene reacts with ·OH as a proxy for the concentration of ·OH. Approximately 10 g of pyrite was ground under a grade 5.0 Argon anoxic atmosphere using a Fritsch Planetary Mono Mill Pulverisette 6.0. Some 0.35 g of pyrite was then weighed out into vials inside a Coy Vinyl Anaerobic Chamber with a 97%N_2/ 3%H_2 atmosphere and a palladium catalyst. They were sealed until the commencement of the experiment. To begin the experiment, the contents of the vials were mixed with 100 ml of 1 mM benzene solution and allowed to react for 1 minute. The solution was then filtered and the phenol produced was analysed using an adapted version of US EPA Method 420.1 (chloroform extraction method). This involved the filtrate being transferred into a 125 ml separatory funnel, 2 ml of a pH 10 buffer (consisting of 16.9 g of NH_4Cl dissolved with 143 ml of concentrated NH_4OH and diluted to 150ml with milliQ water) was added and mixed. Subsequently 0.6 ml of 2% (w/v) aminoantipyrine solution was added and mixed, then 0.6 ml of 8% (w/v) potassium ferricyanide solution was added and mixed in with the solution. Finally, 5 ml of chloroform were drained into quartz cuvettes and measured against a blank at 460 nm.

4.2.2.2 Spectrofluorometer method (Cohn et al., 2009)

The concentration of highly reactive oxygen species (hROS), with particular focus on hydroxyl radicals, was measured using 3'-(p-Aminophenyl) fluorescein (APF), as described by Cohn et al. (2009). A calibration curve was produced using known concentrations of hydrogen peroxide (Analar NORMAPUR® analytical Reagent from VWR International) with 5.9 units/ml type II horseradish peroxidase (HRP) (from Sigma-Aldrich). 1 ml of this solution was pipetted into a 2 ml microcentrifuge tube, together with 10 uM APF (from Santa Cruz biotechnology), which had been previously dissolved in a 50 mM potassium phosphate buffer at pH 7.4 as suggested by the suppliers.

The tubes were closed, covered in tinfoil and placed in an end-over-end rotator for 24 hours. The solutions were next transferred into a 4 ml methycrylate fluorescence cuvette and the fluorescence was measured using either the Cary Eclipse Fluorescence Spectrophotometer (Agilent Technologies) or the Fluorolog 3 Spectrofluorometer (Horiba) with excitation and emission wavelengths set at 490 nm and 520 nm respectively. This calibration curve was then used to calculate the concentration of hROS in terms of "hROS reactivity (uM H_2O_2)".

For the determination of hydroxyl radicals produced from mineral comminution, the crushed pyrite was weighed into a 2 ml centrifuge tube. The sediment loading used for each sample varied depending on the expected surface area of the pyrite (0.5 g L^{-1} for pyrite crushed for 30 mins and 5.0 g L^{-1} for sample crushed for 2 mins). To the crushed sediment the following were added: 1 ml of ultra pure water, and 10 uM APF dissolved in a 50 mM potassium phosphate buffer at pH 7.4. The tubes were then closed covered in tinfoil to avoid UV-degradation and placed in an end-over-end rotator for 24 hours. The suspensions were then filtered using PVDF 0.45µm syringe filters and measured using the spectrofluorometer. For the determination of hROS produced under anoxic conditions, the sediment was crushed under an Ar environment before being transferred into an anaerobic chamber with an atmosphere of 97% N_2 and 3% H_2 with a palladium catalyst. The crushed rock was weighed into the microcentrifuge tubes within the anaerobic chamber. The solutions that were added to these samples were first autoclaved and then bubbled with Ar for over 30 mins to remove any O_2. The microcentrifuge tubes were then transferred into glass tubes which were stoppered with a rubber bung to maintain the anaerobic atmosphere and transferred onto the end-over-end rotator for 24 hours. After this, the samples were transferred back into the anaerobic chamber where they were filtered and transferred into the methycrylate cuvettes. These were covered with Parafilm M before taking them out of the anaerobic chamber and measuring their fluorescence.

4.2.2.3 Phenol HPLC method

A last attempt at measuring ·OH was conducted. This was again based on the phenol produced when benzene reacts with ·OH (Section 4.2.2.1). However, in this case phenol would be quantified using HPLC.

4.2.3 Hydrogen Peroxide

4.2.3.1 Ammonium molybdate method (Graf and Penniston, 1980)

An alternative method to measure H_2O_2, is based on the oxidation of iodide in contact with ammonium molybdate, and the subsequent photometric analysis of the blue starch-iodine complex (Graf and Penniston (1980)). To test the method, as before, pyrite was used as it is a well-known source of H_2O_2. Some 10 g of pyrite were crushed for 30 mins at 500 rpm under a zero grade N_2 atmosphere in a pulverissette mono mill. The ball mill was transferred into the Coy Vinyl Anaerobic Chamber, which was also filled with zero

grade N_2 gas. Here, 0.5 g of freshly ground pyrite were weighed into microcentrifuge tubes and 0.5 ml of anoxic water (previously autoclaved and bubbled with zero grade N_2 for 1hour at 0^{o}C). The tubes were sealed and vortexed, then sediment was allowed to react with the water for 5 mins. After this, the tubes were centrifuged at 4500 rpm for 10 mins. 10 µL of the supernatant solution was pipetted into a 15 ml centrifuge tube, to which 2 ml of 50 mM HCl (analar solution), 0.2 ml of 1 M KI and 0.2 ml of 1 mM ammonium molybdate in 0.5 M H_2SO_4 was added and vortexed. The solution was then left to stand for 20 mins before 0.2 ml of the 50 g L^{-1} starch solution was added. After this, the solution was transferred into a 2 ml cuvette and the absorbance was measured at 570 nm using the UV-VIS mini spectrophotometer.

4.2.3.2 DMP method (Baga et al., 1988)

The concentration of H_2O_2 formed during the reaction of crushed and disaggregated sediments with water was measured using neocuprine (2,9-Dimethyl-1,10-phenanthroline from Sigma-Aldrich), based on the method used by Baga et al. (1988), which was later used in Borda et al. (2001). A set of standards was prepared using known concentrations of H_2O_2 (Analar NORMAPUR® analytical Reagent from VWR International). For the standard calibration, 3 ml of each standard was pipetted into a 10 ml volumetric, and to this, 1 ml of 0.01 M Copper (II) Sulphate, and 1ml of neocuprine solution (10 g L^{-1} in ethanol) were added. The solution was then made up to 10 ml with milliQ water and the absorbance of the solution was measured at 454 nm using the Shimadzu UV min 1240 UV-VIS spectrophotometer. To determine the concentration of H_2O_2 concentration in mineral samples, 0.01 g of crushed mineral were weighed into serum bottles under a grade zero N_2 atmosphere, these were then sealed and crimped shut. Then 5 ml of anoxic water (which had been autoclaved and sparged with grade zero N_2 for 1 hour) was added into the serum bottles. The suspensions were shaken for a minute then filtered using 0.45 µm Puradisc 25PP inline filters. 3 ml of the filtrate was then analysed in the same way as the standards.

4.2.4 FTT and Serpentinization Incubations

4.2.4.1 Sample preparation

FTT/serpentinization experiments were set up much in the same way as gas analysis experiments (Section 3.2.1), however two sources of Fe were tested as possible catalysts for FTT/serpentinization reactions: pyrite and $FeSO_4$ (Table 4-1). Whillans Grounding

Line (GLW) sediments were provided by the Whillans Ice Stream Subglacial Research Drilling (WISSARD) project, by courtesy of Mark Skidmore and John Priscu (Montana State University) and stored at -20°C until used in the experiments. Samples were oven dried overnight at 75°C, once dry, sediments were gently disaggregated in a laminar flow hood using a mortar and pestle, previously cleaned with milliQ water and disinfected with 70% ethanol. The sediment was sieved, and the <200 µm fraction was used for crushing.

Table 4-1 Incubation treatments to test possible FTT reactions as a source of CH_4.

Sample ID	Crushed GLW	Pyrite	$FeSO_4$
GLW	✓		
GLW_Pyr	✓	✓	
GLW_$FeSO_4$	✓		✓
Blank_Pyr		✓	
Blank_$FeSO_4$			✓

An 11 g subsample of the <200 µm fraction was weighed in the laminar flow hood and transferred into a gas tight agate ball mill, together with five agate balls, previously cleaned with 70% ethanol and left to dry in the laminar flow hood. The headspace of the ball mill was flushed for 5 mins with zero grade N_2 gas before the sediment was milled for 30 minutes at 500 rpm in a Fritsch Planetary Mono Mill Pulverisette 6. The headspace of the ball mill was sampled before and after milling. The milled sediment was transferred to the anaerobic chamber, and transferred into a 120 ml borosilicate serum vial, which had been previously acid washed, rinsed six times with milliQ water and furnaced at 450°C for 4 hours. This process was repeated three times, after which the sediments in the borosilicate vial were homogenised by rotating and mixing sediment within the serum vial.

Pyrite (provided by geologysupermarket.com), which had been previously wrapped in thick polyethylene bags and reduced in size using a sledgehammer and plate, which had been cleaned using 100% ethanol, was sieved and the <200 µm fraction was used for crushing. A 10 g subsample of the <200 µm fraction was weighed in the laminar flow hood and transferred into a gas tight agate ball mill, together with five agate balls, previously cleaned with 70% ethanol and left to dry in the laminar flow hood. The headspace of the

ball mill was flushed for 5 mins with zero grade N_2 gas before the sediment was milled for 30 minutes at 500 rpm in a Fritsch Planetary Mono Mill Pulverisette 6. The headspace of the ball mill was sampled before and after milling. The milled sediment was transferred to the anaerobic chamber, into a clean 25 ml borosilicate vial.

GLW: 3 g of sediment were weighed in triplicate into 25 ml borosilicate serum vials, which had been previously acid washed, rinsed six times with milliQ water and furnaced at 450°C for 4 hours. These were sealed with Belco blue butyl rubber stoppers, which had been previously boiled in 0.1M NaOH for an hour, rinsed six times with milliQ water, autoclaved and air dried within the laminar flow hood, and crimp sealed. All the vials for each treatment were taken out of the anaerobic chamber and flushed with zero grade N_2 for 2 minutes to remove any trace of atmospheric gases. This was done by piercing the stopper with a needle connected to a zero grade N_2 gas line, and after two seconds piercing it again with another needle, so keeping the positive pressure out of the vial with a continuous N_2 stream for 2 minutes. After this, both needles were removed when the flush of N_2 out of the vial stopped.

GLW_Pyr: As before, 3 g of sediment were weighed in triplicate into 25 ml borosilicate serum vials, to which 0.006g of pyrite was added, before sealing the vials with Belco blue butyl rubber stoppers and crimping them shut. Vials were then were taken out of the anaerobic chamber and flushed with zero grade N_2 for 2 minutes.

GLW_$FeSO_4$: Again, 3 g of sediment were weighed in triplicate into 25 ml borosilicate serum vials, to which 0.012g of $FeSO_4$ was added, before sealing the vials with Belco blue butyl rubber stoppers and crimping them shut. Vials were then were taken out of the anaerobic chamber and flushed with zero grade nitrogen for 2 minutes.

Blank_Pyr: Here, 0.006 g of pyrite was added to a 25 ml borosilicate serum vials in triplicates, before sealing the vials with Belco blue butyl rubber stoppers and crimping them shut. Vials were then were taken out of the anaerobic chamber and flushed with zero grade nitrogen for 2 minutes.

Blank_$FeSO_4$: 0.012 g of $FeSO_4$ were added to 25 ml borosilicate serum vials in triplicates, before sealing the vials with Belco blue butyl rubber stoppers and crimping them shut. Vials were then were taken out of the anaerobic chamber and flushed with zero grade N_2 for 2 minutes.

4.2.4.2 Gas sampling and analysis

Gas samples were taken before wetting (time = 0) as described in Section 3.2.2. Then, 4 ml of water, previously autoclaved and sparged with zero grade N_2 for at least 30mins, were added to the vial and 4 ml of headspace were removed. After 2 minutes, the headspace was sampled as described before. Subsequent headspace sampling occurred after 24 hours, 48 hours and120 hours. Additional sampling also took place after 26 days, 41 days and 3 months for GLW samples and after 41 days for GLW_Pyr. Gas analysis was carried out in the same way as described in Chapter 3 (Section 3.2.2), using an Agilent 7890A Gas Chromatograph. As before, gas concentrations were converted to molar concentrations using the ideal gas law, corrected for dilution of gases during sampling and for gases dissolved within the water. The results were also blank corrected (using their corresponding blank, or Blank_Pyr for GLW) and normalised to dry sediment mass. A full description of these corrections can be found in Appendix B.

4.2.5 Isotopic Composition

4.2.5.1 Sample Preparation and Incubation

Subglacial Lake Whillans (SL) sediments and Whillans Grounding Line sediments (GL) (provided by the Whillans Ice Stream Subglacial Research Drilling (WISSARD)) were prepared in a laminar flow hood and dried overnight at 75°C (until a constant mass was reached). The dried samples were then disaggregated using a mortar and pestle (previously rinsed six times with milliQ water and then disinfected with 70% ethanol). The sediment was sieved and an 11 g subsample of particles below 200 μm was weighed in the laminar flow hood and transferred into a ball mill (previously disinfected with 70% ethanol and left to dry in a laminar flow hood). The sediment was flushed with zero grade N_2 for 5 mins, within the ball mill, and then milled for 30 minutes at 500 rpm under zero grade N_2 in a gas tight agate ball mill, adapted with two valves for gas sampling, in a Fritsch Planetary Mono Mill Pulverisette 6. Before and after milling, a 1 ml gas aliquot was taken by injecting the same volume of zero grade N_2 into the ball mill as was then taken by the subsample using a gas-tight syringe. This gas sample was analysed using the Varian 3800 GC (by Varian inc.(Palo Alto, CA, USA)) fitted with a HayeSesp T column and 6' x 1/8", 80/100 mesh to get an estimate of CH_4 and CO_2 concentration. Subsequently three 12 ml gas samples were taken following the same method as before and transferred into 12 ml exetainers to be shipped for isotopic analysis. A final subsample of 6 ml was

then injected into a 3.7 ml exetainer for VOC analysis. Sediment was then transported to a Coy Vinyl Anaerobic Chamber with a zero grade N_2 atmosphere and transferred into a large borosilicate serum vial (which had been previously acid washed, rinsed 6 times with milliQ water and furnaced at 450°C for 4 hours) and covered with tinfoil. This procedure was then repeated three times for both the SLW and the GLW samples.

The sediments from all three triplicate crushes for each sediment sample were amalgamated and three 10 g subsamples were weighed into 60 ml borosilicate serum vials (which had been previously acid washed, rinsed 6 times with milliQ water and furnaced at 450°C for 4 hours). The vials were sealed with new grey butyl rubber stoppers (which had been rinsed 6 times with milliQ water, autoclaved and air dried within the laminar flow hood), and crimp sealed. In addition to the sediment samples, three empty vials were prepared in the same way as experimental controls. The headspace in the vials was flushed with zero grade N_2 for 4 mins to remove any trace of atmospheric gases. Then, using a syringe and needle, 12 ml of anoxic water (autoclaved and sparged with zero grade N_2 for an hour) was added to the vials. Samples were gently shaken for 1 min to mix the water and the sediment and were incubated at 0^oC for 21 days, with occasional shaking to ensure the sediment continued to react with the water. Following this incubation, three 12 ml gas samples were taken as before and transferred into 12 ml exetainers for shipping for isotopic analysis and again a 6 ml subsample was also injected into a 3.7 ml exetainer for VOC analysis.

4.2.5.2 Sample analysis (by the Stable Isotope Facility (SIF), UC Davis)

Isotopic analysis of $\delta^{13}C$ in CO_2 and CH_4, and $\delta^{2}H$ in CH_4 in gas samples was performed by the Stable Isotope Facility (SIF) at UC Davis. A ThermoScientific GasBench system interfaced to a ThermoScientific Delta V Plus isotope ratio mass spectrometer (ThermoScientific, Bremen, Germany) was used to measure $\delta^{13}C$ ratios in CO_2. CO_2 was sampled by a six-port rotary valve (Valco, Houston TX) with either a 100 µL, 50 µL, or 10 µL loop programmed to switch at the maximum CO_2 concentration in the He carrier gas. The CO_2 is then separated from any residual gases (such as N_2O) by a Poroplot Q GC column (25 m x 0.32 mm ID, 45°C, 2.5 mL/min (UC Davis Stable Isotope Facility, 2018a). A pure reference gas (CO_2) was used to calculate provisional delta values of the sample peak (UC Davis Stable Isotope Facility, 2018a). The final $\delta^{13}C$ values were calculated by adjusting the provisional values for changes in linearity and instrumental drift, such that

correct $\delta^{13}C$ values for laboratory reference materials are obtained (UC Davis Stable Isotope Facility, 2018a). A minimum of two laboratory reference materials were analysed with every ten samples (UC Davis Stable Isotope Facility, 2018a). Laboratory reference materials were calibrated directly against NIST 8545, and the final $\delta^{13}C$ values were reported relative to the international standard V-PDB (Vienna PeeDee Belemnite) (UC Davis Stable Isotope Facility, 2018a).

For the analysis of $\delta^{13}C$ and $\delta^{2}H$ isotopic ratios in CH_4, a ThermoScientific Precon concentration unit interfaced to a ThermoScientific Delta V Plus isotope ratio mass spectrometer (ThermoScientific, Bremen, Germany) was used (UC Davis Stable Isotope Facility, 2018b). Gas samples were purged from exetainers through a double-needle sampler into a He carrier stream (20 mL/min), which is passed through a H_2O / CO_2 scrubber ($Mg(ClO_4)_2$, Ascarite) and a cold trap (90 cm piece of coiled divinylbenzene 0.32 mm GS-Q column) cooled by liquid N_2 (Yarnes, 2013). CH_4 and residual gases are separated from each other by a GS-CarbonPLOT GC column (30 m x 0.32 mm x 3 µm, 30°C, 1.5 mL/min) (Yarnes, 2013). After CH_4 emerges from the column, one of two processes will occur, depending on the isotope being analysed: CH_4 was either oxidised to CO_2 by reaction with nickel oxide at 1000°C (for $\delta^{13}C$), or it was pyrolyzed in an empty alumina tube then heated to 1400°C ($\delta^{2}H$) and subsequently transferred to the IRMS (Yarnes, 2013). As before, a pure reference gas (either CO_2 or H_2) was used to calculate provisional delta values, and the final δ-values were obtained after adjusting the provisional values for changes in linearity and instrumental drift so that correct δ-values for laboratory reference materials were obtained (Yarnes, 2013). Laboratory reference materials was commercially prepared CH_4 gas diluted in He or air, which was then calibrated against NIST 8559, 8560, and 8561. Final δ-values were reported relative to the international standards V-PDB (Vienna PeeDee Belemnite) for carbon and V-SMOW (Vienna-Standard Mean Ocean Water) for hydrogen (Yarnes, 2013).

4.3 Results

4.3.1 Radicals and Hydrogen Peroxide

Significant amounts of silica radicals (Si·) were measured after crushing of Subglacial Lake Whillans (SLW) sediments in a ball mill for 30 minutes. There was a noticeable decrease in radical production per gram of crushed sediment down the sediment core, going from 8.64 µmol/g of sediment, in the top layer of sediment, to 7.16 µmol/g of

sediment, in the lowermost depth (Table 4-2). This trend was not observed in the disaggregated sediment, probably due to the less homogeneous nature of the sample preparation (Table 4-2). However, it is important to note that there were still significant concentrations of Si· produced by disaggregating sediment (Table 4-2), with concentrations of the same order of magnitude as those found by Telling et al. (2015).

Unfortunately, none of the hydroxyl radial methods were successful. The spectrophotometric method was highly labour intensive and time consuming, and after several attempts at measuring standards, the method was deemed to be too convoluted to be practical. Even more importantly, results were always inconsistent. The fluorometric method provided us with a good and reliable standard curve (Appendix C) when using the Fluorolog3 to make the measurements, despite fluorescence intensities varying from day to day, the R^2 was consistently above 0.998. However, when the concentrations of ·OH was attempted to be measured, despite a clear increase between samples and blanks, they both consistently appeared below 0 µM standard point.

The Fluorolog3 ceased to work during the method development, and attempts were made to measure the same standard curves using the Cary Eclipse Fluorescence Spectrophotometer (Agilent Technologies). Here too, the fluorescence intensities were always variable, and unsuitable to obtain quantitative data.

Table 4-2 Average surface free radical ("Si Radicals") concentrations and H_2O_2 concentrations after 1 min reaction time of crushed and disaggregated SLW samples.

DEPTH (cm)	TREATMENT	"Si radicals" (µmol/g)	H_2O_2 (µmol/g)
2	**Crushed**	**8.64**	**16.9**
2	Disaggregated	1.22	5.15
22	**Crushed**	**7.83**	**13.4**
22	Disaggregated	1.96	3.56
37	**Crushed**	**7.16**	**14.1**
37	Disaggregated	1.49	3.87

4.3.2 FTT and Serpentinization Incubations

Analysis of CH_4 in the headspace of the sediment incubations during the initial 120 hours of incubation appeared to be relatively similar between treatments (Figure 4-1), reaching an average concentration of 0.32 nmol g^{-1} (Table 4-3). As with previous readings (Section 3.3.4) the methane concentration continued to increase after these first 120 hours (Figure 4-1), reaching a concentration of 0.928 nmol g^{-1} in GLW samples (Table 4-3). GLW_Pyr samples also increased, and after the three month incubation had overtaken GLW measurements (Figure 4-1), reaching a concentration of 1.12 nmol g^{-1} (Table 4-3).

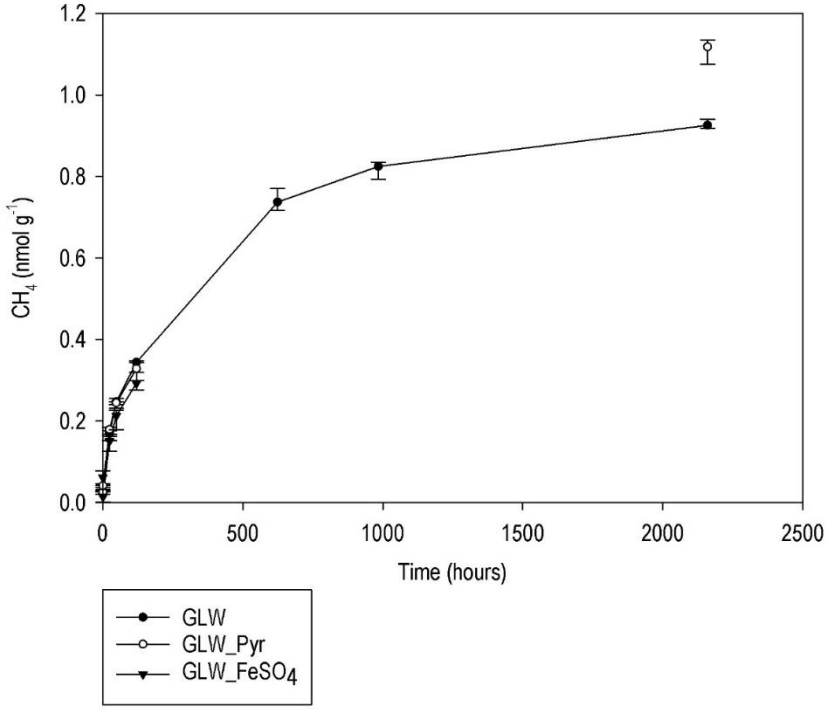

Figure 4-1 CH_4 production during incubations to test possible serpentinization pathways to produce CH_4.

Table 4-3 Average temporal production of CH_4 from crushed Whillans Grounding Line sediments (GLW) and GLW sediments to which crushed pyrite was added (GLW_Pyr) and GLW sediments with $FeSO_4$ salts (GLW_$FeSO_4$). Gas samples were taken before wetting and after the addition of water. All samples (except BLANKs) have been blank corrected. Concentrations for BLANK vials were converted to nmol g^{-1} assuming the mean mass of sediment was in the vial.

TIME POINT (HRS)	GLW	GLW_Pyr	GLW_$FeSO_4$	BLANK
	Mean CH_4 produced (nmol g^{-1})			
0 (DRY)	0.024	0.032	0.054	0.000
0.17	0.025	0.042	0.016	0.043
24	0.171	0.176	0.143	0.062
48	0.244	0.244	0.296	0.061
120	0.337	0.324	0.296	0.060
624	0.741	-	-	0.009
984	0.818	-	-	0.045
2160	0.928	1.11	-	0.083

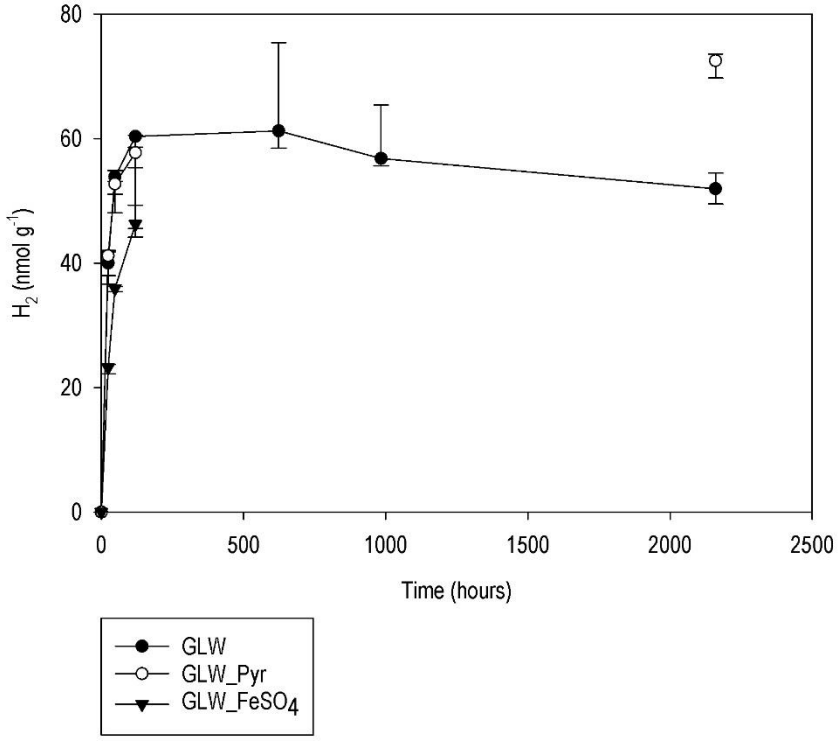

Figure 4-2 H_2 production during incubations to test possible serpentinization pathways.

Table 4-4 . Average temporal production of H_2 from crushed Whillans Grounding Line sediments (GLW) and GLW sediments to which crushed pyrite was added (GLW_Pyr) and GLW sediments with $FeSO_4$ salts (GLW_$FeSO_4$). Gas samples were taken before wetting and after the addition of water. All samples (except BLANKs) have been blank corrected. Concentrations for BLANK vials were converted to nmol g^{-1} assuming the mean mass of sediment was in the vial.

TIME POINT (HRS)	GLW	GLW_Pyr	GLW_$FeSO_4$	BLANK
	Mean H_2 produced (nmol g^{-1})			
0 (DRY)	0.00	0.00	0.00	0.00
0.17	0.00	0.00	0.00	0.00
24	39.6	40.3	23.0	0.00
48	53.3	51.3	35.9	0.00
120	58.8	53.5	47.1	0.00
624	65.0	-	-	0.00
984	59.3	-	-	0.00
2160	52.0	71.9	-	7.28

Hydrogen concentration appeared to follow a similar trend to that found previously in crushed samples of SLW (Section 3.3.2), up until the first 26 days of incubation (Figure 4-2), with GLW reaching concentrations of 65.0 nmol g^{-1} (Table 4-4). Previous analysis of headspace gases concluded after 30 days, therefore these are the longest incubations carried out throughout this project. After 26 days, the concentration of H_2 appeared to decrease in GLW incubations (Figure 4-2), dropping to 52.0 nmol g^{-11} (Table 4-4). GLW_Pyr concentrations increase between the analysis at 120 hours and after 3 months (Figure 4-2), reaching a maximum concentration of 71.9 nmol g^{-11} (Table 4-4), considerably higher than previous results of SLW incubations (Section 3.3.2).

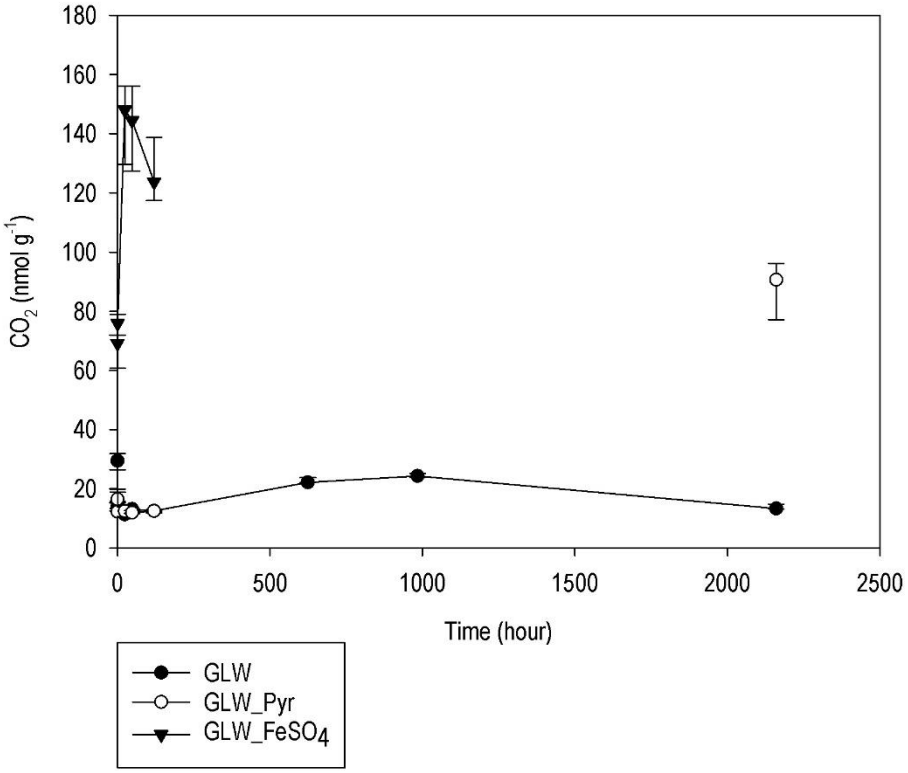

Figure 4-3 CO_2 production during incubations to test possible serpentinization pathways.

Table 4-5 Average temporal production of CO_2 from crushed Whillans Grounding Line sediments (GLW) and GLW sediments to which crushed pyrite was added (GLW_Pyr) and GLW sediments with $FeSO_4$ salts (GLW_$FeSO_4$). Gas samples were taken before wetting and after the addition of water. All samples (except BLANKs) have been blank corrected. Concentrations for BLANK vials were converted to nmol g^{-1} assuming the mean mass of sediment was in the vial.

TIME POINT (HRS)	GLW	GLW_Pyr	GLW_$FeSO_4$	BLANK
	Mean CO_2 produced (nmol g^{-1})			
0 (DRY)	25.5	16.3	55.8	0.250
0.17	14.4	14.8	71.9	1.39
24	11.4	12.3	145	4.79
48	12.6	12.1	143	6.47
120	12.5	12.4	127	7.32
624	22.6	-	-	5.42
984	24.4	-	-	6.81
2160	13.8	88.0	-	14.7

Carbon dioxide production by GLW and GLW_Pyr was significantly lower than that found in SLW time series (Section 3.3.3), with CO_2 reaching a maximum concentration of 24.4 nmol g^{-1} after 41 days (Table 4-5). GLW_Pyr CO_2 production followed a very similar trend to that of GLW during the first 120 hours (Figure 4-3), however the concentration of CO_2 after 3 months was considerably higher than that of GLW (Figure 4-3), reaching a concentration of 88.0 nmol g^{-1} (Table 4-5). The concentration of CO_2 in GLW_$FeSO_4$ rapidly increased immediately after wetting (Figure 4-3), reaching 71.9 nmol g^{-1} after a two minute incubation (Table 4-5), this continued to increase (Figure 4-3), with a concentration of 144 nmol g^{-1} after 24 hours (Table 4-5), and then began to drop off after that point. The sudden increase of CO_2 in GLW_$FeSO_4$ is probably from contamination in the $FeSO_4$ crystals. Due to this contamination, no more samples were taken after the 120 hour time-point.

4.3.3 Isotopic composition

Isotopic composition was measured in gas samples directly after crushing sediments in the ball mill and then again after a 21 day incubation of crushed sediments with water. δ^2D-CH_4 was similar for LW and GL samples taken directly after crushing sediment samples, with values of -263.2‰ and -265.8‰ respectively (Table 4-6). The isotopic fractionation of δ^2D-CH_4 was lower after incubation, with respect to the initial crush values, with values dropping to -269.8‰ and -284.1‰ for LW and GL samples, respectively (Table 4-6).

Unlike δ^2D-CH_4, δ^{13}C-CH_4 values were very different for all samples. LW ball mill sample was -49.0‰ and was lower after the incubation of these crushed sediments with water, with a value of -65.5‰ (Table 4-6). δ^{13}C-CH_4 showed a similar trend, however they were slightly higher, with values of crushed samples at -38.7 ‰ and values of -55.1 ‰ after incubation (Table 4-6).

Finally, δ^{13}C-CO_2 was also analysed, again values for these were very different for each sample. LW samples decreased from -12.2‰, directly after crushing, to -17.6‰, after a 21 day incubation (Table 4-6). Whilst GL samples decreased from -9.6‰, after crushing in the ball mill, to -15.9‰, after the 21 day incubation (Table 4-6).

Table 4-6 Isotopic composition of Lake Whillans and Grounding Line samples after crushing of for 30 minutes in the ball mill, and after incubation of these crushed sediments with water for 21 days.

	$\delta^{2}D\text{-}CH_4$	$\delta^{13}C\text{-}CH_4$	$\delta^{13}C\text{-}CO_2$
LAKE WHILLANS (LW): INITIAL CRUSH - BALL MILL SAMPLE	-263.2	-49.0	-12.2
GROUNDING LINE (GL): INITIAL CRUSH - BALL MILL SAMPLE	-265.8	-38.7	-9.6
LW: 21 DAYS AFTER WETTING SEDIMENT	-269.8	-65.5	-17.6
GL: 21 DAYS AFTER WETTING SEDIMENT	-284.1	-55.1	-15.9

4.4 Discussion

4.4.1 Free Radical Formation

We were unable, despite many attempts when road testing several methods, to find a method which accurately quantified the presence of hydroxyl radicals in solution. However, we did find evidence for the presence of surface Si free radicals. Concentrations of free radicals increased after crushing with respect to disaggregated samples. This is consistent with results from Telling et al. (2015), who found that increasing the duration of crushing increases the presence of Si·. This has been suggested as a possible mechanism for the formation of H_2 (Kita et al., 1982, Telling et al., 2015). SLW sediments are high in silicate minerals, including quartz, plagioclase and other feldspars (Michaud et al., 2016). Therefore, it is likely that the silicate free radicals (detected with DPPH) react with H_20 to form H·, which can then react together to form H_2 (Equations 11, 12 and 13). Telling et al. (2015) found increasing grinding time increased free-radical formation and consequently H_2 production. Contrasting to results found previously, despite increased free-radical formation by crushed samples, H_2 production did not increase significantly between disaggregated and crushed samples. This suggests that there might be other reactions utilising some of the surface free radicals produced.

Here, it was theorised that when the Si≡O≡Si bond in silicates was broken, not only is Si· produced, but also SiO· (Kita et al., 1982). And if this is the case, we would expect ·OH

radicals to form when SiO· comes in contact with water (Equation 22), and in turn ·OH can react together to form H_2O_2 (Equation 23). Results showed that crushing increased H_2O_2 production with respect to disaggregated samples. Despite higher concentrations, increases in H_2O_2 were analogous to those of surface free radicals, suggesting H_2O_2 and Si· might be produced by the same mechanism, namely crushing of silicates.

$$\equiv Si\text{-}O\bullet + H_2O \rightarrow SiOH + \bullet OH \qquad (22)$$

$$\bullet OH + \bullet OH \rightarrow H_2O_2 \qquad (23)$$

Pyrite has also been associated to both ·OH and H_2O_2 formation (Borda et al., 2001, Borda et al., 2003), and in doing so even promotes recycling of Fe (II) and Fe(III) (Gil-Lozano et al., 2014). This occurs when water comes into contact with surface Fe (III) sites (Equation 14 and 15, Borda et al. (2001)). Some pyrite has also been found in SLW sediments (Figure 2-2), either as pyrite clasts or pyrite inclusions within quartz (Michaud et al., 2016). Therefore, it is possible that these reactions also produce H_2O_2 in crushed and disaggregated SLW samples and might account for the difference in concentration of surface silica radicals and H_2O_2.

From these results it is clear that crushing of SLW produces both Si· (which is likely the source of H_2), H_2O_2, and probably ·OH too. Therefore, crushing of SLW can generate end-member REDOX species which could potentially react with many other components of the SLW sediment matrix. Further, this range of REDOX conditions might aid cycling of REDOX sensitive species (e.g. S or Fe) useful to some of the microbial organisms found in SLW (Purcell et al., 2014, Mikucki et al., 2016).

4.4.2 FTT and Serpentinization

During incubations of different depths of the SLW core, it was clear that the top depth produced considerably more H_2 than deeper cores. Analysis of the extractable Fe in the sediment (extracted by ascorbate and dithionite (methods described in (Raiswell et al., 2010, Raiswell et al., 2016)) was higher in the top layer than in any depths below (Appendix D, data (currently unpublished) courtesy of Jon Hawkings). Serpentinization is a well studied abiotic source of H_2 which often uses Fe as a catalyst. However, studies of this phenomenon have focused in its role in fault zones (Kelley et al., 2005), yet it has been detected at low pressures, and temperatures as low as 22^{o}C (Stevens and McKinley, 2000a). Serpentinization occurs when Fe (II) is oxidised to Fe(III) by H_2O, producing H_2

(Equation 16) (Klein et al., 2009). Therefore, we attempted to see if serpentinization had the potential to produce H_2 in SLW but was limited due to low availability of Fe. We did this by adding a mass of $FeSO_4$ and Pyrite which would be provide the equivalent Fe mass difference found in SLW samples (Appendix D). Given the low SLW sample volumes, this was tested with GLW sediments, which were assumed to have a similar composition to SLW, and to which we added some Fe sources. FTT reaction are often associated with serpentinization reactions, therefore CH_4 was also measured during these incubations.

During the first 120 hours of incubation there was no clear difference in concentrations of CH_4 and H_2 between samples (Figure 4-2). However, when a final headspace analysis was carried out after three months, concentrations of both these gases were considerably higher in GLW_Pyr than in GLW samples (Figure 4-2). This could potentially be due to slow serpentinization rates, since H_2 generation by serpentinization is slow and limited below ~150^{o}C, due to slow reaction kinetics and the partitioning of Fe (II) (McCollom, 2009). Despite some evidence of increased H_2 production after the addition of an Fe source to GLW, further analysis of the sediments is necessary to confirm serpentinization is taking place. Such as the analysis of the sediments to look for secondary minerals formed during serpentinization (e.g. brucite or magnetite) (Etiope et al., 2013). If serpentinization is occurring at 0^{o}C, it is possible that the increased H_2 production seen in SLW_Top (Section 3.3.2) is a result of additional Fe sources at this depth resulting in serpentinization, however, as with GLW, further analysis would be necessary.

Secondary minerals, such as magnetite, can catalyse the reaction of CO_2 and H_2 to form CH_4 (Equation 18), these reactions are known as FTT reactions (Neubeck et al., 2011), however this reaction is not that straight forward and is likely to have a number of intermediate reactions, such as the reduction of formate and CO (Okland et al., 2014). If H_2 was produced by serpentinization you would expect these secondary minerals to form. Given the already high concentrations of CO_2, with increased H_2 and increased presence of secondary minerals it could be expected that more CH_4 would also be produced (Equation 18). Methane concentrations during the incubation of GLW and GLW_Pyr, followed a similar trend to H_2, with these samples producing similar concentration of CH_4 during the first 120 hours, but again CH_4 concentration in GLW_Pyr had increased with respect to GLW samples at the three month time-point (Figure 4-1). If this increase in CH_4 is due to the production of H_2 through serpentinization (following Equation 18), it is likely

that there is a correlation between the production of these gases. The linear regression of CH_4 and H_2 in GLW_Pyr samples, after H_2 is detectable, gives an R^2 value of 0.822, suggesting that CH_4 and H_2 are associated (Figure 4-4). The R^2 value for GLW samples was much lower (R^2= 0.234; Figure 4-4). This suggests that serpentinization and FTT reactions are unlikely to control H_2 and CH_4 production in GLW samples. However, the increased H_2 and CH_4 production seen at the three month time point in GLW_Pyr, suggest that they might be relevant after the addition of an Fe source. Nevertheless, if CH_4 was being produced through FTT reactions, you would expect to see a decrease in CO_2 (equation 18), which was not obvious in our results (Figure 4-3). This might just be because of the different orders of magnitude between CH_4 and CO_2 production, which could obscure the associated CO_2 decrease. These results highlight the potential for the additional extractable Fe measured in the top SLW sediments (Appendix D) to lead to serpentinization and FTT reactions in SLW incubations (Section 3.3.2), however the oxidation state of this Fe is unknown and further analysis of the solid and liquid phases would be necessary to confirm this. Interestingly, FTT reactions are often associated to the production of other hydrocarbons, such as ethylene, (McCollom and Seewald, 2001) as well as elevated NH_4^+ concentrations (Okland et al., 2014), both of which were measured in SLW headspaces and waters and will be discussed further in Chapter 5.

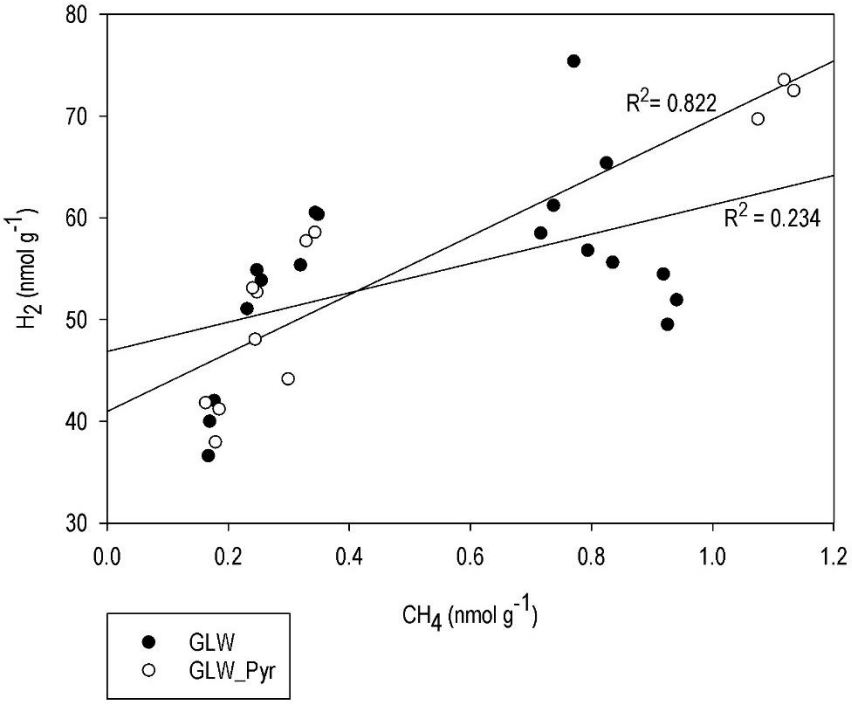

Figure 4-4 CH_4 v. H_2 production in serpentinization/FTT incubations and linear regression lines for GLW ($R^2 = 0.234$) and GLW_Pyr ($R^2 = 0.822$) samples

4.4.3 Isotopic Composition

Lake Whillans (LW) initial crush methane samples crushing (Table 4-1) fell within the "early mature associated humic" signature (Figure 4-5; Whiticar (1999)), suggesting CH_4 analysed might have had some organic sources within it. Whilst the composition of Grounding Line (GL) initial crush results crushing (Table 4-1) fell within "geothermal, hydrothermal, crystalline" origins of formation (Figure 4-5; Whiticar (1999)), suggesting a largely abiotic origin, probably from the release of CH_4 from fluid inclusions. The CH_4 isotopic composition from the initial crushing of both LW and GL could be a result of cracking of complex organic molecules as a result of heating, this is often seen during diagenesis (Potter et al., 2013), which often leads to simpler hydrocarbon species being enriched with lighter isotopes (Potter et al., 2013).

Analysis of isotopic composition of both CH_4 and CO_2 revealed that gases produced after incubation of crushed sediments were lighter than gases released during crushing (Table 4-1). The origin of gases produced during the 21-day incubation is less clear than for the initial crush results. The isotopic composition of CH_4 from both sediment incubations fell within the "mix and transition" signatures (Figure 4-5; Whiticar (1999)), which points

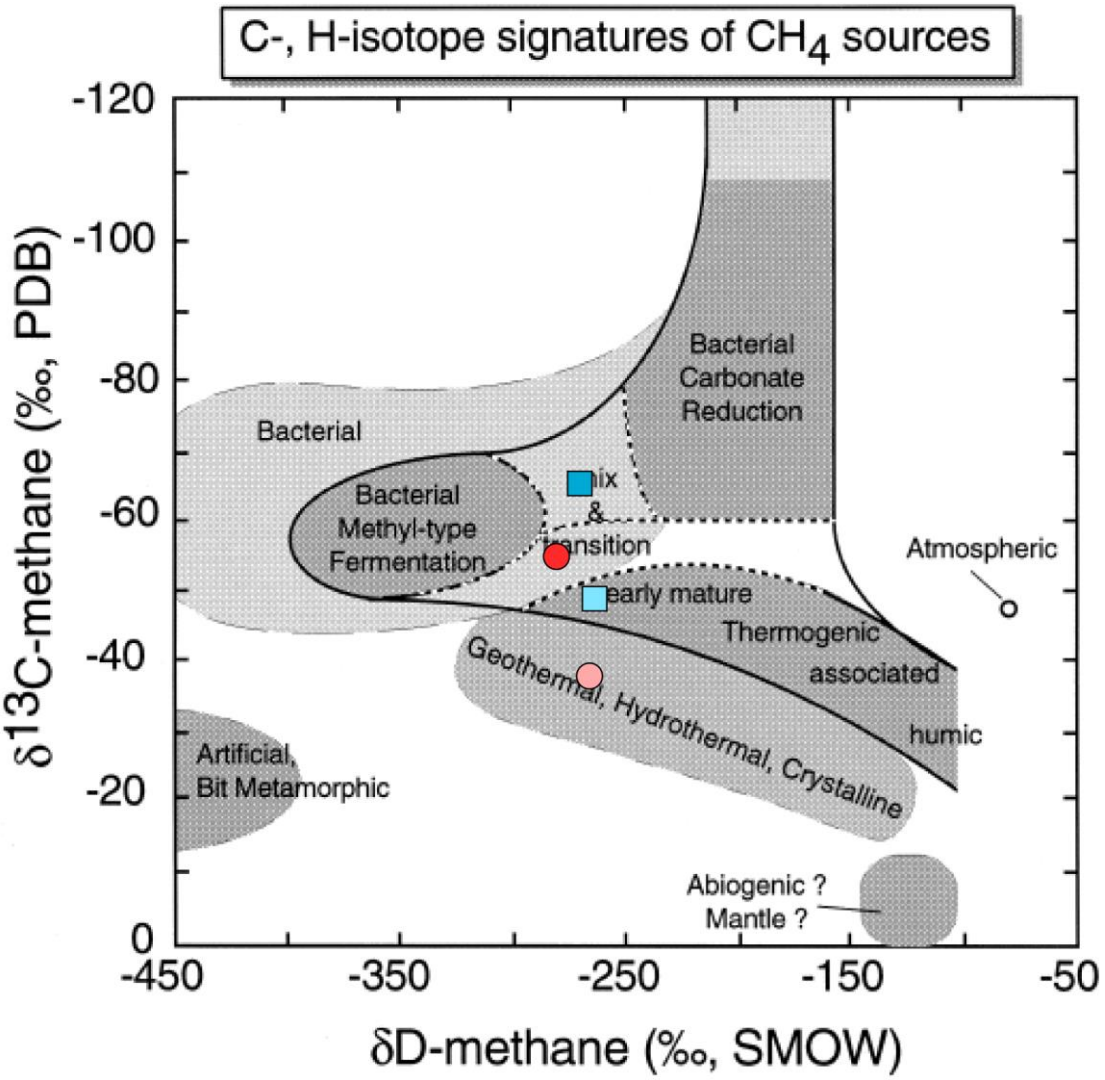

Figure 4-5 Methane stable isotope biplot (modified from Whiticar (1999))with LW_Iso data (blue squares) and GL_Iso data (pink circles), where the ligher colour represents the results after the initial ball mill crush, and the darker colour represents gases after a 21 day incubation.

towards a more bacterial origin. However, interpreting the isotopic signatures of CH_4 can be challenging as it is unlikely to get a fully abiogenic sources of methane (Schoell, 1988), as the abiotic thermal degradation of organic molecules can lead to signal closer to that of microbially derived gases. And so, even when there are no active methanogens, any CH_4 released from thermal degradation of these organisms will have an impact on the isotopic signature of CH_4 (Schoell, 1988). Biologically produced CH_4 is characterised by its lighter δ^2D-CH_4 and δ^{13}C -CH_4 (Potter et al., 2013), which is consistent with our results. However the isotopic composition of CH_4 after incubation of GL sediments, still falls within the isotopic range for CH_4 that has formed as a result of breaking more complex

organic molecules (Potter et al., 2013), with LW CH_4 being just slightly lighter than the range suggested by Potter et al. (2013).

The isotopic composition of CO_2 did not elucidate the origin of these gases any further. $\delta^{13}C$ values of CH_4 and CO_2 in LW samples fell round the edges of values typical of freshwater methyl fermentation (Whiticar, 1999). Whilst GL isotope sigantures of $\delta^{13}C$ in both these gases fell on the edge of methane oxidation processes for gases produced during crushing, and again within methyl fermentation for incubation gases (Whiticar, 1999). The trajectories of the CO_2 - CH_4 carbon isotope partitioning both went against the direction of either oxidation or formation of CH_4 (Whiticar, 1999). It is worth noting isotope analysis of CH_4 did not give results within the range expected for serpentinization reactions (Etiope et al., 2013), although again this would have been unlikely without additional Fe (II) sources. Methane isotopic analysis was also considerably different to that found by Michaud et al. (2017) however this is possibly due to the lack of abiotic effects on gases measured here. These results suggest that isotope data from C and H alone is not enough to draw conclusions of the thermogenic, abiogenic or biogenic origin of gases (Potter et al., 2013).

4.5 Conclusion

This set of experiments shows clearly that crushing of ancient, heavily weathered sediments still produce silica surface radicals. These react with water to produce both H_2 and H_2O_2, as well as their associated radicals, thus producing highly reducing and highly oxidising species and allowing a range of REDOX reactions to take place. Other mechanisms by which these gases might be explained is through serpentinization (in the case H_2) or FTT reactions (in the case of CH_4). Evidence from preliminary incubations with an additional Fe source suggest that these reactions could possibly take place if additional Fe sources were available within the sediment, however, if this is the case, they affect gas concentrations on a longer timescale than is relevant to the SLW incubations carried out here (Chapter 3). Finally, isotopic analysis of CH_4 confirmed initial CH_4 sources are likely to be geothermal, hydrothermal or crystalline in origin, most likely from fluid inclusions. Interpretation of isotopic fractionation of gases analysed after sediment incubation is more complex. Methane had “mix and transition” signatures (Whiticar, 1999), which could suggest some bacterial effects, however caution should be taken when interpreting this data, as there are a lot of factors, such as the origin of C in

the system, which might influence these signatures. Thus, further work is necessary to understand the confounding factors which influence the isotopic composition of CH_4, both in controlled comminution experiments and in subglacial lake samples.

Chapter 5 Other Effects of Crushing

5.1 Introduction

This chapter addresses the third research objective described in the Aims and Objectives (Section 1.4), which is to examine if crushing of SLW sediment releases any other gases or notable solutes. This chapter documents ethylene and other hydrocarbon release using data from GC-MS analysis of head space gases. Solute released during crushing was analysed using a Gallery Automated Analyser and a Dionex Capillary IC-5000 for nutrients and major ions respectively. The fluorescence properties of DOM were analysed using a fluorolog3 spectrofluorometer, while the DOC concentrations was measured by a TOC-L.

5.2 Methods

Samples were prepared as described in Section 3.2.1 for all the "SLW" samples and as described in Section 4.2.5.1 for all the "Whillans:Iso" samples. The samples were kept at 0^{o}C until all the gas time-series analysis were complete and the GC-MS runs were finalised. Only then was the slurry filtered for analysis of the solute. Filtrate was stored at 4^{o}C for any analyses not conducted on the same day of filtering. Sediment samples for grain size distribution were stored in 15 ml centrifuge tubes at 5^{o}C.

5.2.1 Ethylene GC Analysis

Headspace analysis with the Agilent 7890A Gas Chromatograph (GC) revealed a peak, which was suspected of being either ethylene or acetylene. The presence of ethylene (C_2H_4) was confirmed using a Varian 3800 gas chromatograph, on which C_2H_4 was separated from acetylene (C_2H_2) using a 6' x 1/8", 80/100 mesh HayeSep T column at 85 ˚C (He carrier gas). Thereafter, C_2H_4 was quantified, together with other gases, using an Agilent 7890A GC, following the methodology described in Section 3.2.2. The concentrations of headspace gases were calculated based on a 100 ppm C_2H_4 (BOC) standard standard-curve (0.87 ppm to 104 ppm, R^2 = 0.9999, n = 6, linear to 104 ppm). Standards were run daily and gave a coefficient of variation of 3.34 % (n = 5) for C_2H_4, with a detection limit of 0.693 ppm, equivalent to 0.115 nmol g^{-1}.

5.2.2 GC-MS Analysis

Low level concentrations of short chain hydrocarbons were identified using a Medusa GC-MS system. A 2 ml gas sample loop, connected to a 6-port Valco valve, was used to introduce 2 ml of sample into a flowing N_2 stream, originating from a Parker Balston generator. The sample loop was placed in-line with the N_2 stream at the mid-point of sampling. 1 L of the N_2 and gas sample mix were trapped for analysis. The Medusa system used a 'Cryotiger' in order to analyse trace levels of volatile organic compounds. This cools an adsorbent trap to -165^{o}C and then uses two traps, also cooled -165^{o}C, to remove the most abundant gases in air, such as N_2, O_2, H_2O, CO_2 and CH_4, before any further analysis. Isolated trace compounds are desorbed from the first trap onto a smaller second refocusing trap. Analytes are released from the second column by flash heating, and the gas samples are then injected onto a Porabond Q chromatography column, programmed from 40 ^{o}C to 200 ^{o}C at 23 ^{o}C min^{-1}, to separate the compounds of interest. The mass spectral detector then allows accurate detection of a range of complex organic compound mixtures. A more detailed description of the Medusa and set up modifications can be found in Miller et al. (2008) and Arnold et al. (2013). Extensive sampling of N_2 gas from the Parker Balston generator was carried out to determine sample blanks.

5.2.3 Grain Size Distribution

The grain size distribution of the sediments used in the incubation was measured using a Malvern Mastersizer 3000 laser particle size analyser, with a Hydro EV pump accessory (Malvern Instruments Ltd., Worcestershire, UK) and a pump speed set to 2400 rpm. Initially, de-ionised water was used as a dispersant. However, the polarity of some samples resulted in flocculation and unacceptably high RSDs. Sodium Hexametaphosphate was added to the de-ionised water to make a 10% solution, but this did not solve the problem. Finally, isopropanol was used as a dispersant, but again the problem persisted. Unfortunately, this meant no reliable grain size distribution could be collected from these samples.

5.2.4 Water Chemistry

The wet sediment slurry from within the serum bottles was transferred into centrifuge tubes within the anaerobic chamber at the end of the experiment. The tubes were sealed with screw tops, taken out of the anaerobic chamber and centrifuged at 4500 rpm for 10 mins. The tubes were then returned to the anaerobic chamber, where the water was

decanted and filtered using 0.45 µm in-line polypropylene filters, which had previously been left overnight to degas in the anaerobic chamber.

5.2.4.1 Nutrients

Sub-samples of filtered water were diluted 1 in 4 (in anoxic milliQ water) and analysed using the Gallery Automated Photometric Analyzer (Thermofisher). In-built methods were used to analyse for NH_4^+, NO_2, Total Oxidised Nitrogen (TON) as NO_3, Si and PO_4^{3-}. The LOD and coefficient of variance for each analyte can be found in Table 5-1. The Ferrozine method, as described in Viollier et al. (2000), was adapted to run on the Gallery to analyse for Fe^{2+} and total Fe. Analysis of Fe^{2+} was carried out immediately after taking samples out of anaerobic chamber. The LOD and coefficient of variance for this method can also be found in Table 5-1.

5.2.4.2 Major Ions

Sub-samples of filtered water were diluted 1 in 100. The major base cations, Na^+, Mg^{2+}, K^+ and Ca^{2+}, were analysed using a Dionex IC 5000, with an IonPac™ CS12A 2mm column (see Table 5-2 for LOD and Coefficient of Variance). Anions, including: F^-, acetate, Cl^-, Br^-, NO_3^- and SO_4^{2-}, were analysed using a Dionex IC 5000 Capillary, fitted with an IonPac™ AS11-HC capillary column (see Table 5-2 for LOD and Coefficient of Variance).

Table 5-1 LOD and Coefficient of Variance for analytes run on the Gallery.

	LOD (µM)	COEFFICIENT OF VARIANCE (%)	ANALYTICAL ACCURACY (%)
NH_4^+	0.19	2.3	4.1
NO_2	0.005	0.21	6.5
TON	0.10	2.2	2.7
H_4SiO_4 (aq)	0.001	2.1	3.2
PO_4^{3-}	0.14	0.33	3.8
Fe^{2+}	0.03	0.77	2.1
Fe (Total)	0.07	0.56	5.5

Table 5-2 Comparative Limits of Detection (LOD) and coefficients of variance for cations and anions in waters from the experimental slurries, analysed using Dionex IC 5000 and Dionex IC 5000 Capillary, respectively. The actual LOD of the instruments is 100 times lower, and these comparative LOD take account of 1:100 dilution of the waters.

	LOD (µM)	COEFFICIENT OF VARIANCE (%)	ANALYTICAL ACCURACY (%)		LOD (µM)	COEFFICIENT OF VARIANCE (%)	ANALYTICAL ACCURACY (%)
Na^+	0.26	0.27	8.5	F^-	0.21	0.29	1.6
Mg^{2+}	0.29	0.75	7.1	Acetate	0.88	0.76	1.5
K^+	0.21	0.36	15	Cl^-	0.11	0.18	3.1
Ca^{2+}	0.35	2.3	9.9	Br^-	0.21	0.32	1.0
				NO_3^-	0.006	0.1	1.4
				SO_4^-	0.10	0.33	2.5

5.2.4.3 DOM

DOM fluorescence was measured using a Horiba Fluorolog3 fluorometer. Bandwidths were set to 5 nm for both excitation and emission. A series of emission scans (280 - 600 nm, by 2 nm increments) were collected over excitation wavelengths ranging from 250 to 450 nm by 5 nm increments. The resulting fluorescence excitation–emission matrices (EEMs) was processed using the PARAFAC method, as described in Murphy et al. (2013).

5.2.4.4 DOC

DOC (measured as non-purgeable organic carbon) was quantified by high temperature combustion (680^{o}C), using a Shimadzu TOC-L analyser fitted with low sensitivity catalyst. Precision (± 4%) and accuracy (± 4%) were determined by the repeat analysis of a DOC standard solution containing potassium hydrogen phthalate ($C_8H_5KO_4$). The LOD was 5 µM C. Initial analysis of experimental solutions was conducted on amalgamated solutions of Whillans:Iso_GL samples, due to the low sample volume and suspected low concentrations. However, this initial analysis revealed that the concentration of DOC was higher than initially believed and that, in fact, the amalgamated experimental solutions required a 1 in 20 dilution prior to analysis. Therefore, the Whillan:Iso_SL analysis was carried out in triplicate on diluted Whillan:Iso_SL samples.

5.3 Results

5.3.1 Ethylene and Other Hydrocarbons

5.3.1.1 SLW results

Between 1.6 and 3.2 nmol of C_2H_4 g^{-1}, as outlined previously, was detected in the headspace of FIRST-CRUSH SLW samples (Section 3.3.1 - Table 3-2). None was detected in any of the BLANKS (Table 5-3), neither was any above the detection limit in the DIS-WET samples for both the middle and bottom depths (Figure 5-1 and Table 5-3). CRUSH-DRY samples had concentrations above the detection limit after 48 hours of incubation (Table 5-3). This concentration increased steadily from 0.02 nmol to 0.10 nmol C_2H_4 g^{-1}, at the last time point (Figure 5-1), and even overtook C_2H_4 production by its CRUSH-WET counterpart after 120 hours of incubation (Figure 5-1). CRUSH-WET results were slightly unusual compared to the other gases analysed. The amalgamated middle layers of the

core produced considerably less C_2H_4 than the other two depths (Table 5-3 and Figure 5-1), by roughly one order of magnitude. The constant dilution of samples during analysis meant that C_2H_4 levels in the middle layer (crushed) samples fell below the LOD after two weeks of incubation.

A peak, with a retention time that fell between that of propane and iso-butane, was also detected during analysis of the incubation vial headspace. Further analysis of the headspace gases later in the experiment, using fractionation patterns obtained by a Medusa GC-MS on scan mode, identified this peak as propene. However, its concentration could not be quantified at this time. The unidentified peak appeared in all CRUSH-WET samples from time = 0 (before wetting), increased immediately after wetting and continued to increase up to 24 hours after, but then began to decrease, probably from the dilution resulting from successive sampling. For CRUSH-DRY samples, this peak was at its highest at time = 0, and decreased with time, again most likely a result of dilution associated with repeat sampling. DIS-WET samples for middle depths showed no indication of this peak, however, the bottom DIS-WET sediment showed a hint of its presence after 48 hours of incubation, yet the peak area was an order of magnitude smaller than for its crushed counterpart.

The Medusa GC-MS was used to analyse the headspace of the incubation vials after the completion of the experiment. This not only helped to identify the unidentified peak mentioned above, but also highlighted a range of other hydrocarbons produced after crushing and/or disaggregating the SLW sediments (Table 5-4). Compounds which were seen in samples only after undergoing crushing include i-butane and benzene. A surprising result is that a wide range of hydrocarbons appear to have been released just by disaggregation (Table 5-4). However, it is worth noting that there were large uncertainties with the method. Unfortunately, at this time, the concentration of these gases could not be quantified due to a lack of a reliable standard.

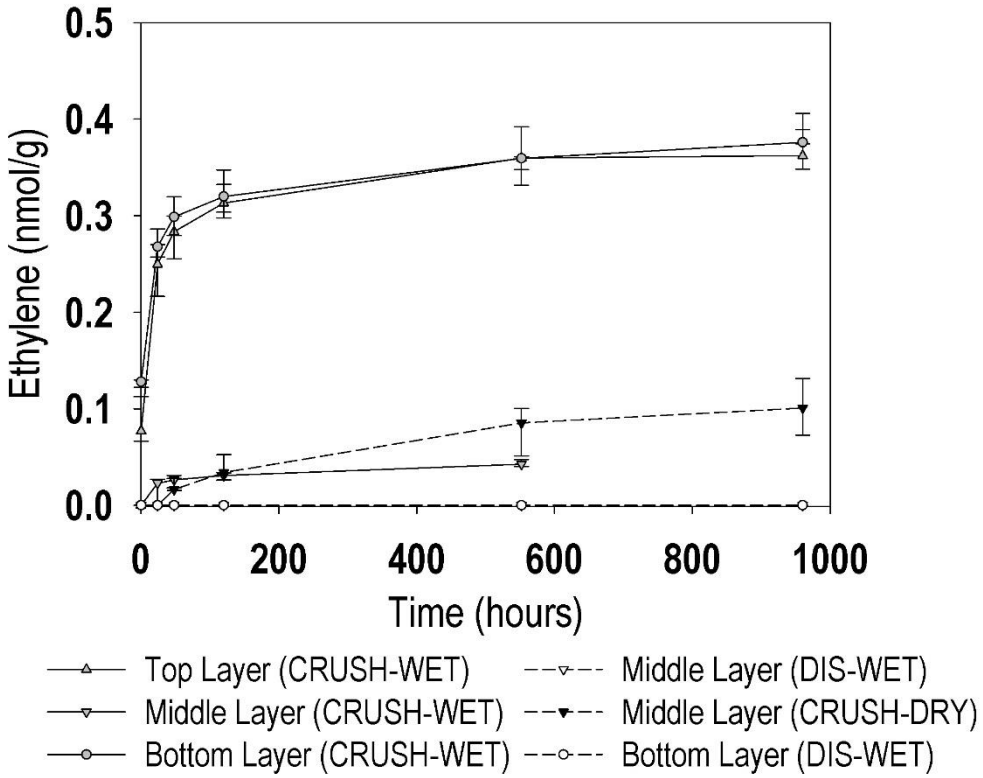

Figure 5-1 Temporal production of C_2H_4 from wetted disaggregated (DIS-WET) and crushed (CRUSH-WET) SLW sediment and crushed but unwetted (CRUSH-DRY) sediment. Each point represents the median value, and error bars denote the maximum and minimum concentrations.

Table 5-3 Average temporal production of C_2H_4 from wetted disaggregated (DIS-WET) and crushed (CRUSH-WET) SLW sediment, and crushed but unwetted (CRUSH-DRY) sediment.

TIME POINT (HRS)	TOP CRUSH-WET	MIDDLE CRUSH-WET	MIDDLE DIS-WET	MIDDLE CRUSH-DRY	BOTTOM CRUSH-WET	BOTTOM DIS-WET	BLANK
	Mean C_2H_4 produced (nmol g^{-1})						
0 (DRY)	0.00	0.00	0.00	0.00	0	0.00	0.00
0.17	0.09	0.00	0.00	0.00	0.12	0.00	0.00
24	0.25	0.02	0.00	0.00	0.26	0.00	0.00
48	0.29	0.03	0.00	0.02	0.29	0.00	0.00
120	0.32	0.03	0.00	0.04	0.32	0.00	0.00
540	0.36	0.04	0.00	0.08	0.36	0.00	0.00
960	0.37	-	0.00	0.10	0.39	0.00	0.00

Table 5-4 Hydrocarbon gases detected using the GC-MS after the completion of the time-series analysis on the GC .

PRESENT ABOVE BLANKS AND ONE STANDARD DEVIATION?	Ethane	Ethyne	Propane	c-Propane	i-Butane	n-Butane	i-Pentane	n-Pentane	Benzene
TOP LAYER: CRUSH-WET	Yes	Yes	Yes	Yes	Yes	Yes	Yes	Yes	Yes
TOP LAYER: DIS-WET	n/a	n/a	n/a	n/a	n/a	n/a	n/a	n/a	n/a
MIDDLE LAYER: CRUSH-WET	Yes	Yes	Yes	Yes	Yes	Yes	Yes	Yes	Yes
MIDDLE LAYER: DIS-WET	No	Yes	Yes	Yes	No	Yes	No	Yes	No
MIDDLE LAYER: CRUSH-DRY	No	Yes	Yes	Yes	Yes	Yes	No	Yes	No
BOTTOM LAYER: CRUSH-WET	No	Yes	Yes	Yes	Yes	Yes	Yes	Yes	Yes
BOTTOM LAYER: DIS-WET	Yes	Yes	Yes	Yes	No	Yes	Yes	Yes	No

Table 5-5 Hydrocarbon gas concentrations in samples for isotope analysis (Whillans:Iso)

NORMALISED TO G OF SEDIMENT (pmol g^{-1})	Ethane	ethyne	propane	n-butane	i-butane	n-pentane	i-pentane	benzene	toluene
WGL: INITIAL CRUSH	97	250	28	5.3	5.8	0.36	2.7	0.38	0.15
SLW: INITIAL CRUSH	120	260	61	2.8	4.8	-	0.39	-	-
WGL: AFTER 21 DAY INCUBATION	6.9	-	3.9	0.70	1.0	0.07	1.0	0.55	-
SLW: AFTER 21 DAY INCUBATION	9.4	8.5	9.8	1.2	1.0	-	-	1.1	-

5.3.1.2 Whillans:Iso Results

The additional experiments carried out to determine the isotopic composition of gases also provided an opportunity to quantify the concentration of hydrocarbons present in the headspace of the ball mill, after the initial crushing of sediments, and the vial headspace, after incubation with water. Results revealed large concentrations of ethane, ethyne and propane after the initial crushing of both the subglacial lake (Whillans:Iso_SL) and grounding line sediments (Whillans:Iso_GL; Table 5-5). N-butane, I-butane and I-pentane were all also found in the headspace gases after initial crushing of sediments, however the concentrations of all these gases were much lower (Table 5-5). N-pentane, benzene and toluene were only found after the initial crush of WGL sediments. However, the concentrations were also very low (Table 5-5).

The concentration of all the above hydrocarbons were much lower after the 21 day incubation of the wetted, crushed samples. Ethane and propane were still relatively high in both SLW and WGL compared to the other hydrocarbons detected (Table 5-5). SLW also had a relatively high ethyne concentration, and lower concentrations of n-butane, i-butane and benzene were also present (Table 5-5). WGL produced no detectable ethyne, however it did have low concentrations of n-butane, i-butane, n-pentane, i-pentane and benzene in the vial headspaces (Table 5-5).

5.3.2 Grain Size Distribution

Despite several attempts at measuring the grain size distribution in several media, the sediment was always too polar to measure.

5.3.3 Water Chemistry

5.3.3.1 Major Ions – SLW

SLW samples were not washed prior to oven drying. This meant that any solute in the pore waters of the samples remained and contributed to the final solute concentrations measured. However, this solute was diluted by the addition of milli-Q water during incubation. To estimate the possible contribution of pre-existing ions to the final solute concentrations measured, the water mass loss for each depth was used to estimate the water volume in each sample (Equation 24). This number was divided by the volume of water added to each sample (4ml) to give a dilution factor. Then the contribution from pre-existing ions in solution was estimated by using average concentration values for ions of interest measured in-situ by Michaud et al. (2016) (unless stated otherwise) for

the depths of the core used in incubation experiment s. The dilution factor was multiplied by these concentrations to estimate the contribution from pre-existing ions in solution. A flow chart explaining the steps taken during this calculation can be seen in Appendix E. The results of these calculations for the top, middle and bottom depth can be seen in Table 5-6, Table 5-7 and Table 5-8 respectively.

Calculated initial pore water contributions to dry sample=

$$\frac{\text{Wet sediment mass(g) – dry sediment mass (g)}}{\text{dry sediment mass}} \quad x \quad \text{average sample mass} \qquad (24)$$

Chloride showed a slight increase in concentration down the core prior to correcting for pre-existing concentrations. However, Cl^- concentrations after correction was relatively constant, with values ranging from 1.18 to 1.43meq L^{-1} (Table 5-6, Table 5-7 and Table 5-8), with the exception of the middle DIS-WET samples which had a much lower Cl^- concentration (0.09 meq L^{-1}; Table 5-7).

The sea water component of pre-existing ions in the sample will contribute to the concentrations of several other ions in solution, such as Br^-, SO_4^{2-}, F^-, Na^+, Mg^{2+}, K^+ and Ca^{2+}. Sea-water is potentially a large component of SLW, particularly deeper within the core (Michaud et al., 2016), therefore correcting solute concentrations, measured here, using estimated contributions from porewaters will simultaneously correct for any sea-water component in the solutions analysed. The Br^- concentration was below the detection limit for all samples and therefore is not included here. SO_4^{2-} concentrations, after correcting for porewaters, , increased down the core, from 0.58 (top CRUSH-WET, Table 5-6) to 5.37 meq L^{-1} (bottom DIS-WET, Table 5-8). The concentrations differed between crushed and disaggregated samples, but one was not consistently higher than the other.

The concentrations of Na^+, after porewater correction, were highest in the middle CRUSH-WET samples (8.05meq L^{-1}; Table 5-7) and lowest in the top CRUSH-WET samples (2.91 meq L^{-1}; Table 5-6). Concentrations of K^+ followed a similar trend within the crushed SLW samples, with concentrations ranging from 1.09 (top CRUSH-WET, Table 5-6) to 1.36 meq L^{-1} (middle CRUSH-WET, Table 5-7). Disaggregated samples had much lower and similar concentrations with 0.400 and 0.417 meq L^{-1} in the middle (Table 5-7) and bottom layer (Table 5-8) respectively. Mg^{2+} concentrations for crushed samples

were similar in the top and middle layer (0.321 (Table 5-6) and 0.309 (Table 5-7) meq L^{-1}, respectively), and increased to 1.07 meq L^{-1} in the bottom depth (Table 5-8). However, corrected Mg^{2+} concentrations in the disaggregated samples became negative (-0.133 and -0.071 meq L^{-1} in the middle and bottom core respectively (Table 5-7 and Table 5-8)). The concentrations of Ca^{2+} ions in solution also became negative after correction, for all depths and treatments, except for bottom DIS-WET samples. Corrected F^- concentrations down the core were all relatively similar, ranging from 0.164 meq L^{-1} (top CRUSH-WET, Table 5-6) to 0.213 meq L^{-1} (middle CRUSH-WET, Table 5-7).

Michaud et al. (2016) only found Si above detection limits in the top centimetre of the core analysed, however the samples analysed here had considerable Si concentrations at all depths. The CRUSH-WET samples had more Si than their disaggregated counterparts, with corrected Si concentrations ranging from 3.78 to 4.69 µmol L^{-1} (Table 5-8 and Table 5-7, respectively) in CRUSH-WET samples and values of 2.52 and 2.90 µmol L^{-1} (Table 5-8 and Table 5-7, respectively) for DIS-WET samples.

Finally, both Fe^{2+} and total iron in solution were measured. Neither Fe^{2+} or total iron values have been reported in the literature, therefore the values could not be corrected. Concentrations of Fe^{2+} increased down the depth of the core within crushed samples, increasing from 0.729 to 1.02 µmol L^{-1} (Table 5-6 and Table 5-8, respectively). DIS-WET samples had much lower Fe^{2+} concentrations, with values of 0.184 (middle, Table 5-7) and 0.134 (bottom, Table 5-8) µmol L^{-1}. Total iron concentrations were considerably higher than those of Fe^{2+}, ranging from 17.4 to 22.7 µmol L^{-1} in CRUSH-WET samples (Table 5-7 and Table 5-8, respectively). Disaggregated samples had lower concentrations than their crushed counterparts, with the middle depth having an average concentration of 16.0 µmol L^{-1} and the bottom, one of 15.9 µmol L^{-1} (Table 5-7 and Table 5-8, respectively).

5.3.3.2 Nutrients – SLW

Total Oxidised Nitrogen (TON) and PO_4^{2-} results were unlike all other ions measured. DIS-WET samples had higher concentrations of these ions than their crushed equivalents. PO_4^{2-} ranged from 0.019 to 0.929 µmol L^{-1} (Table 5-6, Table 5-7 and Table 5-8) in CRUSH-WET samples and 2.62 to 2.90 µmol L^{-1} in DIS-WET samples (Table 5-8 and Table 5-7, respectively). Indeed, blank corrected TON CRUSH-WET samples were negative, from -0.526 to -0.926 µmol L^{-1} (Table 5-6, Table 5-7 and Table 5-8), whereas DIS-WET

samples remained positive, with values of 1.04 and 4.01 μmol L^{-1} (Table 5-7 and Table 5-8, respectively). There was no apparent trend for either of these ions down the core (Table 5-6, Table 5-7 and Table 5-8).

NH_4^+ values were only measured in the lake waters (Christner et al., 2014), and not in the porewaters. The lake concentrations were used to correct concentrations in the top layer sediments, however the correction to the final concentration of NH_4^+ in solution was minimal (Table 5-6). CRUSH-WET samples did not show a clear trend down the core (Table 5-6, Table 5-7 and Table 5-8); values were roughly similar, ranging from 108 to 120 μmol L^{-1}. There was a very marked increase in NH_4^+ with crushed samples versus disaggregated samples, with the middle core increasing its concentration, by ~25 and the bottom core by ~240 times (Table 5-7 and Table 5-8, respectively). Concentrations of NH_4^+ in DIS-WET samples in the middle and bottom core were of 3.78 and 0.480 μmol L^{-1} (Table 5-7 and Table 5-8, respectively).

As with NH_4^+, acetate was only reported in the lake waters (Christner et al., 2014), and this value was used to estimate a maximum contribution to the final concentration in the surface sediment solutions. Acetate concentrations decreased with depth, and there was a markedly higher concentration in the top layer (Table 5-6, Table 5-7 and Table 5-8). Concentrations within CRUSH-WET samples ranged from 340 (in the top layer, Table 5-6) to 280 μmol L^{-1} (in the bottom layer, Table 5-8). Crushing of the sediment increased the concentration of acetate in solution, x3 and x1.7 for the middle (93 μmol L^{-1}; Table 5-7) and bottom (170 μmol L^{-1}; Table 5-8) DIS-WET layers respectively. Acetate concentrations were distinctly higher than in situ lake measurements (Christner et al., 2014), roughly between x70 and x260 times greater in the lowest (middle DIS-WET) and highest (top CRUSH-WET) samples measured, respectively.

5.3.3.3 Major Ions and Nutrients – Whillans:Iso

The water chemistry of the crushed sediment incubations was also analysed. However, issues with the Dionex Capillary IC 5000 meant that only acetate could be analysed using this system. Therefore, analytes were limited to the capabilities of the Gallery Automated Photometric Analyzer. The concentrations of acetate produced in the incubated waters of SLW were very similar to those found in previous SL incubation experiments (ranging from 360 to 380 μmol L^{-1} for replicates; Table 5-9). Conversely, GL sediments did not produce any acetate above the LOD.

NH_4^+ concentrations found in the SL incubations were also similar to those found in previous SLW experiments (average values of 124 μmol L^{-1}), however GL produced a little over twice as much NH_4^+ as SL samples, with an average value of 240 μmol L^{-1} (Table 5-9). There was some evidence of NO_2^-, but no detectable TON, in the GL solute. Conversely, SL showed some evidence of low TON concentrations (Table 5-9), but the NO_2^- in solution was below the limits of detection. Neither of these analytes were detected in previous analyses of the SLW sediment incubations.

The concentration of total Fe in solution from SL was of the same order of magnitude as previous analyses of SLW sediments (average value of 25 μmol L^{-1}), whereas GL Fe concentrations were lower (average value of 2.3 μmol L^{-1}; Table 5-9). However, the SL concentrations, and hence the percentage, of reduced iron were considerably higher than in previous results (Table 5-9), with an average concentration of 2.4 μmol L^{-1}, equivalent to 9.3% of the total iron. GL, despite having lower Fe^{2+} concentrations (average of 0.47 μmol L^{-1}), had a proportionally higher percentage of Fe in its reduced form (21%).

PO_4^{3-} concentrations were similar to those found in previous SLW measurements (Table 5-9), with SL being of the same order of magnitude (average value 0.14 μmol L^{-1}), whilst GL was slightly lower (0.02 μmol L^{-1}). Finally, H_4SiO_4 concentrations were two orders of magnitude higher than in previous SLW measurements presented here (with average values of 260 and 170 μmol L^{-1} for SL and GL samples respectively).

Table 5-6 Concentrations of major ions and nutrients after incubation with crushed top layer SLW sediments. "CONCENTRATION IN LITERATURE" from Michaud et al. (2016) (at depths of 1 and 3 cm), except for * and ** ions. * = from surface sediment measurements in Christner et al. (2014). ** = from lake water measurements in Christner et al. (2014). "FROM POREWATER" calculated as described in Section 5.3.3. "CRUSH-WET" concentrations from water samples incubated with crushed top layer SLW samples. "CORRECTED CONCENTRATION" refer to concentrations not accounted for by the dilution of pre-existing ions in pore waters.

	Cl^-	SO_4^{2-}	Na^+	K^+	Mg^{2+}	Ca^{2+}	F^- *	Si	Fe^{2+}	Fe total	TON	PO_4^{3-}	NH_4^- **	Acetate **
	(meq L^{-1})							(µmol L^{-1})						
CONCENTRATION IN LITERATURE	4.05	1.30	7.05	0.405	0.565	0.920	0.034	0.105	n.r.	n.r.	n.r.	n.r.	2.40	1.30
CONC. FROM POREWATER.	1.05	0.337	1.83	0.105	0.147	0.239	0.009	0.027	0.000	0.000	0.000	0.000	0.623	0.337
CRUSH-WET	2.23	0.918	4.74	1.20	0.468	0.108	0.173	3.90	0.729	21.5	-0.526	0.058	116	338
CORRECTED CONCENTRATION	1.18	0.581	2.91	1.09	0.321	-0.130	0.164	3.87	0.729	21.5	-0.526	0.058	116	338

Table 5-7 Concentrations of major ions and nutrients after incubation with crushed middle layers SLW sediments. "CONCENTRATION IN LITERATURE" from Michaud et al. (2016) (at depths of 21 and 23 cm). "FROM POREWATERS" calculated as described in Section 5.3.3 using average weights of sediments incubated for CRUSH-WET and DIS-WET experiments. "CRUSH-WET" and "DIS-WET" concentrations from water samples incubated with crushed and disaggregated sediments, respectively. "CORRECTED CONCENTRATION" refer to concentrations not accounted for by the dilution of pre-existing ions in pore waters.

	Cl^-	SO_4^{2-}	Na^+	K^+	Mg^{2+}	Ca^{2+}	F^-	Si	Fe^{2+}	Fe total	TON	PO_4^{3-}	NH_4^-	Acetate
	(meq L^{-1})							(µmol L^{-1})						
CONCENTRATION IN LITERATURE	17.0	3.00	20.5	0.570	1.55	1.5	n.r.	n.r.	n.r.	n.r.	n.r.	n.r.	n.r.	n.r.
CONC. FROM POREWATER. (CRUSH)	**3.27**	**0.577**	**3.95**	**0.110**	**0.298**	**0.289**	**0.000**	**0.000**	**0.000**	**0.0**	**0.000**	**0.000**	**0.000**	0.000
CONC.FROM POREWATER. (DIS)	3.25	0.574	3.93	0.109	0.297	0.287	0.000	0.000	0.000	0.0	0.000	0.000	0.000	0.000
CRUSH-WET	**4.70**	**3.43**	**12.00**	**1.472**	**0.608**	**0.192**	**0.213**	**4.69**	**0.884**	**17.4**	**-0.555**	**0.929**	**108**	284
DIS-WET	3.35	3.20	9.99	0.51	0.164	0.148	0.211	2.90	0.184	16.0	4.01	2.37	3.78	92.7
CORRECTED CONCENTRATION (CRUSH-WET)	**1.428**	**2.85**	**8.05**	**1.363**	**0.309**	**-0.097**	**0.213**	**4.69**	**0.884**	**17.4**	**-0.555**	**0.929**	**108**	284
CORRECTED CONCENTRATION (DIS-WET)	0.09	2.63	6.07	0.40	-0.133	-0.139	0.211	2.90	0.184	16.0	4.01	2.37	3.78	92.7

Table 5-8 Concentrations of major ions and nutrients after incubation with crushed bottom layer SLW sediments. "CONCENTRATION IN LITERATURE" from Michaud et al. (2016) (at a depth of 37 cm). "FROM POREWATER" calculated as described in Section 5.3.3 using average weights of sediments incubated for CRUSH-WET and DIS-WET experiments. "CRUSH-WET" and "DIS-WET" concentrations from water samples incubated with crushed and disaggregated sediments, respectively. "CORRECTED CONCENTRATION" refer to concentrations not accounted for by the dilution of pre-existing ions in pore waters.

	Cl^-	SO_4^{2-}	Na^+	K^+	Mg^{2+}	Ca^{2+}	F^-	Si	Fe^{2+}	Fe total	TON	PO_4^{3-}	NH_4^-	Acetate
	(meq L^{-1})							(µmol L^{-1})						
CONCENTRATION IN LITERATURE	22.0	4.10	28.0	0.540	2.30	1.70	n.r.	n.r.	n.r.	n.r.	n.r.	n.r.	n.r.	n.r.
CONC. FROM POREWATER (CRUSH)	**3.62**	**0.674**	**4.60**	**0.089**	**0.378**	**0.279**	**0.000**	**0.000**	**0.000**	**0.000**	**0.000**	**0.000**	**0.000**	**0.000**
CONC.FROM POREWATER (DIS)	3.67	0.685	4.68	0.090	0.384	0.284	0.000	0.000	0.000	0.000	0.000	0.000	0.000	0.000
CRUSH-WET	**4.85**	**5.29**	**9.41**	**1.33**	**1.44**	**0.278**	**0.172**	**3.78**	**1.02**	**22.7**	**-0.926**	**0.019**	**120**	**0.280**
DIS-WET	4.88	6.05	9.81	0.507	0.313	0.301	0.188	2.52	0.134	15.9	1.04	2.62	0.480	0.168
CORRECTED CONCENTRATION (CRUSH-WET)	**1.23**	**4.62**	**4.81**	**1.24**	**1.07**	**-0.002**	**0.172**	**3.78**	**1.02**	**22.7**	**-0.926**	**0.019**	**120**	**0.280**
CORRECTED CONCENTRATION (DIS-WET)	1.21	5.37	5.14	0.417	-0.071	0.017	0.188	2.52	0.134	15.9	1.04	2.62	0.480	0.168

Table 5-9 Concentration of major ions and nutrients after incubation with crushed Whillans:Iso samples.

		AVERAGE RESULTS (BLANK CORRECTED - EXCEPT FOR BLANKS)									
		Acetate	NH_4	NO_2	TON	Fe^{2+}	Fe total	PO_4^{3-}	SiO_4^{4-}	pH	Conductivity (mS/cm)
BLANKS	- µM	0.00	7.12	0.09	1.41	0.108	0.037	0.555	3.33	6.32	0.01
SUBGLACIAL LAKE (SL) - µmol/g		4.48	0.125	-5.1×10^{-4}	1.5×10^{-3}	2.4×10^{-3}	0.026	1.5×10^{-4}	0.260	7.70	0.88
	- µM	371	124	-0.503	1.47	2.37	25.4	0.145	258		
GROUNDING LINE (GL) - µmol/g		0.0	0.238	7.5×10^{-5}	-9.5×10^{-4}	4.8×10^{-4}	2.3E-03	1.8×10^{-5}	0.167	7.29	7.42
	- µM	0.0	238	0.076	-0.953	0.483	2.56	0.018	167		

Table 5-10 Concentration of DOC after incubation Whillans:Iso

	mMOL DOC L^{-1} (SEDIMENT LOADING ~0.75g/mL)	**mg DOC g^{-1} CRUSHED SEDIMENT**
SUBGLACIAL LAKE WHILLANS (SL)	2.87	0.042
WHILLANS GROUNDING LINE (GL)	3.29	0.047

5.3.3.4 DOC

The larger volumes of sediment and water required to produce sufficient gas for the analysis of the isotopic composition meant that DOC analysis could be carried out on the water fraction. DOC concentrations were very similar for both SL and GL incubations (Table 5-10). The mM concentrations of DOC, however, were an order of magnitude higher than the DOC concentrations found in situ in the subglacial lake waters (Christner et al., 2014), despite the likely dilution effect to any pre-existing DOC in solution through sample preparation.

5.3.3.5 DOM

Fluorolog and PARAFAC analysis was carried out in both SLW and Whillans:Iso samples, but only SLW results are discussed here. This is because, although there was some evidence of DOM in both GL and SL Whillans Iso samples (see Appendix F), there were not enough replicates to fit reliable modelled components. DOM for both SL and GL samples appears to fall roughly in the same area as SLW samples, however the fluorescence intensity is as low or lower than for SLW samples. A possible reason for the limited fluorescence intensity, despite the high DOC values, is due to inner-filtering effects which can occur with high DOC concentrations (Hudson et al., 2007).

There was evidence of DOM in disaggregated samples and in some crushed samples. The presence of DOM was not consistent for both treatments (a complete set of results can be found in Appendix G), but we attempted to model the DOM present in crushed and disaggregated samples using the PARAFAC method, as described in Murphy et al. (2013). However, due to low sample numbers, low concentrations and inconsistent results, the modelled components contain significant errors. This is particularly true of crushed samples. The PARAFAC modelled results for CRUSH-WET samples suggested that only

one component is present with excitation peak falling between 320-360 nm and the emission peak falling somewhere between 420-460 nm (Figure 5-3).

One and two components were modelled using PARAFAC on DIS-WET samples (Figure 5-2 and Figure 5-4 respectively). Originally only one component was modelled to describe the EEM signatures for DIS-WET samples (Figure 5-2b). The errors for this model (Figure 5-2c) appeared to concentrate in two areas surrounding the modelled component. Therefore, two components were modelled (Figure 5-4) to describe the composition of fluorescent DOM in DIS-WET waters. The errors found were more evenly spread, suggesting two DOM components exist. However, these still fall within the same range as our modelled CRUSH-WET samples. It is also worth noting there are still very large uncertainties with these models.

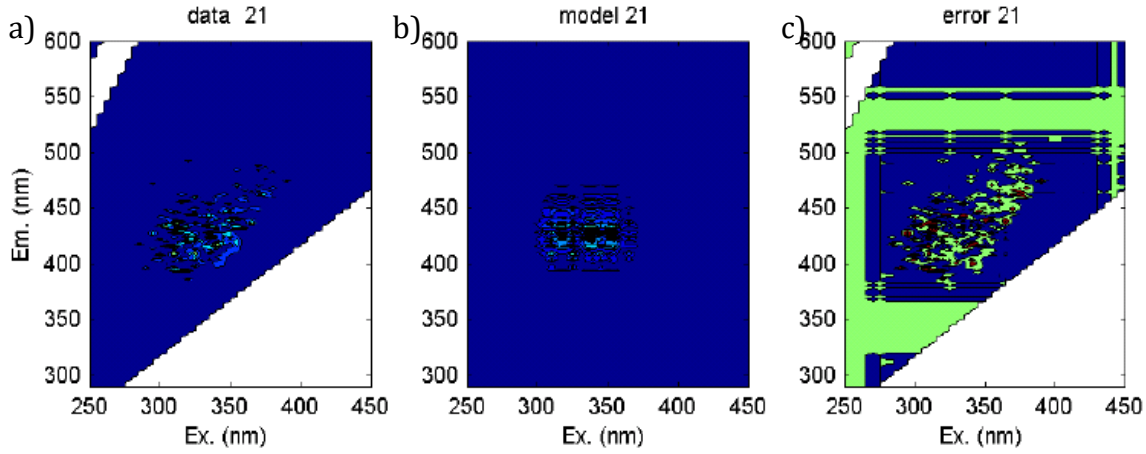

Figure 5-3 CRUSH-WET PARAFAC modelled components. a) average data; b) one component modelled using PARAFAC; c) errors.

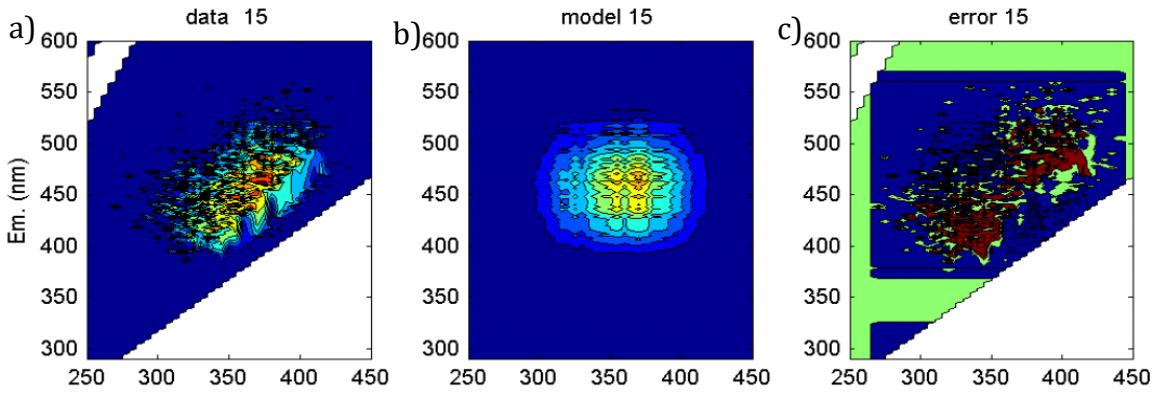

Figure 5-2 DIS-WET PARAFAC modelled component. a) average data; b) one component modelled using PARAFAC; c) errors.

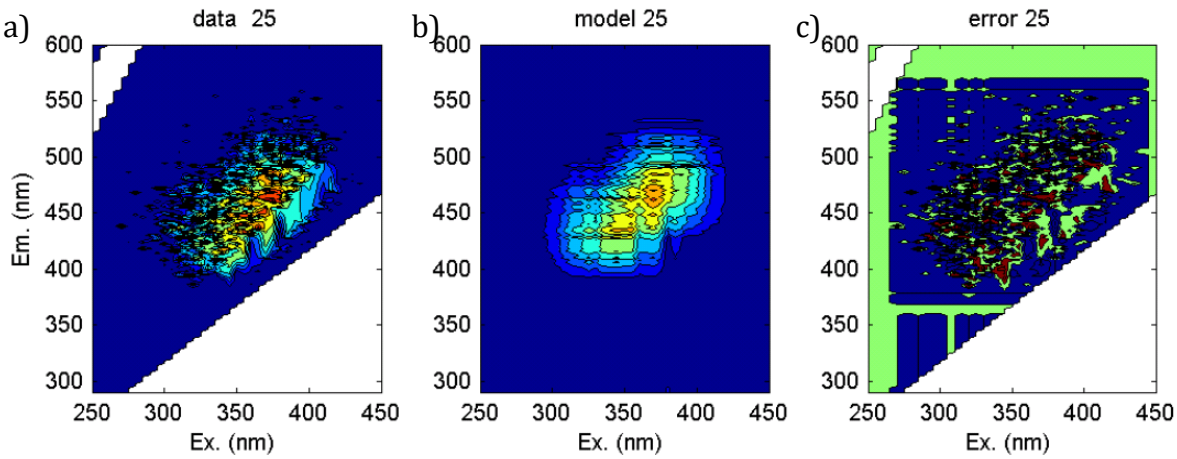

Figure 5-4 DIS-WET PARAFAC modelled components. a) average data; b) two components modelled using PARAFAC; c) errors.

5.4 Discussion

5.4.1 Release of Fluid Inclusions

It was mentioned previously (Section 3.4.1) that there is evidence of the release of gases, and presumably solute, from fluid inclusions during the initial crushing of SLW sediments (Table 3-2). The dominant gases released during the initial crush were CO_2 and H_2, with minor releases of CH_4, consistent with the release of fluid inclusions in granites and quartz syenites (Konnerupmadsen and Rosehansen, 1982). This might be anticipated due to the high percentage of quartz (59%) in SLW (Michaud et al., 2016). The release of ethylene and other hydrocarbons throughout the incubation could also be attributed to the slow release from fluid inclusions, particularly for the gases released by CRUSH-DRY samples.

Further evidence for the release of gases and solutes from fluid inclusions comes from the water chemistry analysis (Table 5-6, Table 5-7 and Table 5-8). The water chemistry was corrected for solutes in porewaters using estimated concentrations calculated from Michaud et al. (2016). After this correction, the ionic contributions from a sea-water component is removed since this component would primarily come from pre-existing concentrations in SLW pore-waters. Therefore, any Cl^- present in solution after correction is potentially due to the release from fluid inclusions. Cl^- was found in all samples, even after porewater correction, consistent with the hypothesis that gases and solutes in fluid inclusions are released during crushing. Fluid inclusions can form in sedimentary and

diagenetic minerals, which are found in a range of environments, quite often marine environments (Goldstein, 2001). Fluid inclusions formed in these minerals will contain microsamples of the sea water and atmosphere at the time of formation (Goldstein, 2001), and will include ions such as Na^{+}, Mg^{2+}, Fl^{-} and SO_4^{2-}. Their composition will also be influenced by the processes of formation, including different diagenesis and deposition environments (Goldstein, 2001), resulting in a highly variable chemical composition. Thus, although the presence of Cl^{-} in the water fraction allows us to confirm that fluid inclusions were indeed released during crushing and disaggregation (except possibly in the middle DIS-WET samples), it is difficult to separate the effect of fluid inclusions from that of weathering on the composition of the water chemistry.

5.4.2 Weathering Influenced by Crushing

Currently, it is believed that carbonate and silicate weathering processes dominate subglacial hydrochemistry (Tranter et al., 2002b). The degree to which each of these contributes depends not only on the mineralogical composition of the sediments, but also on the contact time between water and subglacial sediment (Wadham et al., 2010). Cation exchange will also determine the composition of these waters, with divalent cations in solution exchanging for monovalent cations on the surface of exchange sites (such as mineral surfaces) (Tranter et al., 2002b). Previous analysis of SLW pore waters showed silicate weathering to be the main source of ions in solution, with some evidence of cation exchange (Michaud et al., 2016). This is consistent with reactions inferred for subglacial environments under large ice-sheets (Wadham et al., 2010). Analysis of the water samples after incubation with both crushed and disaggregated sediments not only allows us to confirm fluid inclusions as an additional source of solute, but also allows us to infer if this is a dominant source of solute to subglacial systems.

The contribution from previous weathering environments to the solute was estimated by subtracting the pore water chemistries obtained by Michaud et al. (2016) from our results to identify the possible effects of crushing and disaggregation on the subglacial waters. However, subglacial hydrochemistry arises from a complex set of interacting reactions, which are potentially further complicated by crushed sediment releasing fluid inclusions. Thus, it becomes potentially much harder to unravel the reactions governing the solute composition in these waters.

Carbonate hydrolysis is one of the first weathering reactions to occur in subglacial systems due to its rapid reaction kinetics (Tranter et al., 2002b). Since the sediments used in these experiments are highly weathered, we would expect any carbonates to have weathered away before SLW was sampled. However, our incubations revealed Mg^{2+} to be released after incubation of water with crushed sediment. This is often associated with carbonate weathering. Ca^{2+} is often associated with carbonate weathering, however our results showed negative Ca^{2+} concentrations after corrections for porewaters were carried out (Table 5-6, Table 5-7, Table 5-8). This can be explained by the exchange of divalent cations in solution for monovalent cations on the surface of exchange sites (such as mineral surfaces) which is one of the first reactions to occur when water comes into contact with glacial debris (Tranter et al., 2002b). This could possibly explain the high concentrations of monovalent ions in solution.

Both Mg^{2+} and Ca^{2+} were negative after correcting for porewaters in the disaggregated samples (Table 5-6, Table 5-7, Table 5-8). This suggests that either a sink for both these ions exist in disaggregated samples, or an additional source of these ions exists in crushed samples. Sources of these ions could include previously unreacted calcite, which has become exposed to water and weathering reactions during crushing, or in the case of Mg^{2+}, this could be result of released fluid inclusions. However, the Cl^- concentrations were similar for crushed and disaggregated sediments (Table 5-6, Table 5-7, Table 5-8), suggesting the solute concentrations are not greatly affected by fluid inclusion release. Typical sinks for Mg^{2+} and Ca^{2+} is through cation exchange of divalent ions in solution for monovalent ions in clay minerals (Tranter et al., 2002b).

The presence of both K^+ and Na^+ (Table 5-6, Table 5-7, Table 5-8) indicate silicate hydrolysis is also likely to be taking place during these incubations (Tranter et al., 2002b). As with Mg^{2+}, the concentrations of K^+ were noticeably higher in crushed samples than in their disaggregated counterparts (Table 5-6, Table 5-7, Table 5-8), suggesting crushing can reveal fresh mineral surfaces which are readily weathered. Fluid inclusions, due to their composition, are likely to contribute to Na^+ solute (Goldstein, 2001). This can therefore mask the solute contributions from other processes, such as weathering. However, without knowing the composition of fluid inclusions, it is difficult to separate these processes. A possible reason for the similarity in crushed and disaggregated Na^+ concentrations is the possible increased potential for cation exchange of disaggregated

samples versus crushed samples. DIS-WET samples not only had higher Na^+ with respect to K^+ in solution, but also had negative Mg^{2+} and Ca^{2+} after porewater corrections, suggesting cation exchange between divalent ions in solution and monovalent ions at the surface of clay minerals.

Sulphide oxidation, often coupled to either carbonate or silicate hydrolysis, is another common subglacial weathering reaction (Tranter et al., 2002b). The presence of SO_4^{2-} in solution (Table 5-6, Table 5-7, Table 5-8) indicates that this might also be true during these incubations. It has also been suggested that in anoxic environments, sulphide oxidation might occur through the use of Fe^{3+} instead of oxygen. Our water analysis revealed the presence of both Fe^{3+} and Fe^{2+} in solution (Table 5-6, Table 5-7, Table 5-8, Table 5-9), with increased concentrations of reduced Fe^{2+} in crushed samples. However, increases in reduced Fe^{2+} do not correspond to increased SO_4^{2+} concentrations, as would be expected from equation 8 (Section 1.2.2, Table 1-1) and do not support the stoichiometry of the reactions suggested in this same equation. Therefore, SO_4^{2+} solute is likely to be a result of fluid inclusion releases, although this would likely only be a minor contribution. There remains the possibility that other mechanisms of sulphide oxidation exist, which we have not yet identified. This could include oxidation by H_2O_2, which was detected after the reaction of crushed rocks with water (Section 4.3.1), or even oxidation powered by other metals with various oxidation states (e.g. Manganese; Holmkvist et al. (2011)).

Crushing also increased the NH_4^+ concentration in crushed versus disaggregated samples (Table 5-6, Table 5-7, Table 5-8, Table 5-9). Traditionally, NH_4^+ has been suggested to arise from cation exchange of NH_4^+, within clay minerals (such as illite or tobelite), for K^+ in solution (Manning and Hutcheon, 2004). When this NH_4^+ becomes exposed, through fractures in the clay minerals, it can be exchanged for K^+ as it is of a very similar size (Manning and Hutcheon, 2004). Through crushing, we are likely to increase the fractures in clay minerals, exposing more NH_4^+ for cation exchange. However, there are other sources of NH_4^+ which might also be relevant to SLW.

5.4.3 Re-Activation of Organic Matter

There is evidence of nitrogen-enriched sedimentary organic matter in SLW (Christner et al., 2014). There was a significant concentration of DOC found in both crushed grounding line and subglacial lake sample incubations for isotopic analysis (Section 5.2.4.4).

Unfortunately, DOC was not measured in disaggregated samples or in the original SLW samples. There was a stronger DOM signal in disaggregated samples than in crushed samples, perhaps rather surprisingly, and there was still an indication of DOM presence in some crushed samples (Section 5.2.4.3). DOM present in both CRUSH-WET and DIS-WET (and even Whillans:Iso samples) appeared to fall within the range of "visible humic-like material" (Stedmon et al., 2003), even when more than one component was modelled. Humic-like material was initially thought to be highly refractory, but studies have shown that it can degrade to low-molecular-weight carbonyl compounds through the production of free radicals associated to UV photodegradation (Kieber et al., 1990).

A possible reason for the decrease in fluorescent DOM found after crushing is the degeneration of this organic matter into more bio-available forms through the process of crushing. We caution that fluorescence intensity can be affected by the composition of our waters, and thus these results should be interpreted with caution. Perhaps the most likely source of interference in our water samples is the presence of iron in solution (see Table 5-6, Table 5-7 and Table 5-8) which could quench fluorescence intensity, by the formation of organo-metal complexes (Hudson et al., 2007), or possibly even inner-filtering effects from high DOC concentrations, which could also be reducing fluoresce intensity (Hudson et al., 2007). Nevertheless, these results still offer some insight into the possible effects of crushing on OM, particularly when taken in combination with other results found.

Crushing was shown to produce H_2O_2 (Section 4.3.1, Table 4-2) which not only have we interpreted here to be a proxy for the presence of ·OH, but has also been suggested to be able to reverse between H_2O_2, ·OH and HOO· states (Anastasio and Jordan, 2004). The reaction of photochemically produced ·OH with OM has been widely studied in snowpack, as described below (Domine and Shepson, 2002, Dibb and Arsenault, 2002, Anastasio and Jordan, 2004, Swanson et al., 2002, Grannas et al., 2004). However, the possible reaction of mechanochemically formed ·OH with OM has not been explored to date.

The production of ethylene and other alkenes has been linked to the reaction of organic matter with ·OH (Swanson et al., 2002). Therefore, the presence of alkenes in the headspace (Table 5-3, Table 5-4 and Table 5-5) could be a result of the reaction of particulate OM with ·OH after crushing, which leaves less DOM in solution. Further, the oxidation of alkenes is believed to be a major source of monocarboxylic acids which act

as precursors to carboxylate ions (such as acetate) (Dibb and Arsenault, 2002), thus ethylene measured in SLW samples (Section 5.3.1) might be further oxidised by ·OH to produce acetate.

Acetate can also be produced directly by the reaction of OM with ·OH (Anastasio et al., 2007). Therefore, DOM in solution found after crushing could be converted to other, more available forms after reacting with ·OH. Acetate was found in both crushed and disaggregated SLW samples (Table 5-6, Table 5-7, Table 5-8) and in SL samples for isotopic composition (Table 5-9), and its concentration was considerably higher in crushed than in disaggregated samples, indicating that these mechanisms might indeed be transforming any OM into more bio-available forms. Furthermore, although methane concentrations found in SLW have been suggested to be produced by hydrogenotrophic methanogenesis (Michaud et al., 2017), previous models have proposed that methane reservoirs found under the West Antarctic Ice Sheet (WAIS) are formed through acetoclastic methanogenesis (Wadham et al., 2012). There is also evidence suggesting that the subglacial lakes beneath the Whillans Ice Stream (WIS) are hydrologically connected (Carter et al., 2013). Therefore, even if the acetate is not used in-situ for methanogenesis, it might be transported to areas where acetoclastic methanogenesis is dominant.

Finally, NH_4^+ has not only been linked to cation exchange, it is also associated to organic matter degradation. Lingle et al. (2017) suggested the degradation of organic matter in sedimentary glacial sediments as the source of NH_4^+ in a glacial drift aquifer in Michigan. In geothermal areas, increased NH_4^+ concentrations have been suggested to be a result of thermal degradation of the organic matter which is contained within sedimentary rocks (Holloway et al., 2011). There is evidence of nitrogen-enriched sedimentary organic matter in SLW (Christner et al., 2014), the degradation of this could be enhanced by crushing, as a larger surface area is exposed to weathering and the effects of free-radicals, as well as any possible thermal degradation that might have occurred during crushing, providing the CRUSH-WET samples with large NH_4^+ concentrations.

5.5 Conclusions

Although results are somewhat limited by the low sample levels and lack of pH measurements, there is evidence of increased carbonate and silicate weathering

reactions after crushing of sediments. This is likely due to the increased surface area associated with sediment comminution. Further, there is some indication of cation exchange. However, the weathering results may be masked by the solute released from fractured fluid inclusions. Quite interestingly, these preliminary results hint at the potential organic matter reactivation, from more re-calcitrant organic matter forms (i.e. visible humic-like material) to more labile forms of carbon (in the form of acetate and carboxylic acids) and nitrogen (in the form of NH_4^+). Further investigation is required to establish the mechanisms by which this might happen, however, hydroxyl radicals are likely to play a key role in this.

Chapter 6 Synthesis of Results and Conclusions

6.1 Summary

This project set out to investigate the potential impact that crushing and its associated mechanochemical reactions has on subglacial environments. More specifically, it focused on the potential effects of crushing at the bed of the ice sheet on the release of nutrients and energy to the microbial ecosystems found in these environments. It is known that crushing of unweathered rocks can release microbially relevant compounds (Telling et al., 2015). Throughout the course of this thesis, it has been shown that erosion of highly weathered subglacial lake sediments, sampled directly from SLW, could potentially also release similar bio-utilisable compounds.

The possible effects of subglacial crushing of sediments was studied via three objectives. First, we wanted to confirm H_2 was not only produced when crushing unweathered rocks, but also when crushing highly weathered subglacial sediments (Objective 1). Objective 1 also attempted to measure any other gasses which might be relevant to the microbial populations found in SLW (e.g. methanogens and methanotrophs (Michaud et al., 2017)). Therefore, CO_2 and CH_4 production were also monitored. Our results showed that H_2 is produced during incubations of crushed highly weathered sediments, such as those found in SLW, under atmospheric pressures and at 0°C. H_2 was instantly produced during the crushing, with concentrations of up to 110 nmol of H_2 g^{-1}. Considerable CO_2 concentrations were also recorded, both during crushing and during the subsequent incubation of crushed sediments. The existence of several methanogen species in a range of subglacial environments (Boyd et al., 2010, Michaud et al., 2017, Stibal et al., 2012b, Wadham et al., 2008) makes both these gases relevant to not only SLW but the wider subglacial environment. The concentration of H_2 released from a 30 minute crush and the subsequent incubation of the top centimetre of sediment from SLW was calculated to account for approximately 10% of the H_2 necessary for the CH_4 flux estimated in SLW (Michaud et al., 2017), and CO_2 from this same process could account for about a third of the CO_2 necessary for that same CH_4 flux. Thus, crushing of SLW sediments has the potential to produce gases which support the methane flux which has been suggested to be produced by methanogenic bacteria in SLW (Michaud et al., 2017). Further, we found crushing of SLW sediments and their incubation also produced CH_4, another gas of

microbial relevance, particularly given the presence of methanotrophs found in SLW (Michaud et al., 2017). The CH_4 contributions from crushing of SLW sediments were considerably lower than H_2 and CO_2 but could still contribute to the methane flux estimated in SLW. Thus, crushing can support some of the microbial carbon cycling processes which are essential for the maintenance of the microbial populations found in SLW (Achberger et al., 2016).

The second objective of this project was to gain a better understanding of the processes by which gases detected in Objective 1 are being produced during crushing and incubation of SLW sediments. Understanding the detail of these reactions is challenging, particularly when looking at free-radical reactions which are highly reactive and unstable, and which are not well understood. Like in Telling et al. (2015), silicate surface radicals were detected, preferentially in crushed samples, but considerable Si· concentrations were also detected after relatively gentle disaggregation of the sediment. Silicate surface radicals have been credited for H_2 production (Kita et al., 1982, Telling et al., 2015). Here, we suggest that is also the case, but we further suggest that other radicals might be involved in different reactions too. In Chapter 4, it was also suggested that SiO· could form as the counterpart to Si· when Si≡O≡Si bonds are broken, and that these can react with water to produce ·OH. Unfortunately, despite attempting several methods to measure ·OH, all the attempts were unsuccessful. It has been suggested that two ·OH can react together to produce H_2O_2, which was successfully measured in SLW samples. Like surface radicals, the concentration of H_2O_2 increased after crushing, supporting the hypothesis that ·OH are formed simultaneously with Si· during crushing. Both ·OH and H_2O_2 could be subglacially relevant, as they are strong oxidising agents. Combined with the H_2 detected, it was suggested that crushing can produce microenvironments which expand the whole natural range of REDOX conditions on crushed subglacial debris. This is particularly relevant to the nutrient cycling of REDOX sensitive species, such as Fe and S, which are utilised by some of the species found in SLW (Purcell et al., 2014, Mikucki et al., 2016). The presence of H_2O_2, and consequently ·OH, can also elucidate the presence of other hydrocarbons and carboxylates which were detected after the incubation of crushed sediments in water (Chapter 5). Isotopic analysis of the gases and other incubations looking at potential serpentinization and FTT reactions were also carried out. However, the results of these were inconclusive.

The final objective of this project (Objective 3) was to explore other previously unimagined effects of crushing on the subglacial environment. To do this, the gases released during initial crushing and the incubation were analysed in order to measure any hydrocarbons present, and the aqueous phase of the incubation was also analysed. It was discovered that crushing appeared to not only release considerable amounts of bio-utilisable gases, such as H_2, CH_4 and CO_2, but also released trace amounts of a number of hydrocarbons. It was suggested that the initial release of these gases could be a result of fluid inclusions, which had been suggested to potentially release solute and gases to subglacial environments during erosion (Telling et al., 2015), but which had not been quantified. Chapter 5 showed gases released from fluid inclusions could provide an important source of energy to subglacial microbial ecosystems.

Analysis of the trace gases released during crushing and in the headspace of incubated sediments contained several hydrocarbons. This, together with the presence of acetate in the aqueous fraction of sediment slurry, suggests that crushing can increase the available C to microbial communities. This increased availability of labile C sources has been linked to recalcitrant OM reacting with ·OH more bio-available forms of OM (Anastasio et al., 2007). Thus, crushing or erosion of heavily weathered SLW sediments could potentially assist the C-cycling necessary for sustaining the microbial communities found in SLW.

Water chemistry analysis of the incubated fraction also revealed the increase in concentration of several inorganic ions, and the decrease of others, suggesting increased cation exchange after crushing. The considerable increase in salinity supported the theory that fluid inclusions, which contain traces of salts and other evaporites (Goldstein, 2001), could be released to this environment through crushing and, to a lesser extent, through disaggregation of sediments. Crushing of sediments can potentially increase their surface area. Our results suggested that this also leads to increased chemical weathering of sediments. Some of the most common subglacial weathering reactions are often catalysed by microbes, thus this increased surface area could potentially also contribute to the microbial ecosystem within SLW.

6.2 Theoretical Implications

The results presented here demonstrate that crushing and even (to a certain extent) gentle disaggregation of SLW sediments has the potential to increase the availability of nutrients and energy sources relevant to the microbial communities found to date in SLW. However, it is difficult to know with any certainty to what extent SLW sediments undergo erosion in-situ. Hodson et al. (2016b) suggest that sediments under SLW undergo ductile deformation. However, there is still evidence of sheared fabrics, suggesting some level of erosion occurs in SLW. Our results showed that even gentle disaggregation of sediment for a few minutes could release significant amounts of H_2, CO_2 and some CH_4. Thus, it is suggested that only minimal erosion would be necessary to release these gases in the subglacial environment. Furthermore, continuous erosion of these sediments would be expected to continue to release gases. The erosional processes by which these gases are released are particularly likely to take place in active lakes, such as SWL, since they are likely to become (at least) partly grounded on the edges of the lake during draining events, and can even become fully grounded (e.g. 2004 (Hodson et al., 2016b)), during these events. Shear and further comminution may then occur. SLW is part of a wider hydrological network (Fricker and Scambos, 2009), therefore despite Hodson et al. (2016b) suggesting there is not much erosion taking place at SLW and not much sediment transport occurring, several others have identified a till wedge at WGL (Anandakrishnan et al., 2007, Christianson et al., 2016, Muto et al., 2013) which has been suggested to be formed as a result of subglacially transported till (Alley et al., 1987, Blankenship et al., 1987) which has been deposited at WGL. Consequently, it is likely that at least some level of erosion exists throughout this hydrological system and the gases and nutrients released can be transported throughout the subglacial system. Some erosion might also be occurring at "sticky-spots", which have been identified below the WIS (Luthra et al., 2016), where there is high basal drag and likely high erosive power.

As mentioned in the previous section (Section 6.1), the effects of crushing and erosion can sustain several of the microbial consortia which have been found in SLW so far and could sustain nutrient cycling necessary for the maintenance of some of the microbial communities found. This includes C-cycling and cycling of REDOX sensitive species such as Fe and S. Mechanochemical reactions and their effects could also explain some of the distinctive features found in SLW, such as the relatively high NH_4^+ concentration and high

DOC concentration (Christner et al., 2014), which were also seen in waters incubated with crushed samples. Further, Vick-Majors et al. (2016) suggested N was a limiting factor for microbial growth, and crushing could potentially provide a previously unaccounted source of NH_4^+ to the system.

Finally, although the samples studied were only from SLW, these processes are unlikely to be limited to SLW. Yet, until samples are collected from other subglacial environments, we should be cautious of extending our results to the whole of the subglacial environment. Finally, as highlighted earlier, SLW is an active lake, which ultimately drains into the Southern Ocean, and thus the nutrients which are produced during comminution can be discharged into the wider global system.

6.3 Limitations of this Study

Trying to reproduce natural processes in the laboratory is always challenging and the results obtained are not without their limitations. Such is the case when trying to emulate subglacial sediment crushing in the laboratory. There are several factors which cannot presently be fully controlled and a large number of unknowns. Thus, although our results show clearly that SLW sediments could produce a number of bio-utilisable gases, when crushed and during the incubation of crushed sediments at 0°C, we do not know to what extent subglacial erosion takes place and how it relates to our crushing. It is speculated that at least some form of erosion is taking place at the lake edges and at the lake bed itself (during periods of grounding, e.g. 2004 (Hodson et al., 2016b)), as well as further up and down the hydrological system. However, further research and further samples would be necessary to understand how this relates to the degree and periodicity of crushing.

Further, there are a number of limitations related to the laboratory set up. One of these is the temperature control during grinding. Although the reaction of sediments with water were carried out with water at 0°C and vials maintained at 0°C to attempt to reproduce subglacial conditions, it was not possible to control the temperature during grinding. We do not know what temperature is reached in the ball mill at individual comminution sites or if temperature influences radical formation. Subglacial till temperatures during erosion are very poorly constrained, but there is likely much more thermal inertia in these natural erosional environments. Moreover, erosion in subglacial environments, particularly in the context of SLW, will potentially occur in wet sediments.

By contrast, the laboratory experiments occurred without temperature buffering and in a dry environment. More realistic experiments are clearly called for in the future.

There are also a number of limitations that arise from our restricted understanding of the science. SLW was the first of subglacial lake to be sampled, whereas before environmental reactions and conditions in these ecosystems have largely been inferred from subglacial run-off. This offered some great insight into subglacial conditions, but without direct sampling our understanding was restricted. Likewise, free radical reactions are difficult to identify and monitor. Studies on their nature, and the effects of external factors, such as temperature, or how different free-radicals interact, are limited. SLW sediments were composed of a range of minerals and other components, and it follows that trying to understand the reactions which were occurring within this mixed matrix is challenging. As yet, we have only limited understanding of the complex interactions which might arise between different mineralogies and their response to crushing.

Finally, one of the main limitations associated to this study was the sample volumes. Throughout the course of this project there were a number of controls which would have ideally been ran alongside SLW incubations, such as autoclaved incubations (though this could also have its limitations), or different crush times. However, SLW sediments samples are in very scarce supply, and our experimental designs were limited by the mass of sample made available to us. In order to achieve some form of replication, small sample volumes were used, which in turn limited the analysis that could be carried out on the water fraction of incubations. An example of this is the analysis of DOC. Currently, a minimum water volume of 9 ml was necessary for analyses with the level of detail and replication that we would ideally require, and yet only a maximum of 3 ml was extracted from the incubated slurry, precluding detailed analysis of DOC concentrations and quality.

6.4 Future Work

Some of the limitations to this study can be easily addressed in future work. First, this set of experiments were ideal to show the potential for subglacial sediments to produce bioavailable sources of energy and nutrients. However, further work needs to be carried out to understand the processes by which they from. This could be done by crushing model phases (such as quartz, sulphide, carbonates and organic substrates) and analysing the gases released and the solid phases which remain for isotopic composition

to better understand the possible sources of gases and the reactions by which they might form. Then, matrixes of varying mineralogical compositions should be crushed to understand not only the mechanochemical reactions one mineral can undergo during crushing but also to show how these minerals and their products might interact.

The effects of external factors on the formation of radicals and gases should also be explored. This could include crushing of either subglacial sediments or model phases and reacting them with water at different temperatures, then measuring gases or H_2O_2. The timeline of H_2O_2 production and how it might relate to H_2 formation would also inform us on how these reactions might interact. The effect of wet crushing on gas formation should also be explored, as this will more closely emulate crushing in subglacial lake environments. Another external factor that can affect the ability for certain reactions to take place is atmospheric pressure. Subglacial environments are often found under pressure, this can potentially increase the probability of reactions between gases to take place, such as the production of CH_4 from the reactions CO_2 with H_2, or the production of NH_3 from N_2 and H_2, both of which are favourable at high pressure. In subglacial environments high energy erosion will be relatively localised, however there is likely to be some widespread low-energy erosion under large fraction of the ice-sheet bed, where the sediments are saturated with water. To further emulate the possible erosion and crushing that takes place in subglacial environments, experiments looking at the possible releases of gas during low-energy crushing should also be explored.

Finally, although it can be inferred that the processes highlighted here are likely to be taking place in other locations within the wider hydrological system, more sediment and rock samples from the subglacial environment should be analysed to confirm these reactions could potentially occur elsewhere in the hydrological system.

6.5 Concluding Remarks

Despite SLW sediments being heavily weathered, crushing of these sediments produced microbially relevant H_2 concentrations, with concentrations comparable to those of unweathered rocks (Telling et al., 2015). Methanogenic bacteria found deeper within the short SLW sediment cores can potentially utilise this H_2 as an energy source to produce CH_4. Furthermore, these methanogens would also require CO_2, which was also produced during crushing and incubation of the crushed sediments. The production of methane is essential for the maintenance of the methanotrophs in the surface layers of SLW

sediments. This methane has been suggested to be produced by methanogens, however our results showed some of the methane could also be produced abiotically during crushing and incubation of SLW sediments, which could compliment CH_4 production from methanogens.

Crushing can produce extreme REDOX end-members which could assist in the cycling of other REDOX sensitive species. Further, crushing might help C-cycling within these environments, not only through the production of inorganic gases which sustain microbial life, but also in the water phase. Acetate concentrations increased considerably after crushing. This is particularly relevant to some of the methanogenic communities found in SLW which follow an acetoclastic pathway. Therefore, crushing could be essential to these methanogens. Another notable effect of crushing was the increased NH_4^+ concentration after crushing. NH_4^+ concentrations were found to limit the growth of the microbial populations in SLW, and thus crushing might be essential to sustaining these microbial communities.

To conclude, it is clear crushing of SLW sediments could explain some of the phenomena found in SLW waters and be a previously unidentified source of energy and nutrients to these environments. However, our understanding of the reactions taking place is very limited, and further work is required to understand to what extent this might be occurring in SLW or throughout the WIS subglacial hydrological system. Additional sampling of subglacial environments is necessary to confirm these potential reactions are not limited to sediments found in SLW. Results so far show an exciting new aspect of the subglacial environments which could contribute to a fuller and better understanding of the mechanisms by which life is sustained in these extreme environments.

Appendix A

SLW sediment samples.

Appendix B

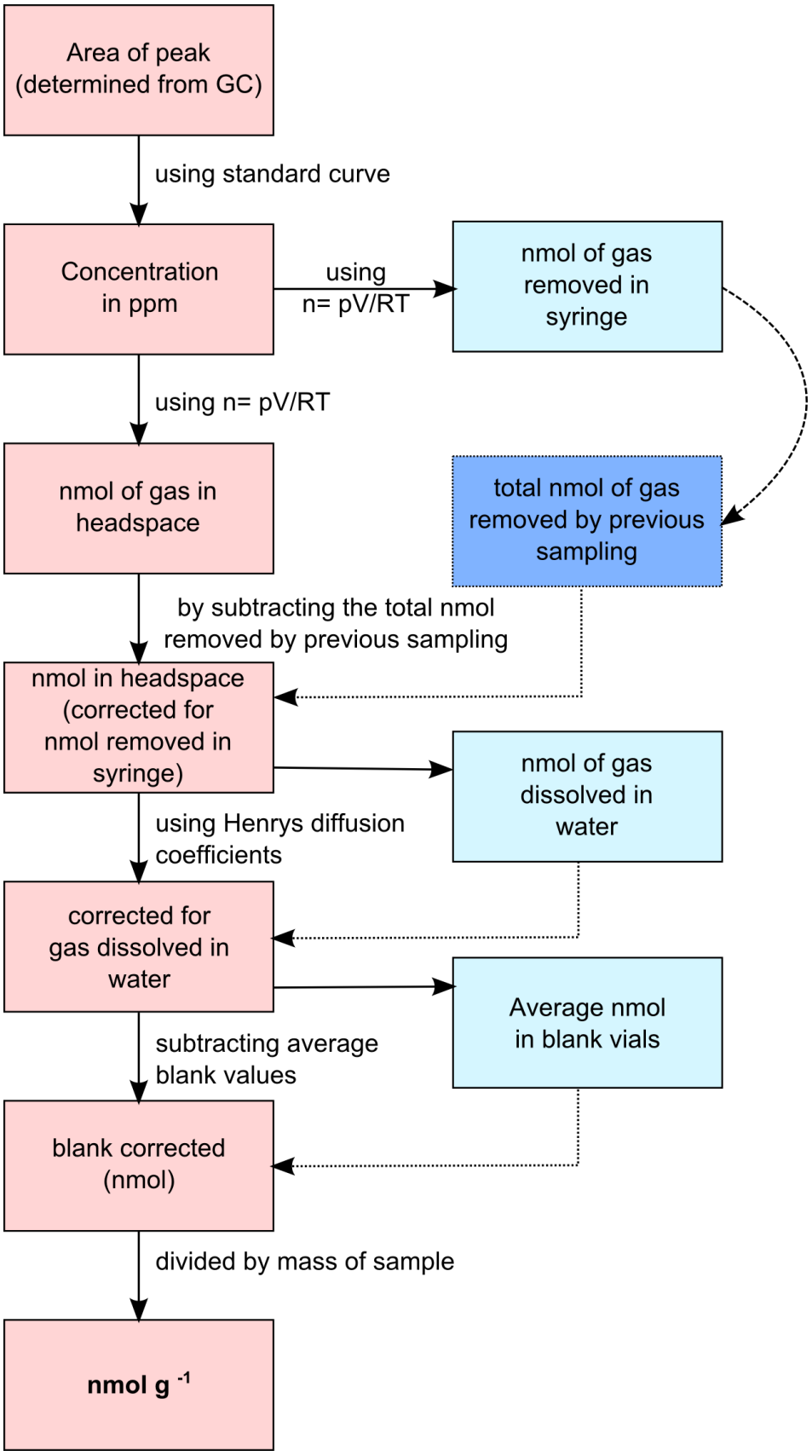
Area of peak (determined from GC)
using standard curve
Concentration in ppm
using n= pV/RT
nmol of gas removed in syringe
using n= pV/RT
nmol of gas in headspace
total nmol of gas removed by previous sampling
by subtracting the total nmol removed by previous sampling
nmol in headspace (corrected for nmol removed in syringe)
nmol of gas dissolved in water
using Henrys diffusion coefficients
corrected for gas dissolved in water
Average nmol in blank vials
subtracting average blank values
blank corrected (nmol)
divided by mass of sample
nmol g -1

Appendix C

One of the pyrite OH-radical formation standard curves produced using the spectrofluorometric method described in Section 4.2.2.2.

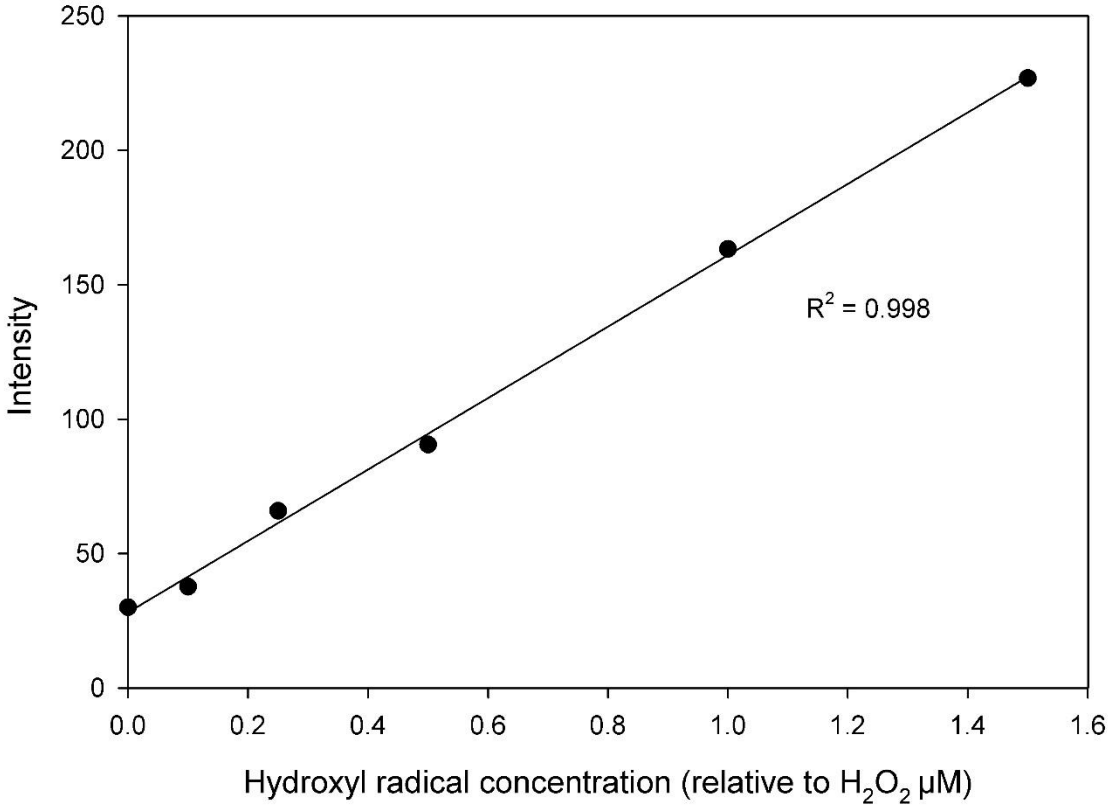

Appendix D

Iron extracted through ascorbate (FeA) and dithionite (FeD) wet chemical extractions, following methods described in Raiswell et al. (2010), Raiswell et al. (2016). Data (currently unpublished), courtesy of Jon Hawkings).

SLW CORE AND DEPTH	%FeA (WET WEIGHT)	%FeD (WET WEIGHT)
SLW(AM)-MC2 0-2CM	0.103	0.083
SLW(AM)-MC3B 14-16 CM	0.040	0.035
SLW(AM)-MC2 20-22CM	0.039	0.028
SLW(AM)-MC3B 28-30 CM	0.032	0.038
SLW(AM)-MC3B 36-38 CM	0.035	0.056

Appendix E

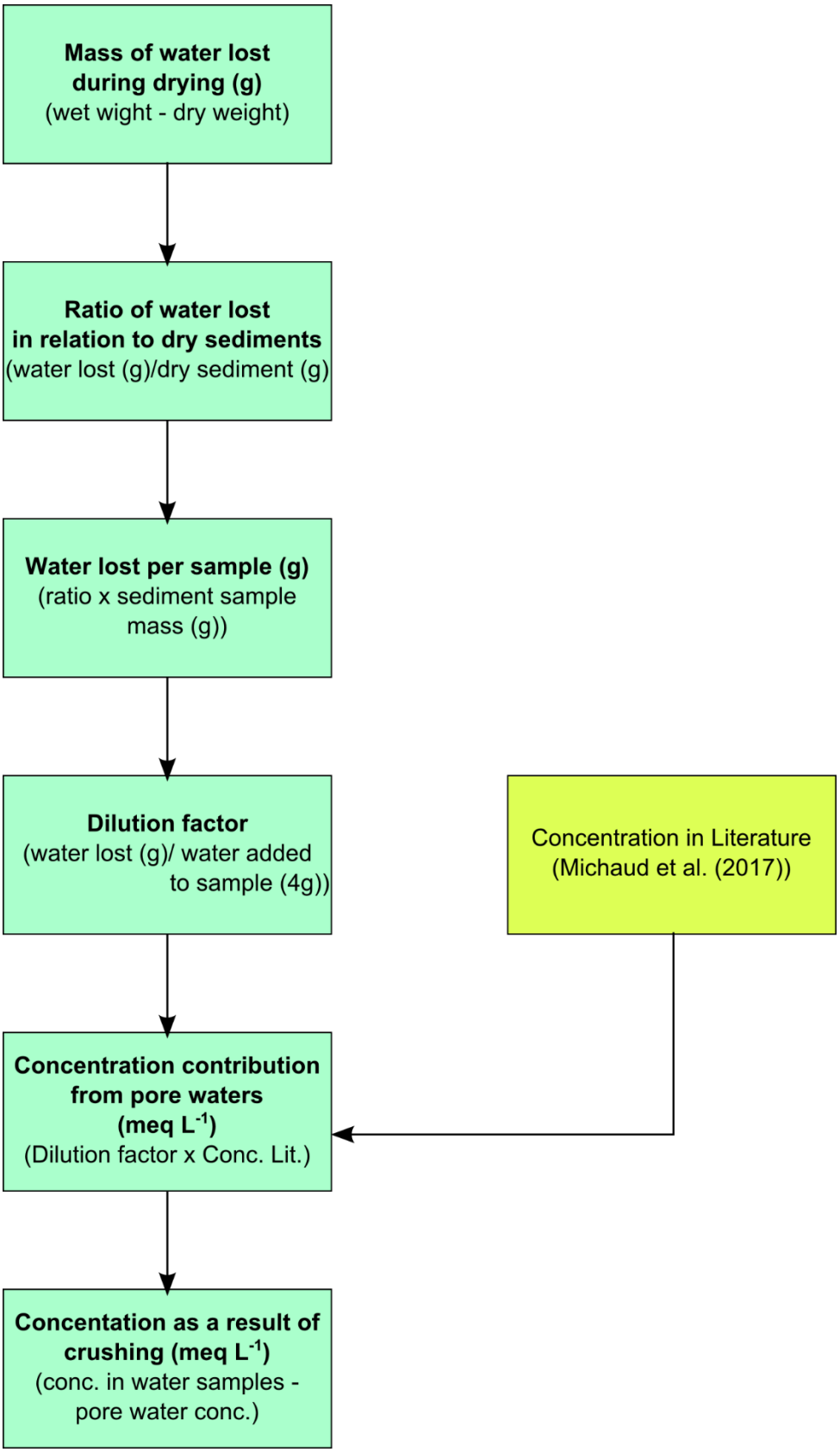
Mass of water lost during drying (g)
(wet wight - dry weight)
Ratio of water lost in relation to dry sediments
(water lost (g)/dry sediment (g)
Water lost per sample (g)
(ratio x sediment sample mass (g))
Dilution factor
(water lost (g)/ water added to sample (4g))
Concentration in Literature
(Michaud et al. (2017))
Concentration contribution from pore waters (meq L-1)
(Dilution factor x Conc. Lit.)
Concentation as a result of crushing (meq L-1)
(conc. in water samples - pore water conc.)

Appendix F

Whillans:Iso SL, GL and Blank eems.

SAMPLE	EEMS FOR TRIPLICATE SAMPLES
WHILLANS:ISO GL	GLW1d1, GLW2d1 and GLW3d1
WHILLANS:ISO SL	LWW1d1, LWW2d1, LWW3d1
BLANKS	SLWBLK2d1, SLWBLK3d1, SLWblk1d1

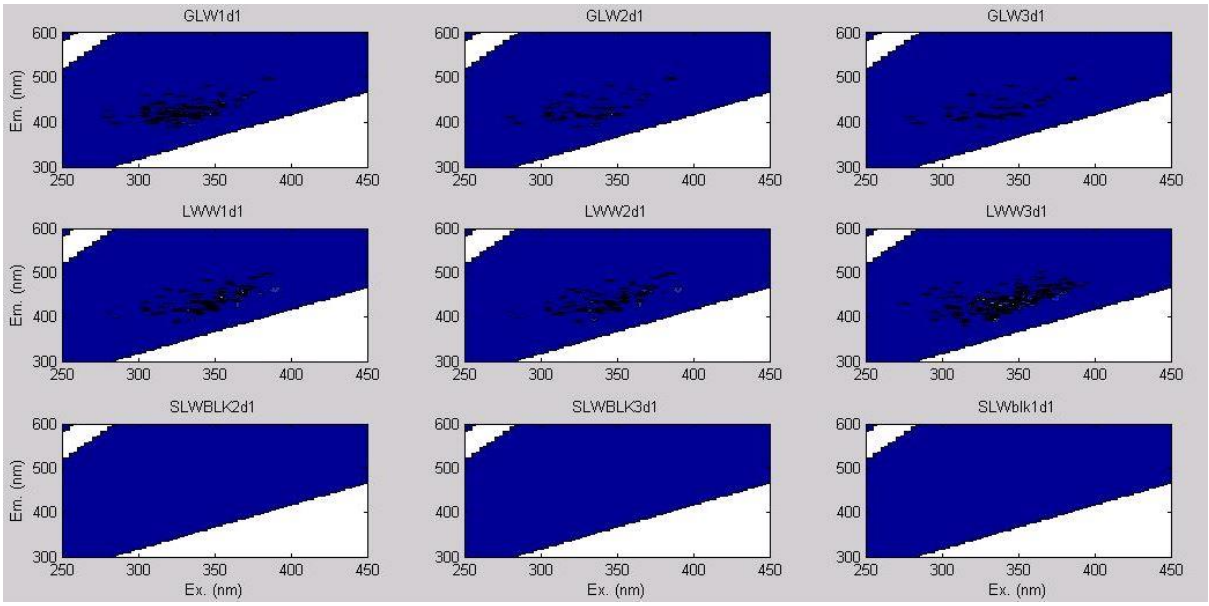

Appendix G

Complete set of EEMs for DOM analysis of CRUSH-WET, DIS-WET, and BLANK waters.

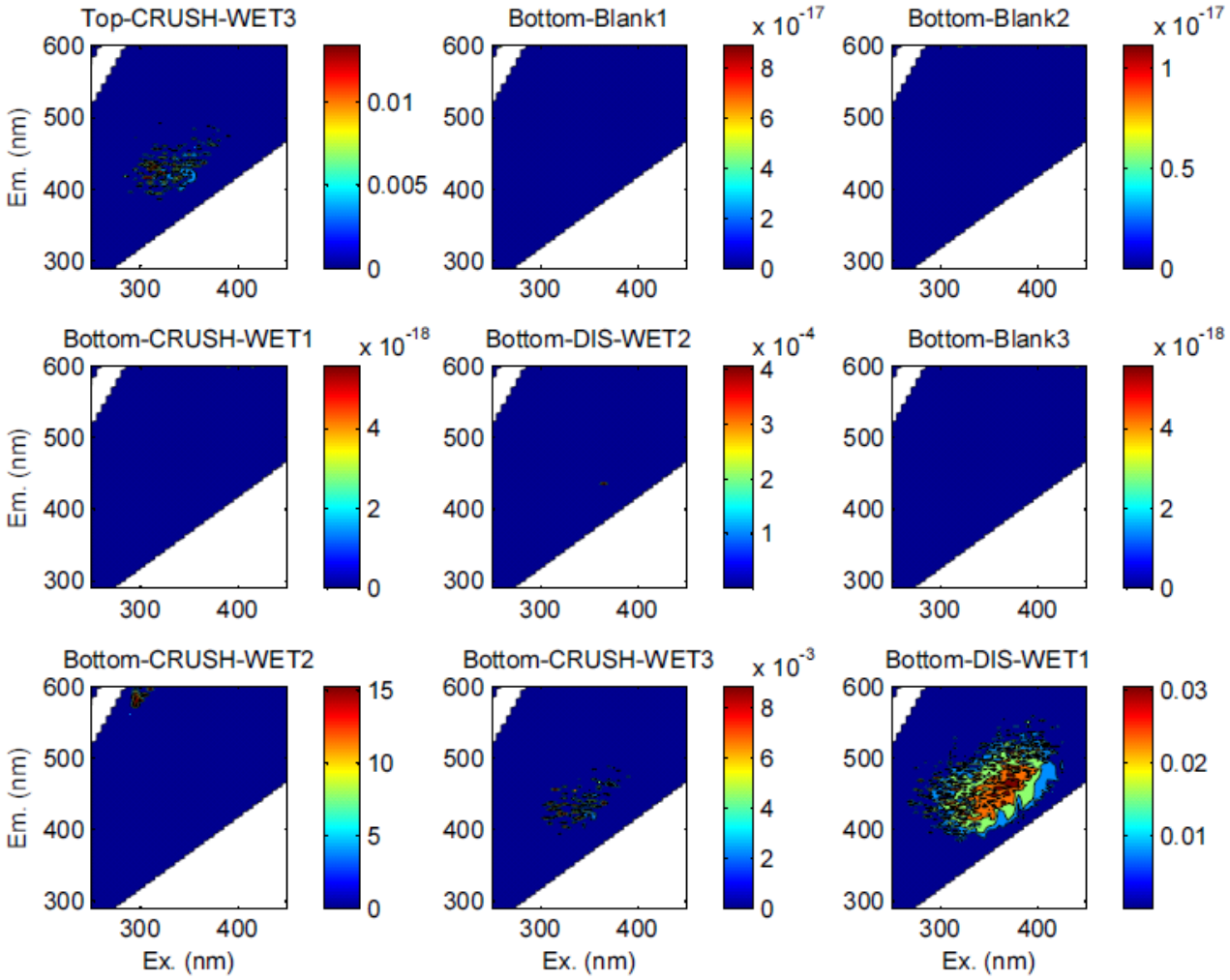

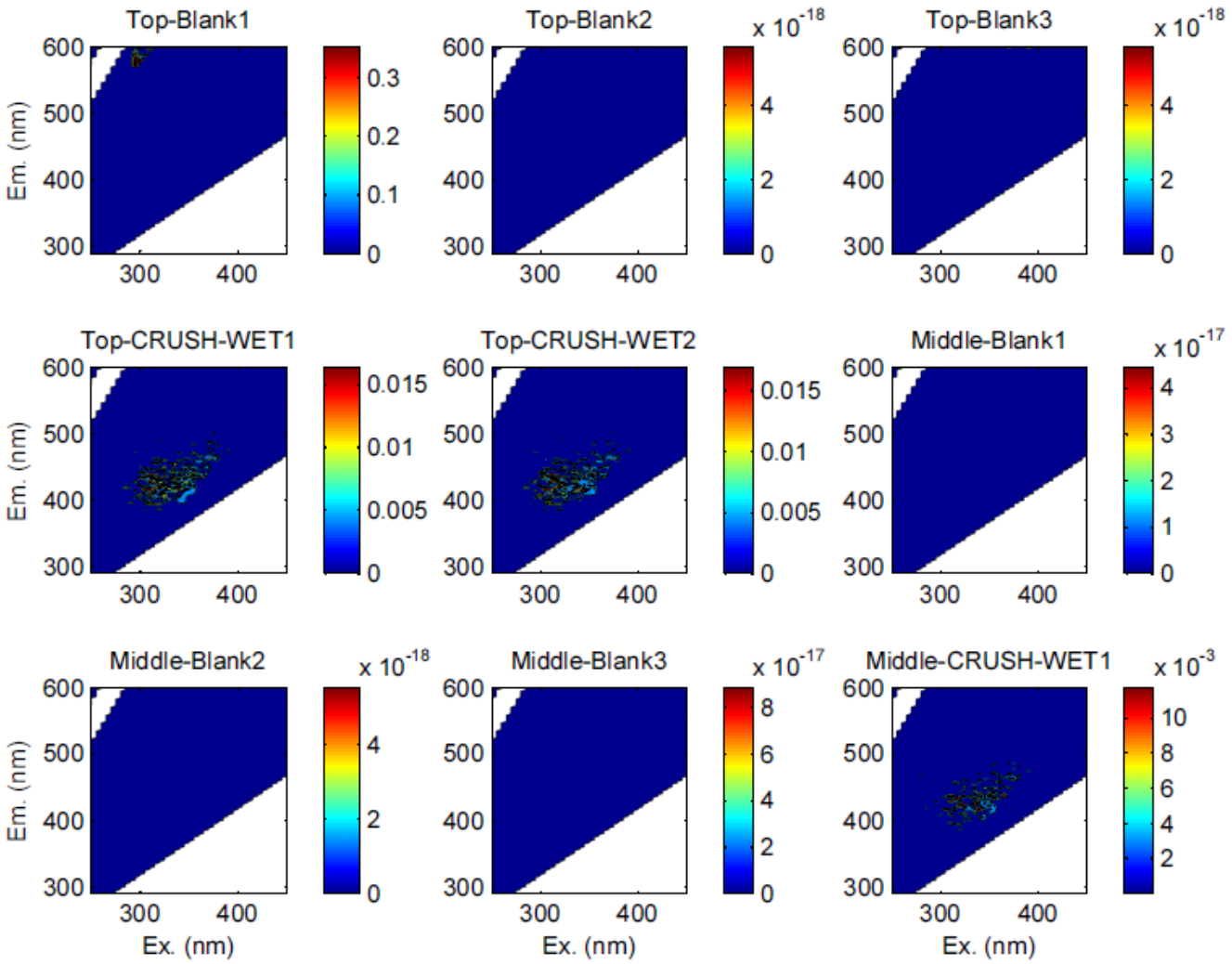
Top-Blank1
Top-Blank2
Top-Blank3
Top-CRUSH-WET1
Top-CRUSH-WET2
Middle-Blank1
Middle-Blank2
Middle-Blank3
Middle-CRUSH-WET1
Em. (nm)
Ex. (nm)
x 10^-18
x 10^-17
x 10^-3

Appendix E

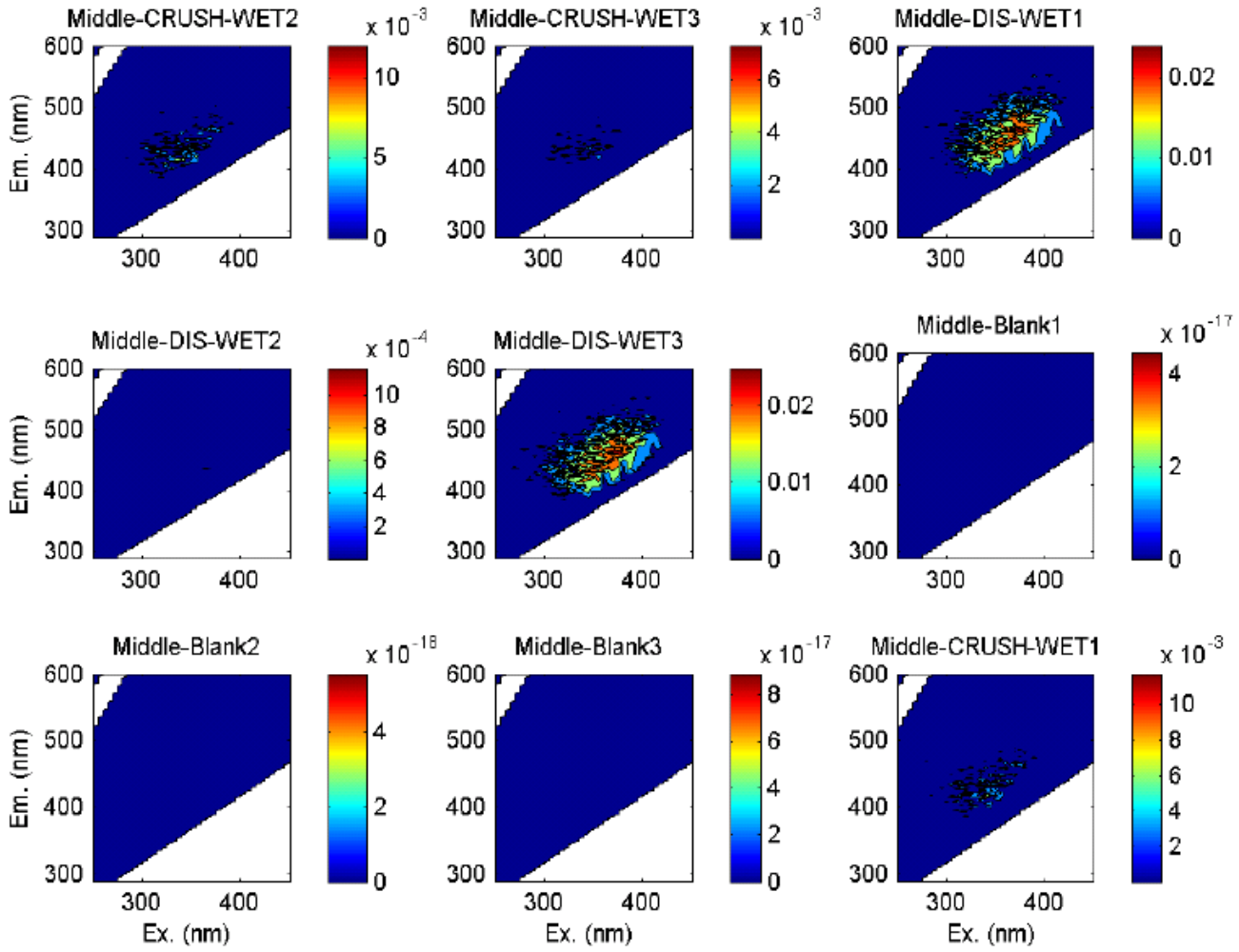
Middle-CRUSH-WET2
Middle-CRUSH-WET3
Middle-DIS-WET1
Middle-DIS-WET2
Middle-DIS-WET3
Middle-Blank1
Middle-Blank2
Middle-Blank3
Middle-CRUSH-WET1
Em. (nm)
Ex. (nm)
600
500
400
300
300
400

References

ACHBERGER, A. M., CHRISTNER, B. C., MICHAUD, A. B., PRISCU, J. C., SKIDMORE, M. L., VICK-MAJORS, T. J., , T. W. S. T., ADKINS, W., ANANDAKRISHNAN, S., BARBANTE, C., BARCHECK, G., BEEM, L., BEHAR, A., BEITCH, M., BOLSEY, R., BRANECKY, C., CARTER, S., CHRISTIANSON, K., EDWARDS, R., FISHER, A., FRICKER, H., FOLEY, N., GUTHRIE, B., HODSON, T., JACOBEL, R., KELLEY, S., MANKOFF, K., MCBRYAN, E., MIKUCKI, J., MITCHELL, A., POWELL, R., PURCELL, A., SAMPSON, D., SCHERER, R., SHERVE, J., SIEGFRIED, M. & TULACZYK, S. 2016. Microbial Community Structure of Subglacial Lake Whillans, West Antarctica. *Frontiers in Microbiology,* 7.

ALLEY, R. B., BLANKENSHIP, D. D., BENTLEY, C. R. & ROONEY, S. T. 1987. TILL BENEATH ICE STREAM-B .3. TILL DEFORMATION - EVIDENCE AND IMPLICATIONS. *Journal of Geophysical Research-Solid Earth and Planets,* 92**,** 8921-8929.

ANANDAKRISHNAN, S., CATANIA, G. A., ALLEY, R. B. & HORGAN, H. J. 2007. Discovery of till deposition at the grounding line of Whillans Ice Stream. *Science,* 315**,** 1835-1838.

ANASTASIO, C., GALBAVY, E. S., HUTTERLI, M. A., BURKHART, J. F. & FRIEL, D. K. 2007. Photoformation of hydroxyl radical on snow grains at Summit, Greenland. *Atmospheric Environment,* 41**,** 5110-5121.

ANASTASIO, C. & JORDAN, A. L. 2004. Photoformation of hydroxyl radical and hydrogen peroxide in aerosol particles from Alert, Nunavut: implications for aerosol and snowpack chemistry in the Arctic. *Atmospheric Environment,* 38**,** 1153-1166.

ANDERSON, S. P., DREVER, J. I. & HUMPHREY, N. F. 1997. Chemical weathering in glacial environments. *Geology,* 25**,** 399-402.

ANESIO, A. M. & LAYBOURN-PARRY, J. 2012. Glaciers and ice sheets as a biome. *Trends in Ecology & Evolution,* 27**,** 219-225.

ARNOLD, T., HARTH, C. M., MUHLE, J., MANNING, A. J., SALAMEH, P. K., KIM, J., IVY, D. J., STEELE, L. P., PETRENKO, V. V., SEVERINGHAUS, J. P., BAGGENSTOS, D. & WEISS, R. F. 2013. Nitrogen trifluoride global emissions estimated from updated atmospheric measurements. *Proceedings of the National Academy of Sciences of the United States of America,* 110**,** 2029-2034.

BAGA, A. N., JOHNSON, G. R. A., NAZHAT, N. B. & SAADALLA-NAZHAT, R. A. 1988. A simple spectrophotometric determination of hydrogen peroxide at low concentrations in aqueous solution. *Analytica Chimica Acta,* 204**,** 349-353.

BEGEMAN, C. B., TULACZYK, S. M. & FISHER, A. T. 2017. Spatially Variable Geothermal Heat Flux in West Antarctica: Evidence and Implications. *Geophysical Research Letters,* 44**,** 9823-9832.

BENN, D. I. & EVANS, D. J. A. 2010a. Erosion processes, forms and landscapes. *Glaciers and Glaciation.* London: Hodder Education.

BENN, D. I. & EVANS, D. J. A. 2010b. Glacier Hydrology. *Glaciers and Glaciation.* London: Hodder education.

BEYER, M. K. & CLAUSEN-SCHAUMANN, H. 2005. Mechanochemistry: The mechanical activation of covalent bonds. *Chemical Reviews,* 105**,** 2921-2948.

BHATIA, M., SHARP, M. & FOGHT, J. 2006. Distinct bacterial communities exist beneath a high arctic polythermal glacier. *Applied and Environmental Microbiology,* 72**,** 5838-5845.

BLANKENSHIP, D. D., BENTLEY, C. R., ROONEY, S. T. & ALLEY, R. B. 1987. TILL BENEATH ICE STREAM-B .1. PROPERTIES DERIVED FROM SEISMIC TRAVEL-TIMES. *Journal of Geophysical Research-Solid Earth and Planets,* 92**,** 8903-8911.

BORDA, M. J., ELSETINOW, A. R., SCHOONEN, M. A. & STRONGIN, D. R. 2001. Pyrite-Induced Hydrogen Peroxide Formation as a Driving Force in the Evolution of Photosynthetic Organisms on an Early Earth. *Astrobiology,* 1**,** 283-288.

BORDA, M. J., ELSETINOW, A. R., STRONGIN, D. R. & SCHOONEN, M. A. 2003. A mechanism for the production of hydroxyl radical at surface defect sites on pyrite. *Geochimica et Cosmochimica Acta,* 67**,** 935-939.

BOTTRELL, S. H. & TRANTER, M. 2002. Sulphide oxidation under partially anoxic conditions at the bed of the Haut Glacier d'Arolla, Switzerland. *Hydrological Processes,* 16**,** 2363-2368.

BOYD, E. S., SKIDMORE, M., MITCHELL, A. C., BAKERMANS, C. & PETERS, J. W. 2010. Methanogenesis in subglacial sediments. *Environmental Microbiology Reports,* 2**,** 685-692.

BRADLEY, A. S. & SUMMONS, R. E. 2010. Multiple origins of methane at the Lost City Hydrothermal Field. *Earth and Planetary Science Letters,* 297**,** 34-41.

BRANTLEY, S. L. 2003. Reaction Kinetics of Primary Rock-forming Minerals under Ambient Conditions. *In:* HOLLAND, H. D. & TUREKIAN, K. K. (eds.) *Treatise on Geochemistry: Surface and Ground Water Weathering, and Soils.* first ed. Oxford: Elseiver-Permagon.

BROWN, G. H., HUBBARD, B. & SEAGREN, A. G. 2001. Kinetics of solute acquisition from the dissolution of suspended sediment in subglacial channels. *Hydrological Processes,* 15**,** 3487-3497.

BROWN, G. H., TRANTER, M. & SHARP, M. J. 1996. Experimental investigations of the weathering of suspended sediment by Alpine glacial meltwater. *Hydrological Processes,* 10**,** 579-597.

CARTER, S. P., FRICKER, H. A. & SIEGFRIED, M. R. 2013. Evidence of rapid subglacial water piracy under Whillans Ice Stream, West Antarctica. *Journal of Glaciology,* 59**,** 1147-1162.

CHRISTIANSON, K., JACOBEL, R. W., HORGAN, H. J., ALLEY, R. B., ANANDAKRISHNAN, S., HOLLAND, D. M. & DALLASANTA, K. J. 2016. Basal conditions at the grounding zone of Whillans Ice Stream, West Antarctica, from ice-penetrating radar. *Journal of Geophysical Research-Earth Surface,* 121**,** 1954-1983.

CHRISTIANSON, K., JACOBEL, R. W., HORGAN, H. J., ANANDAKRISHNAN, S. & ALLEY, R. B. 2012. Subglacial Lake Whillans - Ice-penetrating radar and GPS observations of a shallow active reservoir beneath a West Antarctic ice stream. *Earth and Planetary Science Letters,* 331**,** 237-245.

CHRISTNER, B. C., PRISCU, J. C., ACHBERGER, A. M., BARBANTE, C., CARTER, S. P., CHRISTIANSON, K., MICHAUD, A. B., MIKUCKI, J. A., MITCHELL, A. C., SKIDMORE, M. L., VICK-MAJORS, T. J. & TEAM, W. S. 2014. A microbial ecosystem beneath the West Antarctic ice sheet. *Nature,* 512**,** 310-+.

COHN, C. A., PEDIGO, C. E., HYLTON, S. N., SIMON, S. R. & SCHOONEN, M. A. 2009. Evaluating the use of 3'-(p-Aminophenyl) fluorescein for determining the formation of highly reactive oxygen species in particle suspensions. *Geochemical Transactions,* 10**,** 1-9.

COMPTON, R. G., DALY, P. J. & HOUSE, W. A. 1986. THE DISSOLUTION OF ICELAND SPAR CRYSTALS - THE EFFECT OF SURFACE-MORPHOLOGY. *Journal of Colloid and Interface Science,* 113**,** 12-20.

COWTON, T., NIENOW, P., BARTHOLOMEW, I., SOLE, A. & MAIR, D. 2012. Rapid erosion beneath the Greenland ice sheet. *Geology,* 40**,** 343-346.

DAMM, C. & PEUKERT, W. 2009. Kinetics of Radical Formation during the Mechanical Activation of Quartz. *Langmuir,* 25**,** 2264-2270.

DAVIES, D., BINGHAM, R. G., KING, E. C., SMITH, A. M., BRISBOURNE, A. M., SPAGNOLO, M., GRAHAM, A. G. C., HOGG, A. E. & VAUGHAN, D. G. 2018. How dynamic are ice-stream beds? *Cryosphere,* 12**,** 1615-1628.

DIBB, J. E. & ARSENAULT, M. 2002. Shouldn't snowpacks be sources of monocarboxylic acids? *Atmospheric Environment,* 36**,** 2513-2522.

DICKINSON, J. T., JENSEN, L. C., LANGFORD, S. C. & ROSENBERG, P. E. 1992. FRACTURE-INDUCED EMISSION OF ALKALI ATOMS FROM FELDSPAR. *Physics and Chemistry of Minerals,* 18**,** 453-459.

DIESER, M., BROEMSEN, E., CAMERON, K. A., KING, G. M., ACHBERGER, A., CHOQUETTE, K., HAGEDORN, B., SLETTEN, R., JUNGE, K. & CHRISTNER, B. C. 2014. Molecular and biogeochemical evidence for methane cycling beneath the western margin of the Greenland Ice Sheet. *Isme Journal,* 8**,** 2305-2316.

DOMINE, F. & SHEPSON, P. B. 2002. Air-snow interactions and atmospheric chemistry. *Science,* 297**,** 1506-1510.

ETIOPE, G. & IONESCU, A. 2015. Low-temperature catalytic CO2 hydrogenation with geological quantities of ruthenium: a possible abiotic CH4 source in chromitite-rich serpentinized rocks. *Geofluids,* 15**,** 438-452.

ETIOPE, G., VANCE, S., CHRISTENSEN, L. E., MARQUES, J. M. & DA COSTA, I. R. 2013. Methane in serpentinized ultramafic rocks in mainland Portugal. *Marine and Petroleum Geology,* 45**,** 12-16.

FOGHT, J., AISLABIE, J., TURNER, S., BROWN, C. E., RYBURN, J., SAUL, D. J. & LAWSON, W. 2004. Culturable bacteria in subglacial sediments and ice from two Southern Hemisphere glaciers. *Microbial Ecology,* 47**,** 329-340.

FRICKER, H. A. & SCAMBOS, T. 2009. Connected subglacial lake activity on lower Mercer and Whillans Ice Streams, West Antarctica, 2003-2008. *Journal of Glaciology,* 55**,** 303-315.

FRICKER, H. A., SCAMBOS, T., BINDSCHADLER, R. & PADMAN, L. 2007. An Active Subglacial Water System in West Antarctica Mapped from Space. *Science,* 315**,** 1544.

G. MILLER, J. & OULTON, T. D. 1970. *Prototropy in Kaolinite During Percussive Grinding*.

GIL-LOZANO, C., LOSA-ADAMS, E., DAVILA, A. F. & GAGO-DUPORT, L. 2014. Pyrite nanoparticles as a Fenton-like reagent for in situ remediation of organic pollutants. *Beilstein Journal of Nanotechnology,* 5**,** 855-864.

GOLDSTEIN, R. H. 2001. Fluid inclusions in sedimentary and diagenetic systems. *Lithos,* 55**,** 159-193.

GRAF, E. & PENNISTON, J. T. 1980. METHOD FOR DETERMINATION OF HYDROGEN-PEROXIDE, WITH ITS APPLICATION ILLUSTRATED BY GLUCOSE ASSAY. *Clinical Chemistry,* 26**,** 658-660.

GRANNAS, A. M., SHEPSON, P. B. & FILLEY, T. R. 2004. Photochemistry and nature of organic matter in Arctic and Antarctic snow. *Global Biogeochemical Cycles,* 18**,** 10.

HALLET, B., HUNTER, L. & BOGEN, J. 1996. Rates of erosion and sediment evacuation by glaciers: A review of field data and their implications. *Global and Planetary Change,* 12**,** 213-235.

HAMILTON, T. L., PETERS, J. W., SKIDMORE, M. L. & BOYD, E. S. 2013. Molecular evidence for an active endogenous microbiome beneath glacial ice. *The Isme Journal,* 7**,** 1402.

HASEGAWA, M., OGATA, T. & SATO, M. 1995. MECHANO-RADICALS PRODUCED FROM GROUND QUARTZ AND QUARTZ GLASS. *Powder Technology,* 85**,** 269-274.

HODSON, A., TRANTER, M., GURNELL, A., CLARK, M. & HAGEN, J. O. 2002. The hydrochemistry of Bayelva, a high Arctic proglacial stream in Svalbard. *Journal of Hydrology,* 257**,** 91-114.

HODSON, A., TRANTER, M. & VATNE, G. 2000. Contemporary rates of chemical denudation and atmospheric CO2 sequestration in glacier basins: An Arctic perspective. *Earth Surface Processes and Landforms,* 25**,** 1447-1471.

HODSON, T. O., POWELL, R., BRACHFIELD, S., TULACZYK, S., SCHERER, R. P. & TEAM, W. S. 2016a. 4.2. Bulk density and magnetic susceptibility of sediment core SLW1_PC1. *In supplement to: Hodson, TO et al. (2016): Physical processes in Subglacial Lake Whillans, West Antarctica: inferences from sediment cores. Earth and Planetary Science Letters, 444, 56-63, https://doi.org/10.1016/j.epsl.2016.03.036.* PANGAEA.

HODSON, T. O., POWELL, R. D., BRACHFELD, S. A., TULACZYK, S., SCHERER, R. P. & TEAM, W. S. 2016b. Physical processes in Subglacial Lake Whillans, West Antarctica: Inferences from sediment cores. *Earth and Planetary Science Letters,* 444**,** 56-63.

HOLLOWAY, J. M. & DAHLGREN, R. A. 2002. Nitrogen in rock: Occurrences and biogeochemical implications. *Global Biogeochemical Cycles,* 16.

HOLLOWAY, J. M., NORDSTROM, D. K., BOHLKE, J. K., MCCLESKEY, R. B. & BALL, J. W. 2011. Ammonium in thermal waters of Yellowstone National Park: Processes affecting speciation and isotope fractionation. *Geochimica Et Cosmochimica Acta,* 75**,** 4611-4636.

HOLMKVIST, L., KAMYSHNY, A., VOGT, C., VAMVAKOPOULOS, K., FERDELMAN, T. G. & JØRGENSEN, B. B. 2011. Sulfate reduction below the sulfate–methane transition in Black Sea sediments. *Deep Sea Research Part I: Oceanographic Research Papers,* 58**,** 493-504.

HORGAN, H. J., ANANDAKRISHNAN, S., JACOBEL, R. W., CHRISTIANSON, K., ALLEY, R. B., HEESZEL, D. S., PICOTTI, S. & WALTER, J. I. 2012. Subglacial Lake Whillans - Seismic observations of a shallow active reservoir beneath a West Antarctic ice stream. *Earth and Planetary Science Letters,* 331**,** 201-209.

HUDSON, N., BAKER, A. & REYNOLDS, D. 2007. Fluorescence analysis of dissolved organic matter in natural, waste and polluted waters - A review. *River Research and Applications,* 23**,** 631-649.

ITALIANO, F., MARTINELLI, G. & PLESCIA, P. 2008. CO2 degassing over seismic areas: The role of mechanochemical production at the study case of Central Apennines. *Pure and Applied Geophysics,* 165**,** 75-94.

JANECKY, D. R. & SEYFRIED, W. E. 1986. Hydrothermal serpentinization of peridotite within oceanic crust: experimental investigations of mineralogy and major element chemistry. *Geochimica et Cosmochimica Acta,* 50.

JONES, L. C., ROSENBAUER, R., GOLDSMITH, J. I. & OZE, C. 2010. Carbonate control of H2 and CH4 production in serpentinization systems at elevated P-Ts. *Geophysical Research Letters,* 37**,** L14306.

KAMEDA, J., SARUWATARI, K. & TANAKA, H. 2004. H-2 generation during dry grinding of kaolinite. *Journal of Colloid and Interface Science,* 275**,** 225-228.

KELLEY, D. S., KARSON, J. A., FRUH-GREEN, G. L., YOERGER, D. R., SHANK, T. M., BUTTERFIELD, D. A., HAYES, J. M., SCHRENK, M. O., OLSON, E. J., PROSKUROWSKI,

G., JAKUBA, M., BRADLEY, A., LARSON, B., LUDWIG, K., GLICKSON, D., BUCKMAN, K., BRADLEY, A. S., BRAZELTON, W. J., ROE, K., ELEND, M. J., DELACOUR, A., BERNASCONI, S. M., LILLEY, M. D., BAROSS, J. A., SUMMONS, R. T. & SYLVA, S. P. 2005. A serpentinite-hosted ecosystem: The lost city hydrothermal field. *Science,* 307**,** 1428-1434.

KIEBER, R. J., ZHOU, X. L. & MOPPER, K. 1990. FORMATION OF CARBONYL-COMPOUNDS FROM UV-INDUCED PHOTODEGRADATION OF HUMIC SUBSTANCES IN NATURAL-WATERS - FATE OF RIVERINE CARBON IN THE SEA. *Limnology and Oceanography,* 35**,** 1503-1515.

KITA, I., MATSUO, S. & WAKITA, H. 1982. H-2 GENERATION BY REACTION BETWEEN H2O AND CRUSHED ROCK - AN EXPERIMENTAL-STUDY ON H-2 DEGASSING FROM THE ACTIVE FAULT ZONE. *Journal of Geophysical Research,* 87**,** 789-795.

KLEIN, F., BACH, W., JÖNS, N., MCCOLLOM, T., MOSKOWITZ, B. & BERQUÓ 2009. Iron partitioning and hydrogen generation during serpentinization of abyssal peridotites from 15°N on the Mid-Atlantic Ridge. *Geochimica et Cosmochimica Acta,* 73.

KNIGHT, P. G. 1997. The basal ice layer of glaciers and ice sheets. *Quaternary Science Reviews,* 16**,** 975-993.

KONNERUPMADSEN, J. & ROSEHANSEN, J. 1982. VOLATILES ASSOCIATED WITH ALKALINE IGNEOUS RIFT ACTIVITY - FLUID INCLUSIONS IN THE ILIMAUSSAQ INTRUSION AND THE GARDAR GRANITIC COMPLEXES (SOUTH GREENLAND). *Chemical Geology,* 37**,** 79-93.

LANGENHORST, F. & POIRIER, J.-P. 2000. Anatomy of black veins in Zagami: clues to the formation of high-pressure phases. *Earth and Planetary Science Letters,* 184**,** 37-55.

LANGMUIR, D. 1997. *Aqueous environmental geochemistry*, Upper Saddle River, N.J : Prentice Hall

LANOIL, B., SKIDMORE, M., PRISCU, J. C., HAN, S., FOO, W., VOGEL, S. W., TULACZYK, S. & ENGELHARDT, H. 2009. Bacteria beneath the West Antarctic Ice Sheet. *Environmental Microbiology,* 11**,** 609-615.

LASAGA, A. C. 1984. CHEMICAL-KINETICS OF WATER-ROCK INTERACTIONS. *Journal of Geophysical Research,* 89**,** 4009-4025.

LERMAN, A. 1988. Dissolution of Feldspars. *Geochemical Processes Water and Sediment Environments.* Malabar, florida: Robert E. Krieager Publishing Company.

LIN, L. H., HALL, J., LIPPMANN-PIPKE, J., WARD, J. A., LOLLAR, B. S., DEFLAUN, M., ROTHMEL, R., MOSER, D., GIHRING, T. M., MISLOWACK, B. & ONSTOTT, T. C. 2005. Radiolytic H-2 in continental crust: Nuclear power for deep subsurface microbial communities. *Geochemistry Geophysics Geosystems,* 6**,** 13.

LINGLE, D. A., KEHEW, A. E. & KRISHNAMURTHY, R. V. 2017. Use of nitrogen isotopes and other geochemical tools to evaluate the source of ammonium in a confined glacial drift aquifer, Ottawa County, Michigan, USA. *Applied Geochemistry,* 78**,** 334-342.

LUTHRA, T., ANANDAKRISHNAN, S., WINBERRY, J. P., ALLEY, R. B. & HOLSCHUH, N. 2016. Basal characteristics of the main sticky spot on the ice plain of Whillans Ice Stream, Antarctica. *Earth and Planetary Science Letters,* 440**,** 12-19.

MANNING, D. A. C. & HUTCHEON, I. E. 2004. Distribution and mineralogical controls on ammonium in deep groundwaters. *Applied Geochemistry,* 19**,** 1495-1503.

MARQUES, J. M., CARREIRA, P. M., CARVALHO, M. R., MATIAS, M. J., GOFF, F. E., BASTO, M. J., GRACA, R. C., AIRES-BARROS, L. & ROCHA, L. 2008. Origins of high pH mineral waters from ultramafic rocks, Central Portugal. *Applied Geochemistry,* 23**,** 3278-3289.

MARTINELLI, G. & PLESCIA, P. 2004. Mechanochemical dissociation of calcium carbonate: laboratory data and relation to natural emissions of CO2. *Physics of the Earth and Planetary Interiors,* 142**,** 205-214.

MARTINELLI, G. & PLESCIA, P. 2005. Carbon dioxide and methane emissions from calcareous-marly rock under stress: experimental tests results. *Annals of Geophysics,* 48**,** 167-173.

MAYHEW, L. E., ELLISON, E. T., MCCOLLOM, T. M., TRAINOR, T. P. & TEMPLETON, A. S. 2013. Hydrogen generation from low-temperature water-rock reactions. *Nature Geosci,* 6**,** 478-484.

MCCOLLOM, T. M. 2009. Thermodynamic constraints on hydrogen generation during serpentinization of ultramafic rocks. *Geochimica et Cosmochimica Acta,* 73.

MCCOLLOM, T. M. & SEEWALD, J. S. 2001. A reassessment of the potential for reduction of dissolved CO2 to hydrocarbons during serpentinization of olivine. *Geochimica et Cosmochimica Acta,* 65**,** 3769-3778.

MEISTER, P. 2013. Two opposing effects of sulfate reduction on carbonate precipitation in normal marine, hypersaline, and alkaline environments. *Geology,* 41**,** 499-502.

MICHAUD, A. B., DORE, J. E., ACHBERGER, A. M., CHRISTNER, B. C., MITCHELL, A. C., SKIDMORE, M. L., VICK-MAJORS, T. J. & PRISCU, J. C. 2017. Microbial oxidation as a methane sink beneath the West Antarctic Ice Sheet. *Nature Geoscience,* 10**,** 582-+.

MICHAUD, A. B., SKIDMORE, M. L., MITCHELL, A. C., VICK-MAJORS, T. J., BARBANTE, C., TURETTA, C., VANGELDER, W. & PRISCU, J. C. 2016. Solute sources and geochemical processes in Subglacial Lake Whillans, West Antarctica. *Geology,* 44**,** 347-350.

MIKUCKI, J. A., LEE, P. A., GHOSH, D., PURCELL, A. M., MITCHELL, A. C., MANKOFF, K. D., FISHER, A. T., TULACZYK, S., CARTER, S., SIEGFRIED, M. R., FRICKER, H. A., HODSON, T., COENEN, J., POWELL, R., SCHERER, R., VICK-MAJORS, T., ACHBERGER, A. A., CHRISTNER, B. C., TRANTER, M. & TEAM, W. S. 2016. Subglacial Lake Whillans microbial biogeochemistry: a synthesis of current knowledge. *Philosophical Transactions of the Royal Society a-Mathematical Physical and Engineering Sciences,* 374.

MIKUCKI, J. A., PEARSON, A., JOHNSTON, D. T., TURCHYN, A. V., FARQUHAR, J., SCHRAG, D. P., ANBAR, A. D., PRISCU, J. C. & LEE, P. A. 2009. A Contemporary Microbially Maintained Subglacial Ferrous "Ocean". *Science,* 324**,** 397-400.

MILLER, B. R., WEISS, R. F., SALAMEH, P. K., TANHUA, T., GREALLY, B. R., MUHLE, J. & SIMMONDS, P. G. 2008. Medusa: A sample preconcentration and GC/MS detector system for in situ measurements of atmospheric trace halocarbons, hydrocarbons, and sulfur compounds. *Analytical Chemistry,* 80**,** 1536-1545.

MONTROSS, G. G., MCGLYNN, B. L., MONTROSS, S. N. & GARDNER, K. K. 2013. Nitrogen production from geochemical weathering of rocks in southwest Montana, USA. *Journal of Geophysical Research-Biogeosciences,* 118**,** 1068-1078.

MORTIMER, R. J. G., GALSWORTHY, A. M. J., BOTTRELL, S. H., WILMOT, L. E. & NEWTON, R. J. 2011. Experimental evidence for rapid biotic and abiotic reduction of Fe (III) at low temperatures in salt marsh sediments: a possible mechanism for formation of modern sedimentary siderite concretions. *Sedimentology,* 58**,** 1514-1529.

MURPHY, K. R., STEDMON, C. A., GRAEBER, D. & BRO, R. 2013. Fluorescence spectroscopy and multi-way techniques. PARAFAC. *Analytical Methods,* 5**,** 6557-6566.

MUTO, A., CHRISTIANSON, K., HORGAN, H. J., ANANDAKRISHNAN, S. & ALLEY, R. B. 2013. Bathymetry and geological structures beneath the Ross Ice Shelf at the mouth of Whillans Ice Stream, West Antarctica, modeled from ground-based gravity measurements. *Journal of Geophysical Research-Solid Earth,* 118**,** 4535-4546.

NAUMOV, V. B., DOROFEEVA, V. A. & MIRONOVA, O. F. 2009. Principal physicochemical parameters of natural mineral-forming fluids. *Geochemistry International,* 47**,** 777-802.

NEUBECK, A., DUC, N. T., BASTVIKEN, D., CRILL, P. & HOLM, N. G. 2011. Formation of H2 and CH4by weathering of olivine at temperatures between 30 and 70°C. *Geochemical Transactions,* 12**,** 6.

NEUBECK, A., DUC, N. T., HELLEVANG, H., OZE, C., BASTVIKEN, D., BACSIK, Z. & HOLM, N. G. 2014. Olivine alteration and H2 production in carbonate-rich, low temperature aqueous environments. *Planetary and Space Science,* 96**,** 51-61.

OKLAND, I., HUANG, S., THORSETH, I. H. & PEDERSEN, R. B. 2014. Formation of H2, CH4 and N-species during low-temperature experimental alteration of ultramafic rocks. *Chemical Geology,* 387**,** 22-34.

PETROVICH, R. 1981. KINETICS OF DISSOLUTION OF MECHANICALLY COMMINUTED ROCK-FORMING OXIDES AND SILICATES .1. DEFORMATION AND DISSOLUTION OF QUARTZ UNDER LABORATORY CONDITIONS. *Geochimica Et Cosmochimica Acta,* 45**,** 1665-1674.

PLUMMER, L. N., WIGLEY, T. M. & PARKHURST, D. L. 1978. The kinetics of calcite dissolution in CO 2 -water systems at 5 degrees to 60 ^{o}C and 0.0 to 1.0 atm CO_2. *American Journal of Chemistry,* 278**,** 179 - 216.

POTTER, J., SALVI, S. & LONGSTAFFE, F. J. 2013. Abiogenic hydrocarbon isotopic signatures in granitic rocks: Identifying pathways of formation. *Lithos,* 182**,** 114-124.

PRISCU, J. C., ACHBERGER, A. M., CAHOON, J. E., CHRISTNER, B. C., EDWARDS, R. L., JONES, W. L., MICHAUD, A. B., SIEGFRIED, M. R., SKIDMORE, M. L., SPIGEL, R. H., SWITZER, G. W., TULACZYK, S. & VICK-MAJORS, T. J. 2013. A microbiologically clean strategy for access to the Whillans Ice Stream subglacial environment. *Antarctic Science,* 25**,** 637-647.

PRISCU, J. C., ADAMS, E. E., LYONS, W. B., VOYTEK, M. A., MOGK, D. W., BROWN, R. L., MCKAY, C. P., TAKACS, C. D., WELCH, K. A., WOLF, C. F., KIRSHTEIN, J. D. & AVCI, R.

1999. Geomicrobiology of subglacial ice above Lake Vostok, Antarctica. *Science,* 286**,** 2141-2144.

PRISCU, J. C., TULACZYK, S., STUDINGER, M., KENNICUTT, M., CHRISTNER, B. C. & FOREMAN, C. M. 2008. Antarctic subglacial water: origin, evolution and ecology. *Polar lakes and rivers: limnology of Arctic and Antarctic aquatic ecosystems. Oxford University Press, Oxford***,** 119-135.

PROSKUROWSKI, G., LILLEY, M. D., SEEWALD, J. S., FRUH-GREEN, G. L., OLSON, E. J., LUPTON, J. E., SYLVA, S. P. & KELLEY, D. S. 2008. Abiogenic hydrocarbon production at Lost City hydrothermal field. *Science,* 319**,** 604-607.

PURCELL, A. M., MIKUCKI, J. A., ACHBERGER, A. M., ALEKHINA, I. A., BARBANTE, C., CHRISTNER, B. C., GHOSH, D., MICHAUD, A. B., MITCHELL, A. C., PRISCU, J. C., SCHERER, R., SKIDMORE, M. L., VICK-MAJORS, T. J. & TEAM, W. S. 2014. Microbial sulfur transformations in sediments from Subglacial Lake Whillans. *Frontiers in Microbiology,* 5.

RAISWELL, R. 1984. CHEMICAL-MODELS OF SOLUTE ACQUISITION IN GLACIAL MELT WATERS. *Journal of Glaciology,* 30**,** 49-57.

RAISWELL, R., HAWKINGS, J. R., BENNING, L. G., BAKER, A. R., DEATH, R., ALBANI, S., MAHOWALD, N., KROM, M. D., POULTON, S. W., WADHAM, J. & TRANTER, M. 2016. Potentially bioavailable iron delivery by iceberg-hosted sediments and atmospheric dust to the polar oceans. *Biogeosciences,* 13**,** 3887-3900.

RAISWELL, R., VU, H. P., BRINZA, L. & BENNING, L. G. 2010. The determination of labile Fe in ferrihydrite by ascorbic acid extraction: Methodology, dissolution kinetics and loss of solubility with age and de-watering. *Chemical Geology,* 278**,** 70-79.

RICKARD, D. & SJOBERG, E. L. 1983. MIXED KINETIC CONTROL OF CALCITE DISSOLUTION RATES. *American Journal of Science,* 283**,** 815-830.

ROGERS, J. R. & BENNETT, P. C. 2004. Mineral stimulation of subsurface microorganisms: release of limiting nutrients from silicates. *Chemical Geology,* 203**,** 91-108.

SARUWATARI, K., KAMEDA, J. & TANAKA, H. 2004. Generation of hydrogen ions and hydrogen gas in quartz-water crushing experiments: an example of chemical processes in active faults. *Physics and Chemistry of Minerals,* 31**,** 176-182.

SCHERER, R., POWELL, R., COENEN, J., HODSON, T., PUTTKAMMER, R. & TULACZYK, S. Geological and paleontological results from the WISSARD (Whillans Ice Stream Subglacial Access Research Drilling) Project. AGU Fall Meeting Abstracts, 2015.

SCHILLAWSKI, S. & PETSCH, S. 2008. Release of biodegradable dissolved organic matter from ancient sedimentary rocks. *Global Biogeochemical Cycles,* 22.

SCHINK, B. 2006. Microbially Driven Redox Reactions in Anoxic Environments: Pathways, Energetics, and Biochemical Consequences. 6**,** 228-233.

SCHOELL, M. 1988. MULTIPLE ORIGINS OF METHANE IN THE EARTH. *Chemical Geology,* 71**,** 1-10.

SCHULZ, H. 1999. Short history and present trends of Fischer-Tropsch synthesis. *Applied Catalysis A: General,* 186.

SHARP, M., PARKES, J., CRAGG, B., FAIRCHILD, I. J., LAMB, H. & TRANTER, M. 1999. Widespread bacterial populations at glacier beds and their relationship to rock weathering and carbon cycling. *Geology,* 27**,** 107-110.

SHARP, M. & TRANTER, M. 2017. Glacier biogeochemistry. *Geochemical Perspectives,* 6**,** 1-177.

SISSON, V. B., LOVELACE, R. W., MAZE, W. B. & BERGMAN, S. C. 1993. DIRECT OBSERVATION OF PRIMARY FLUID-INCLUSION FORMATION. *Geology,* 21**,** 751-754.

SKIDMORE, M., ANDERSON, S. P., SHARP, M., FOGHT, J. & LANOIL, B. D. 2005. Comparison of microbial community compositions of two subglacial environments reveals a possible role for microbes in chemical weathering processes. *Applied and Environmental Microbiology,* 71**,** 6986-6997.

SKIDMORE, M., TRANTER, M., TULACZYK, S. & LANOIL, B. 2010. Hydrochemistry of ice stream beds - evaporitic or microbial effects? *Hydrological Processes,* 24**,** 517-523.

SKIDMORE, M. L., FOGHT, J. M. & SHARP, M. J. 2000. Microbial life beneath a high Arctic glacier. *Applied and Environmental Microbiology,* 66**,** 3214-3220.

SMITH, A. M., BENTLEY, C. R., BINGHAM, R. G. & JORDAN, T. A. 2012. Rapid subglacial erosion beneath Pine Island Glacier, West Antarctica. *Geophysical Research Letters,* 39.

SMITH, A. M., MURRAY, T., NICHOLLS, K. W., MAKINSON, K., AOALGEIRSDOTTIR, G., BEHAR, A. E. & VAUGHAN, D. G. 2007. Rapid erosion, drumlin formation, and changing hydrology beneath an Antarctic ice stream. *Geology,* 35**,** 127-130.

STEDMON, C. A., MARKAGER, S. & BRO, R. 2003. Tracing dissolved organic matter in aquatic environments using a new approach to fluorescence spectroscopy. *Marine Chemistry,* 82**,** 239-254.

STEVENS, T. O. & MCKINLEY, J. P. 2000a. Abiotic Controls on H2 Production from Basalt–Water Reactions and Implications for Aquifer Biogeochemistry. *Environmental Science & Technology,* 34**,** 826-831.

STEVENS, T. O. & MCKINLEY, J. P. 2000b. Abiotic controls on H-2 production from basalt-water reactions and implications for aquifer biogeochemistry. *Environmental Science & Technology,* 34**,** 826-831.

STIBAL, M., HASAN, F., WADHAM, J. L., SHARP, M. J. & ANESIO, A. M. 2012a. Prokaryotic diversity in sediments beneath two polar glaciers with contrasting organic carbon substrates. *Extremophiles,* 16**,** 255-265.

STIBAL, M., WADHAM, J. L., LIS, G. P., TELLING, J., PANCOST, R. D., DUBNICK, A., SHARP, M. J., LAWSON, E. C., BUTLER, C. E. H., HASAN, F., TRANTER, M. & ANESIO, A. M. 2012b. Methanogenic potential of Arctic and Antarctic subglacial environments with contrasting organic carbon sources. *Global Change Biology,* 18**,** 3332-3345.

SUDGEN, D. E. & JOHN, B. S. 1976. The process of glacial erosion. *Glaciaers and Landscape.* London, UK: Edward Arnold.

SWANSON, A. L., BLAKE, N. J., DIBB, J. E., ALBERT, M. R., BLAKE, D. R. & ROWLAND, F. S. 2002. Photochemically induced production of CH3Br, CH3I, C2H5I, ethene, and propene within surface snow at Summit, Greenland. *Atmospheric Environment,* 36**,** 2671-2682.

TAKEHIRO, H., SHINSUKE, K. & KATSUHIKO, S. 2011. Mechanoradical H2 generation during simulated faulting: Implications for an earthquake-driven subsurface biosphere. *Geophysical Research Letters,* 38.

TELLING, J., BOYD, E. S., BONE, N., JONES, E. L., TRANTER, M., MACFARLANE, J. W., MARTIN, P. G., WADHAM, J. L., LAMARCHE-GAGNON, G., SKIDMORE, M. L., HAMILTON, T. L., HILL, E., JACKSON, M. & HODGSON, D. A. 2015. Rock comminution as a source of hydrogen for subglacial ecosystems. *Nature Geosci,* 8**,** 851-855.

TRANTER, M. 2003. Geochemical Weathering in Glacial and Proglacial Environments. *In:* HOLLAND, H. D. & TUREKIAN, K. K. (eds.) *Treatise on Geochemistry.* Oxford: Elsevier-Permagon.

TRANTER, M. 2006. Glacial chemical weathering, runoff composition and solute fluxes. *In:* KNIGHT, P. G. (ed.) *Glacier Science and Environmental Change.* Oxford: Blackwell Science Ltd.

TRANTER, M., BROWN, G., RAISWELL, R., SHARP, M. & GURNELL, A. 1993. A CONCEPTUAL-MODEL OF SOLUTE ACQUISITION BY ALPINE GLACIAL MELTWATERS. *Journal of Glaciology,* 39**,** 573-581.

TRANTER, M., HUYBRECHTS, P., MUNHOVEN, G., SHARP, M. J., BROWN, G. H., JONES, I. W., HODSON, A. J., HODGKINS, R. & WADHAM, J. L. 2002a. Direct effect of ice sheets on terrestrial bicarbonate, sulphate and base cation fluxes during the last glacial cycle: minimal impact on atmospheric CO2 concentrations. *Chemical Geology,* 190**,** 33-44.

TRANTER, M., SHARP, M. J., BROWN, G. H., WILLIS, I. C., HUBBARD, B. P., NIELSEN, M. K., SMART, C. C., GORDON, S., TULLEY, M. & LAMB, H. R. 1997. Variability in the chemical composition of in situ subglacial meltwaters. *Hydrological Processes,* 11**,** 59-77.

TRANTER, M., SHARP, M. J., LAMB, H. R., BROWN, G. H., HUBBARD, B. P. & WILLIS, I. C. 2002b. Geochemical weathering at the bed of Haut Glacier d'Arolla, Switzerland - a new model. *Hydrological Processes,* 16**,** 959-993.

TRANTER, M., SKIDMORE, M. & WADHAM, J. 2005. Hydrological controls on microbial communities in subglacial environments. *Hydrological Processes,* 19**,** 995-998.

TRANTER, M. & WADHAM, J. L. 2013. Geochemical Weathering in Glacial and Proglacial Environments. *Treatise on Geochemistry: Second Edition.* JAI-Elsevier Science Inc.

TULACZYK, S., KAMB, B., SCHERER, R. P. & ENGELHARDT, H. F. 1998. Sedimentary processes at the base of a West Antarctic ice stream: Constraints from textural and compositional properties of subglacial debris. *Journal of Sedimentary Research,* 68**,** 487-496.

TULACZYK, S., MIKUCKI, J. A., SIEGFRIED, M. R., PRISCU, J. C., BARCHECK, C. G., BEEM, L. H., BEHAR, A., BURNETT, J., CHRISTNER, B. C., FISHER, A. T., FRICKER, H. A., MANKOFF, K. D., POWELL, R. D., RACK, F., SAMPSON, D., SCHERER, R. P., SCHWARTZ, S. Y. & WISSARD SCI, T. 2014. WISSARD at Subglacial Lake Whillans, West Antarctica: scientific operations and initial observations. *Annals of Glaciology,* 55**,** 51-58.

TUNG, H. C., PRICE, P. B., BRAMALL, N. E. & VRDOLJAK, G. 2006. Microorganisms metabolizing on clay grains in 3-km-deep Greenland basal ice. *Astrobiology,* 6**,** 69-86.

TURCHYN, A. V., SIVAN, O. & SCHRAG, D. P. 2006. Oxygen isotopic composition of sulfate in deep sea pore fluid: evidence for rapid sulfur cycling. 4**,** 191-201.

UC DAVIS STABLE ISOTOPE FACILITY. 2018a. *Analysis of Carbon Dioxide (CO2) by GasBench-IRMS* [Online]. Available: https://stableisotopefacility.ucdavis.edu/co2.html [Accessed 14th November 2018].

UC DAVIS STABLE ISOTOPE FACILITY. 2018b. *Analysis of Methane (CH4) by GasBench-Precon-IRMS* [Online]. Available: https://stableisotopefacility.ucdavis.edu/ch4.html [Accessed].

VICK-MAJORS, T. J., MITCHELL, A. C., ACHBERGER, A. M., CHRISTNER, B. C., DORE, J. E., MICHAUD, A. B., MIKUCKI, J. A., PURCELL, A. M., SKIDMORE, M. L., PRISCU, J. C. & , T. W. S. T. 2016. Physiological Ecology of Microorganisms in Subglacial Lake Whillans. *Frontiers in Microbiology,* 7.

VIOLLIER, E., INGLETT, P. W., HUNTER, K., ROYCHOUDHURY, A. N. & VAN CAPPELLEN, P. 2000. The ferrozine method revisited: Fe(II)/Fe(III) determination in natural waters. *Applied Geochemistry,* 15**,** 785-790.

WADHAM, J. L., ARNDT, S., TULACZYK, S., STIBAL, M., TRANTER, M., TELLING, J., LIS, G. P., LAWSON, E., RIDGWELL, A., DUBNICK, A., SHARP, M. J., ANESIO, A. M. & BUTLER, C. E. H. 2012. Potential methane reservoirs beneath Antarctica. *Nature,* 488**,** 633-637.

WADHAM, J. L., BOTTRELL, S., TRANTER, M. & RAISWELL, R. 2004. Stable isotope evidence for microbial sulphate reduction at the bed of a polythermal high Arctic glacier. *Earth and Planetary Science Letters,* 219**,** 341-355.

WADHAM, J. L., COOPER, R. J., TRANTER, M. & BOTTRELL, S. 2007. Evidence for widespread anoxia in the proglacial zone of an Arctic glacier. *Chemical Geology,* 243**,** 1-15.

WADHAM, J. L., TRANTER, M., SKIDMORE, M., HODSON, A. J., PRISCU, J., LYONS, W. B., SHARP, M., WYNN, P. & JACKSON, M. 2010. Biogeochemical weathering under ice: Size matters. *Global Biogeochemical Cycles,* 24**,** 11.

WADHAM, J. L., TRANTER, M., TULACZYK, S. & SHARP, M. 2008. Subglacial methanogenesis: A potential climatic amplifier? *Global Biogeochemical Cycles,* 22.

WAKITA, H., NAKAMURA, Y., KITA, I., FUJII, N. & NOTSU, K. 1980. HYDROGEN RELEASE - NEW INDICATOR OF FAULT ACTIVITY. *Science,* 210**,** 188-190.

WHITE, A. F. & BRANTLEY, S. L. 2003. The effect of time on the weathering of silicate minerals: why do weathering rates differ in the laboratory and field? *Chemical Geology,* 202**,** 479-506.

WHITICAR, M. J. 1999. Carbon and hydrogen isotope systematics of bacterial formation and oxidation of methane. *Chemical Geology,* 161**,** 291-314.

WRIGHT, A. & SIEGERT, M. 2012. A fourth inventory of Antarctic subglacial lakes. *Antarctic Science,* 24**,** 659-664.

YARNES, C. 2013. δ13C and δ2H measurement of methane from ecological and geological sources by gas chromatography/combustion/pyrolysis isotope-ratio mass spectrometry. 27**,** 1036-1044.

YDE, J. C., FINSTER, K. W., RAISWELL, R., STEFFENSEN, J. P., HEINEMEIER, J., OLSEN, J., GUNNLAUGSSON, H. P. & NIELSEN, O. B. 2010. Basal ice microbiology at the margin of the Greenland ice sheet. *Annals of Glaciology,* 51**,** 71-79.

ZHANG, L. & LUETTGE, A. 2009. Theoretical approach to evaluating plagioclase dissolution mechanisms. *Geochimica Et Cosmochimica Acta,* 73**,** 2832-2849.